SPECIFICITY AND COMPETITION DURING MATURATION OF NEUROMUSCULAR SYNAPSES

Thesis by

James Martin Soha

In Partial Fulfillment of the Requirements

for the Degree of

Doctor of Philosophy

California Institute of Technology

Pasadena, California

1988

(Submitted April 26, 1988)

ACKNOWLEDGEMENTS

I am grateful to my wife Linda, my daughter Jill, and my son Aron for their patience, cheerfulness, and support.

I thank my research advisor, David Van Essen, for his personal kindness, for his thoughtful guidance, and for teaching by example the virtues of care and precision. In addition to my advisor, two individuals contributed significantly to the work described in this thesis. Chris Yo, a Caltech undergraduate, diligently assisted in the dye labeling experiments of Chapter 3. Ed Callaway collaborated in the reinnervation study of Chapter 2 and the computer modeling effort described in Chapter 4. I particularly thank Ed for the many hours of stimulating discussions, and for his logistical support when I was in Connecticut.

Many other people provided valuable help. Kathy Tazumi prepared Ringer's and slides and helped in countless other ways. David Bilitch freely contributed his time and computer expertise in support of the modeling work. Mike Walsh and Dave Hodge provided hardware support. Bill Lease and Angelo Delise helped locate essential supplies. Milton Grooms and Robert Vega furnished animal care. Susan Kallenbach, Sandy Koceski and Nancy Gill contributed indispensable administrative help. I thank John and Elspeth Benton for taking me into their home. Finally, I thank Mary Kennedy for an introduction to biochemistry during an extended rotation, and Karl Herrup for his unflagging encouragement.

I gratefully acknowledge my financial support, which included National Research Service Awards under NIH training grants T32 GM07616 and T32 GM07737, an Evelyn Wood fellowship, Caltech Institute fellowships, and a Graduate Research Assistantship funded by NSF grant BNS-8408213 to David Van Essen.

ABSTRACT

Fast and slow contracting fibers in neonatal mammalian skeletal muscle are each innervated in a highly specific manner by motor neurons of the corresponding type, even at an age when polyinnervation is widespread. Chemospecific recognition is a possible mechanism by which this pattern of innervation could be established. I have investigated this possibility by studying the degree of specificity during reinnervation of neonatal rabbit soleus muscle. Fiber type composition was assayed by measuring the twitch rise times of motor units within two days of the onset of functional reinnervation. In contrast to the broad, bimodal distribution of single motor unit twitch rise times seen in normal muscles, motor units in reinnervated muscles yielded a narrower, unimodal distribution of rise times. Rise times of reinnervated units were intermediate to those of normal fast and slow units, suggesting that reinnervated units were composed of a mixture of fast and slow contracting muscle fibers. An alternative possibility, that specific reinnervation was masked by contractile de-differentiation of muscle fibers, was examined by maintaining a transmission blockade induced by botulinum toxin poisoning for an equivalent interval. Twitch rise times of treated motor units exhibited the distinctly bimodal distribution characteristic of normal muscles, suggesting that muscle fibers can retain contractile diversity during a transient period of denervation. Computer simulations were employed to estimate the amount of rise time diversity induced by varying degrees of specificity during reinnervation. Based on this analysis, I conclude that there is little if any selective reinnervation of muscle fiber types at the ages studied.

In a second experiment, I compared the development of fast and slow motor innervation in the neonatal rabbit soleus, a muscle which contains two distinct motor

unit types during the early period of polyneuronal innervation. The innervation state of individual muscle fibers was ascertained using an intracellular electrode; a fluorescent dye was then injected into particular fibers to permit subsequent identification of histochemical type. No significant difference in the time course of synapse elimination was observed for fast and slow motor units as judged by the percentage of fibers remaining polyneuronally innervated at two ages: 7–8 days, when most fibers are multiply innervated, and 10–11 days, when the level of polyinnervation is low.

In a third experiment, I examined a phenomenon in which compound endplate potentials were occasionally seen in muscle fibers at an age (17–23 days) well past the major episode of synapse elimination. Several lines of evidence indicate that this apparent polyinnervation in fact derives from an electrode-induced electrical coupling artifact, and that genuinely polyinnervated fibers are very rare at this stage, if present at all.

A computer model of neuromuscular synapse elimination was developed to serve as an analytical tool in exploring the potential roles of candidate mechanisms in regulating the normal process and in shaping its response to experimental perturbations. Synapse elimination is a complex process likely to involve the dynamic interaction of several specific mechanisms. This situation limits the reliability of a strictly inductive theoretical investigation into how these mechanisms might act. Three mechanisms which have been previously proposed and discussed in the literature are simulated, including a synaptic stabilization molecule, a muscle derived trophic factor, and a hypothesized intrinsic tendency of motor neurons to limit their arbor. The model is stochastic rather than deterministic in character, and is also dynamic, tracing the growth and retraction of individual presynaptic terminals at each iteration as they compete for limited synaptic space.

Nine experimental observations were selected to guide development of the model and evaluate its performance. All but one of the experimental observations can be simulated by at least one of the mechanisms studied. No single mechanism, however, is adequate to duplicate the entire body of experimental evidence. A relative advantage for larger terminals appears critical for convergence in both the scaffolding and trophic factor mechanisms. Several alternative roles for activity are compared.

TABLE OF CONTENTS

Chapter 1

GENERAL INTRODUCTION: THE DEVELOPMENT OF SPECIFICITY IN THE PERIPHERAL MOTOR SYSTEM

INTRODUCTION

The mammalian nervous system is exceedingly intricate and complex. Precise connections are required to support coordinated and purposeful behavior. A fundamental goal in the study of the nervous system is to achieve a clear understanding of the events and processes by which this precise cellular connectivity arises during development. Beyond the intellectual challenge, the issue is a practical one with obvious therapeutic implications. Grasping developmental strategies should also provide important clues to how the completed assemblage functions.

The formation and organization of so complex a system involves many distinct activities. Cellular proliferation and its regulation, differentiation and commitment, and cellular migration are processes which define neural populations and their spatial relationships during embryonic development. Guidance and pathfinding functions during axonal outgrowth are crucial in assuring appropriate patterns of projection. Once axons reach their target tissue, a process of mutual recognition is essential for axons to form synaptic connections at the appropriate locations with the correct target cells. Equally important is the development of appropriate cellular morphology, to encourage the proper number and relative positioning of synaptic inputs.

The peripheral motor system offers an accessible system for the study of these important developmental processes. The mature organization of spinal motor pools focuses attention upon the mitotic and migratory processes which may produce these functional groupings (Hollyday and Hamburger, 1977). Muscle fibers develop independently from somitic precursors (Chevallier *et al.*, 1977; Shellswell, 1977), although the final number of fibers in a muscle is neurogenically regulated (Betz *et al.*, 1980; Ross *et al.*, 1987). Motor axons follow highly stereotyped pathways to

find and innervate their appropriate target muscles (Landmesser, 1984). Within a muscle, the projection may be ordered topographically (Hardman and Brown, 1985) and according to muscle fiber contractile type (Thompson *et al.*, 1984).

Operating together with these active, expansionary processes are two apparently regressive events, naturally occurring cell death, and an episode of synaptic remodeling generally referred to as synapse elimination. While seemingly wasteful of developmental energy or resources, each may play an essential role in assuring functional integrity. Occurring during the early phase of interactions between afferent neurons and their targets, cell death is a widespread phenomenon apparently affecting all aspects of the central and peripheral nervous systems (Cowan *et al.*, 1984). Unlike the programmed cell death common in simple invertebrates (Sulston and Horvitz, 1977), the mammalian version of the process is not lineage dependent, acting upon specifically identifiable cells, but rather affects neuronal populations, albeit in a repeatable and predictable fashion. Two potential roles for cell death have been suggested: error correction and numerical matching. While cell death has been shown to selectively remove incorrectly projecting ganglion cells from the rat retina (O'Leary *et al.*, 1986), aberrant pathfinding is very rare in the peripheral motor system (Lance-Jones and Landmesser, 1981a), so error correction is apparently unnecessary to achieve muscle specificity. Whether cell death refines the organization of the projection at an intramuscular scale, perhaps by contributing to the early formation of compartmentalized innervation (English and Weeks, 1984; Balice-Gordon and Thompson, 1988), is not known. Population matching appears to be a more significant consequence of cell death. Its function in achieving the appropriate numerical ratio between afferent and target neural populations (Hamburger, 1975; Katz and Lasek, 1978) has been clearly demonstrated in both the motor system (Lanser *et al.*, 1986) and the central nervous

system (Herrup and Sunter, 1987).

The second process, in which an initial hyperinnervation is followed by developmental elimination of the excessive synaptic connections, also occurs throughout the nervous system. In the neonatal cerebellum, Purkinje cells are initially innervated by climbing fibers originating from as many as five distinct olivary neurons, and then lose all but one of these inputs during subsequent development (Crepel *et al.*, 1976; Mariani and Changeux, 1981). Similar events have been documented in autonomic ganglia: in rat submandibular ganglion (Lichtman, 1977), hamster superior cervical ganglion (Lichtman and Purves, 1980), and rabbit ciliary ganglion (Johnson and Purves, 1981), there is a significant reduction during early maturation in the number of preganglionic axons innervating a particular cell, although the total number of synaptic boutons actually increase significantly during this period of cell growth (Purves and Lichtman, 1985). Intrahemispheric cortical projections passing through the corpus callosum are substantially reduced during early development through a process of axon collateral withdrawal (Innocenti, 1981; O'Leary *et al.*, 1981; Ivy and Killackey, 1982). The developmental restriction of the geniculo-cortical projection which gives rise to ocular dominance columns in visual cortex provides another well documented example of synaptic rearrangement in the central nervous system (LeVay *et al.*, 1978, 1980).

Synapse elimination is most accessible in the neuromuscular system, and hence it is here that it has been most thoroughly studied. The phenomenon is widespread, having been described in a number of mammalian species (Bagust *et al.*, 1973; Brown *et al.*, 1976; Bixby and Van Essen, 1979a; Fladby, 1987), as well as chicks (Bennett and Pettigrew, 1974) and amphibians (Letinsky, 1974; Bennett and Pettigrew, 1975). During the interval of neuromuscular synaptogenesis which occurs in late embryonic development, muscle fibers readily accept innervation

well in excess of the normal adult complement of one presynaptic motor axon per muscle fiber. A corollary of this polyneuronal innervation is that the neonatal motor projection is considerably more divergent than that found in adults. Motor unit size, defined as the number of muscle fibers innervated by a single motor neuron, is typically three to six times the mature value. In the weeks that follow, excessive synaptic inputs gradually disappear, apparently through a process of axonal retraction (Riley, 1977a, 1981; Bixby, 1981). The fact that denervated muscle fibers are not observed in significant numbers demonstrates that the process is an orderly one, and that the loss of connections is not random. Experimental perturbations, such as partial denervation (Brown *et al.*, 1976; Thompson and Jansen, 1977) or partial activity blocks (Callaway *et al.*, 1987) further suggest that the process is competitive, at least in the sense that the behavior of a presynaptic terminal depends upon the presence and relative status of other terminals at the endplate. Cell death among motor neurons takes place before birth (Oppenheim, 1986), when neuromuscular connections are first forming, whereas the bulk of synapse elimination occurs neonatally (Bixby and Van Essen, 1979a). Hence the timing of cell death and synapse elimination are distinct in the neuromuscular system (Brown *et al.*, 1976; Dennis *et al.*, 1981; but see Bennett *et al.*, 1983), so that cell death does not contribute to synapse loss in any meaningful way.

The developmental rationale underlying this phenomenon remains unclear. One possibility is that the excess innervation is necessary to establish full connectivity; specifically, in the neuromuscular case, to ensure that each muscle fiber receives at least one input. The observed levels of polyinnervation are in fact adequate to guarantee that virtually all muscle fibers will be innervated under the assumption that initial synapse formation in a muscle is completely random (Willshaw, 1981). Error correction is another possible motive, although excepting a certain degree

of topographic sharpening (Brown and Booth, 1983; Bennett and Lavidis, 1984a; Callaway *et al.*, 1987; Bennett and Ho, 1988), there is little evidence from the neuromuscular system to support this view. Early hyperinnervation may allow for developmental plasticity, in which the adult pattern of connectivity emerges based upon early activity or other expressions of developmental requirements. It has been suggested, for example (Callaway *et al.*, 1987), that synapse elimination may help establish the recruitment ordering of motor units found in mature muscles (Henneman and Olson, 1965; Zajac and Faden, 1985). Alternatively, the processes of neuronal outgrowth, arborization, and synapse formation may require a degree of neuronal vigor so great that a substantial degree of polyinnervation is inevitable. Beyond offering a logic for the phenomenon, elucidating the mechanisms of the competitive interactions of motor nerve terminals at muscle endplates might contribute to understanding the strategies employed by the nervous system to establish the appropriate pattern of connectivity during development. A portion of the research described in this thesis (Chapter 4) compares the ability of several proposed mechanisms to account for several of the experimental findings which currently describe the synapse elimination process.

The remainder of this thesis (Chapters 2 and 3) presents research relating to fiber type selectivity in early motor unit development. The mammalian soleus muscle provides an interesting opportunity to study the origin of neuromuscular specificity during neonatal synaptic development. Although maturing to become a predominantly slow contracting muscle, the soleus exhibits a mixed composition during early postnatal development, containing substantial numbers of both fast contracting and slow contracting twitch fibers. These two fiber types are also distinguishable based upon metabolic enzyme histochemistry (Burke *et al.*, 1973), actomyosin ATPase activity (Stein and Padykula, 1962; Guth and Samaha, 1969),

and the presence of immunologically distinct contractile protein isoforms (Butler-Browne and Whalen, 1984).

Two complementary experiments have recently demonstrated that the innervation of these two fiber types is distinctly non-random, even at early postnatal ages when a substantial degree of polyinnervation is present. Using the glycogen depletion technique to label most of the fibers belonging to single motor units, Thompson *et al.* (1984) established that motor units in polyinnervated muscle are each composed predominantly, but not exclusively, of a single fiber type. An independent approach has yielded a similar conclusion: By stimulating isolated single motor units and recording the time required to achieve maximal twitch tension, Gordon and Van Essen (1985) demonstrated two clearly separable populations of fast contracting and slow contracting units, again indicating that single motor units are largely homogeneous in their fiber type composition. These findings also suggest, but do not prove, that distinct fast and slow motor axons are present at birth. It should be noted that Jones *et al.* (1987), in a study of fiber type specificity in the fourth deep lumbrical muscle of the neonatal rat, found only small variations from random fiber type composition. Five of twelve units appeared marginally selective; the remainder were randomly innervated. The lumbrical muscle is not an ideal choice for a study of selectivity, however. The fiber count in this muscle is relatively low at birth, and secondary myotubes continue to form in parallel with synapse elimination (Betz *et al.*, 1979). It is a small, predominantly fast muscle innervated by few (about 10) motor axons, and hence a simple numerical dominance of fast motor axons could effectively prevent selective innervation. Because of its fiber type balance, the soleus is a more appropriate candidate for study. The case for specificity in this muscle is a strong one, based upon two independent measures of motor unit fiber type composition.

Several developmental mechanisms have been proposed to account for this early fiber type specificity. Motor neurons could innervate undifferentiated muscle fibers at random and subsequently specify their fiber type. Alternatively, an early wave of selective synapse elimination, representing a form of error correction, could occur following an initially random innervation. Developmental timing differences in the early maturation of fast and slow muscle fibers might passively yield fiber type specificity. Or ingrowing axons might recognize muscle fiber types according to the presence of specific chemical markers and selectively innervate those of the corresponding type. These alternatives will be discussed at greater length in a subsequent section.

The remainder of this chapter will analyze the development of peripheral motor specificity in more detail. For specific recognition to be a viable route to achieving fiber type selectivity, it is essential that myotubes express some type specific characteristics prior to innervation. The next section addresses this issue by considering the timing and neural dependence of muscle fiber differentiation. The third section compares the development of specificity at three distinct levels: the matching of motor axons to correct target muscles, topographic relationships between spinal motor pools and intramuscular motor unit localization, and selective innervation of muscle fiber types. It is interesting to consider whether all three matching processes utilize similar strategies, or whether independent mechanisms are required. Based upon this background, the final section introduces the studies described in this thesis.

THE ORIGIN OF FIBER TYPE DIVERSITY

In a mature animal, all muscle fibers of a single motor unit share the same metabolic and contractile properties (Edstrom and Kugelberg, 1968; Burke *et al.*, 1973; Kugelberg, 1973; Nemeth *et al.*, 1981). This pattern suggests an instructive role for the motor neuron, and indeed there is considerable evidence that a motor neuron regulates the phenotype of the muscle fibers which it innervates. Cross reinnervation experiments demonstrate that when a nerve which normally innervates a fast muscle, such as the extensor digitorum longus (EDL), is severed and positioned so that it reinnervates a slow muscle such as the soleus (or vice versa), the reinnervated muscle is altered so that both its contractile rate (Buller *et al.*, 1960) and histochemical properties (Buller *et al.*, 1969; Barany and Close, 1971; Mommaerts *et al.*, 1977) match its new nerve supply. A similar neuron directed conversion of muscle fiber type can be recognized in self reinnervated muscle (Kugelberg *et al.*, 1970). Artificial nerve stimulation using implanted electrodes has identified the pattern of neural activity as the critical parameter in fiber type regulation (Salmons and Vrbová, 1969; Sréter *et al.*, 1973; Salmons and Sréter, 1976; Pette *et al.*, 1976), and in fact the direct activation of denervated muscle using an appropriate stimulus pattern is sufficient to elicit fiber type transformation (Lømo *et al.*, 1974).

Innervation also influences muscle development in neonates. Secondary myotubes, which normally form as satellites of primary myofibers, fail to appear in the absence of functional innervation (Harris, 1981; McLennan, 1983; Ross *et al.*, 1987). Transection of the rat sciatic nerve soon after birth inhibits the growth and differentiation of muscle fibers in denervated muscles (Shafiq *et al.*, 1972; Dhoot and Perry, 1983). Although subject to atrophy following denervation, fast

muscle fibers progress through a normal sequence of contractile protein expression, whereas postnatal maturation of slow contracting fibers appears to be innervation dependent (Rubinstein and Kelly, 1978; Butler-Browne *et al.*, 1982; Butler-Browne and Whalen, 1984).

Does this instructive role for motor neurons apply to the earliest stages of muscle fiber differentiation, when muscle fibers first express their contractile identity, or do muscle fibers establish their contractile phenotype according to an intrinsic developmental program? This question is particularly relevant when considering the origin of the selective innervation of muscle fiber types: information about the timing and regulation of phenotypic development can provide a sharper focus to the analysis of how specific innervation arises, and whether chemospecific recognition is a viable possibility. Motor unit type homogeneity could result from neurogenic regulation of muscle fiber type, or from the specific matching of motor neurons and muscles fibers, each of which have become committed to a particular developmental program. In the event of neurogenic regulation, the most plausible scenario features the random innervation of undifferentiated muscle fibers, although it is conceivable that neurons might specifically recognize markers unrelated to fiber type, or that fiber type differences might exist but not affect synaptogenesis. If selective association of neurons and muscle fibers is the rule, then this process could involve active recognition mediated by molecular markers, or could be governed by some passive process, such as matched developmental timing. Evidence favoring autonomous contractile development of muscle fibers supports the feasibility of specific recognition in that differentiated targets are potentially available for selective recognition. The absence of detectable early contractile commitment does not preclude molecular recognition, as it could still be mediated by markers expressed in advance of the type specific array of intracellular proteins.

Nevertheless, it seems reasonable to expect that the two phenotypic characteristics would be coordinately expressed.

Experimental evidence regarding fiber type differentiation is most complete for the chick. Muscle colony forming cells cultured from the early chick limb bud form at least two distinct populations based on the time at which they first appear, their culture requirements, and the morphology of myotubes which subsequently form (White *et al.*, 1975). Cloned myoblasts retain their identity by these criteria through many generations (Rutz and Hauschka, 1982). Early and late myoblasts also exhibit differential expression of myosin light chain isoforms (Toutant *et al.*, 1984). Myogenic precursors migrate into the developing limb bud from their source in the somitic mesoderm (Chevallier *et al.*, 1977; Jacob *et al.*, 1979). By transplanting limb buds at various stages, Seed and Hauschka (1984) demonstrated that precursors to the two populations enter the wing buds at different stages of maturation. Based on their developmental timing, it would appear likely that these two populations contribute selectively to the formation of primary and secondary myotubes.

Immunocytochemical labeling using antibodies specific to fast and slow myosin heavy chain isoforms has shown that cultured early stage myoblasts give rise to three distinct classes of myotubes: fast, fast/slow, and slow (Miller *et al.*, 1985). Using these antibodies, each of the three classes is found among primary myofibers in embryonic chick limb in a pattern which remains consistent during early development (Crow and Stockdale, 1986; Miller and Stockdale, 1986a). Clonal analysis in culture demonstrates that the early myoblasts themselves comprise three distinct populations, each of which reliably and exclusively gives rise to one of the three classes of myotubes (Miller and Stockdale, 1986b). In these experiments, multiple types of myotubes were never seen together in a single clonal culture.

Late stage myoblasts primarily form myotubes of the fast class, although fast/slow myotubes also occur infrequently (Miller *et al.*, 1985). Serial subcloning reveals that fast myoblasts occasionally undergo further differentiation to yield a fast/slow lineage (Schaefer *et al.*, 1987). Taken together, these studies demonstrate that myoblasts sharing a common lineage selectively fuse to produce myotubes of a particular type, thereby establishing a stable pattern of fiber types in the developing chick limb. The fact that this process also occurs in culture in the absence of neurons is strong evidence that the contractile identity of muscle fibers follows from an intrinsic developmental program which does not require neural supervision (Stockdale and Miller, 1987).

Further evidence that muscle fiber contractile development in the chick is initially independent of neural influences arises from experiments in which innervation is either removed, or its pattern altered, during early development. Excision of an appropriate region of the neural tube prior to axon outgrowth yields wing buds which are totally devoid of innervation (Butler *et al.*, 1982). While secondary myotubes do not appear, primary myofibers develop normally for the first few days in these aneurogenic wings, and display the same pattern of fiber type expression according to ATPase histochemistry as do control limbs (Butler *et al.*, 1982; Phillips and Bennett, 1984). Laing and Lamb (1983) transplanted wing buds to an ectopic position near the hindlimb, causing them to receive innervation from a novel set of motor neurons. Subsequent ATPase staining revealed a normal pattern of fiber types in the ulnimetacarpalis dorsalis muscle of the wrist. In similar experiments, Vogel and Landmesser (1987) altered the pattern of chick hindlimb innervation using both hindlimb shifts and spinal cord reversals. Aberrant innervation was verified by EMG recording of muscle activation patterns and by retrograde labeling of spinal motor pools using HRP. In 85% of muscles analyzed,

the spatial distribution of fiber types defined by ATPase activity appeared normal. These findings suggest that muscle fiber type develops intrinsically, and that either these fiber types were selectively innervated or neural activity differences had not yet produced fiber type transitions. In the remaining 15% of cases in the latter study, alterations of the normal pattern were seen. These indicate that fiber type respecification was possible during the experimental interval, but their relatively low frequence of occurrence is consistent with inappropriate innervation arising only when there was a gross numerical mismatch between neural and muscle fiber types (Vogel and Landmesser, 1987).

While less information is available regarding the initial phases of fiber type differentiation in mammalian skeletal muscle, there are indications that it may occur prior to functional innervation. Little concrete information regarding early type expression has emerged from tissue culture studies. Ecob and Whalen (1986) have studied the appearance of myosin heavy chain isozymes among newly formed myotubes which arise from satellite cells present when adult muscle fibers are introduced into culture. In the context of the chick culture studies, these mature cells would be expected to yield fast myotubes. While embryonic and neonatal heavy chains were always found, the appearance of adult fast myosin required the presence of spinal explants. In contrast, Weydert *et al.* (1987) observed the expression of adult myosin mRNA in maturing myotubes arising from cultured myogenic cell lines in the absence of nerve, although no information is available concerning whether the resulting protein is of the fast or slow type. Clearly such data is extremely sketchy in regard to the present issue.

In vivo, primary myotubes exhibit a pronounced preference to mature as slow fibers, while secondary myotubes initially adopt the fast pathway (Rubinstein and Kelly, 1981). Using an antibody specific to myosin heavy chain, Narusawa *et al.*

(1987) have demonstrated that slow myosin accumulates in all primary myofibers in the hindlimb of 16 day rat fetuses, an age at which synaptic connections are still forming (Rubinstein and Kelly, 1981). Expression of slow myosin is then inhibited in those primary cells which diverge to a fast developmental pathway. Neonatal denervation led to a decrease in slow myosin, suggesting that innervation is required to maintain or protect the maturation of slow fibers. In a similar study, Dhoot (1986) was able to distinguish between presumptive fast and slow fibers within predominantly fast muscles at 17 days gestation, using a slow type specific antibody. In this study, fiber type differentiation in the soleus muscle did not become apparent until about 4 days postnatal. While secondary myofibers will not form if primary muscle fibers are not innervated (Harris, 1981; Ross *et al.*, 1987), subsequent denervation does not prevent fast fibers from continuing their normal developmental sequence of myosin isozyme expression (Butler-Browne *et al.*, 1982). This does not conclusively establish, however, that secondary myotubes express a recognizable type identity prior to innervation.

The fact that primary and secondary myotubes are connected by gap junctions during early development (Schmalbruch, 1982) has implications for the early development of muscle fiber type. Even if the activity patterns of embryonic motor neurons are differentiated into tonic and phasic forms, it would seem that the spread of activity between fibers in a cluster would expose individual fibers to an ambiguous pattern of activation. A further interesting consideration is that individual motor terminals are occasionally observed to form dual synapses with both a primary and secondary myotube (Duxson *et al.*, 1986), suggesting that at least some of the innervation of secondary myotubes may develop by a transfer of existing terminals. The implications of this observation for either fiber type differentiation or the formation of specific innervation remain unclear.

DEVELOPMENT OF SPECIFIC INNERVATION

An organized, accurate pattern of neural connections within the motor system is essential for the precise execution of complex and coordinated behaviors. Specificity is present at several loci within the system. In the spinal cord, both descending and afferent sensory inputs must be correctly organized. Motor axons originating from reproducibly positioned longitudinal pools within the spinal cord follow consistent neural pathways to innervate appropriate muscles. Within individual muscles, fiber type selectivity is prevalent, and motor units are at least occasionally organized topographically. While most of the experiments described in this thesis relate to the organization of motor units according to muscle fiber type, it is interesting and worthwhile to examine and compare the development of specificity at various points within the system, searching both for common principles and distinctive features.

Innervation of Appropriate Muscles

Considerable research attention has been devoted to understanding the sequence of events through which motor specificity arises. Much of this work has been performed in chick, both because of the relative accessibility of this preparation for embryonic surgical manipulations and the extensive description of its early development (Hamburger and Hamilton, 1951). The earliest motor axons emerge from the spinal column while the generation of motor neurons is still in progress (Hollyday and Hamburger, 1977). Axonal pathways into the developing limb appear to be permissively regulated by the limb itself, as these define a highly stereotyped pattern of plexuses and nerve trunks even in supernumerary limbs innervated by axons from unusual spinal segments (Hamburger, 1939; Morris, 1978). By the time that growing axons have reached their targets, neurons innervating a particular muscle are organized into longitudinal motor pools (Landmesser, 1978a). During

early axonal outgrowth, the developing limb bud consists largely of undifferentiated mesenchyme cells, although cells of precartilage and premuscle regions can be distinguished ultrastructually based on their cell-cell contacts (Hilfer *et al.*, 1973; Tosney and Landmesser, 1985a). Differentiation and fusion of myogenic cells soon define the dorsal and ventral primary muscle masses. Motor neuron pools located medially in the spinal cord grow into the ventral muscle mass, while those from lateral pools innervate muscles deriving from the dorsal muscle mass (Landmesser, 1978a; Hollyday, 1980).

When considering the process by which motor axons find and establish connections with the appropriate muscle, an early question to arise is whether specificity follows from precise and ordered outgrowth, or whether an initially less accurate projection is refined by an error correction process. One experimental approach to this issue has been to retrogradely label motor axons projecting to a limited region in a developing limb. In this procedure, horseradish peroxidase (HRP) is injected locally into a region of the premuscle mass believed to give rise to a particular muscle, and the positions of labeled motor neurons in the spinal cord are subsequently analyzed. HRP labeled motor neurons found beyond the boundaries of the relevant motor pool are presumed to have projected incorrectly. Experiments of this nature in amphibian hind limb (Lamb, 1976, 1977; McGrath and Bennett, 1979) and chick wing (Pettigrew *et al.*, 1979) indicated a significant fraction of initial projections to be in error. In contrast to these reports, other studies in chick hindlimb, involving both retrograde HRP labeling (Landmesser, 1978a,b) and the electrophysiological association of muscle nerves and spinal nerves (Landmesser and Morris, 1975), suggested that motor projections are remarkably specific and free of errors from the earliest stages analyzed. Retrograde labeling studies in early embryos are unfortunately clouded by a technical complication,

namely that it is difficult to completely rule out the possibility that HRP may have leaked or diffused into other regions of the uncleaved muscle mass.

More recent experiments have used superior labeling strategies to describe the accuracy of axonal outgrowth. The injection of HRP into embryonic chick spinal cord permits the positions of axons labeled by orthograde transport to be assessed at intermediate times during their outgrowth, before they actually reach their target tissue. Using this technique, Lance-Jones and Landmesser (1981a) found that axons from any of the lumbar spinal roots followed consistent pathways through the plexus region and along major nerve tracts into the growing hindlimb. Furthermore, they saw virtually no significant deviations from these normal pathways, arguing that not only do axons rarely grow to an incorrect muscle, but in fact seldom make inappropriate choices at nerve branch points. It remained possible that axons might reach their target muscle by correct routes and then ramify across future boundaries, thereby accounting for errors detected by retrograde transport. Tosney and Landmesser (1985b) analyzed this possibility by observing the projections of segmentally labeled axons between their time of entry into the primary muscle masses and the completion of muscle cleavage. They found that early projections were spatially restricted to the central portion of the appropriate target region, and did not begin to fully invade the muscle until cleavage had occurred.

Another technique with great promise involves the injection of dextran, conjugated with a fluorescent dye, directly into individual cells. This method has been used to follow the actual outgrowth of pioneer motor axons in zebrafish embryos. As these embryos are conveniently transparent, the pathway selection process employed by growing axons can be observed over time by using enhanced video imaging (Eisen *et al.*, 1986). Preliminary studies have shown that pioneering axons consistently select the appropriate pathway, avoiding even transient errors

(Westerfield and Eisen, 1988). Whether differences in the timing of outgrowth control the pathway selections made by these pioneering axons requires additional study. On balance, current evidence would appear to refute the conjecture that error correction plays a major role in establishing the mature pattern of motor innervation.

If directed neural outgrowth along consistent, predictable pathways is an established feature of embryonic limb development, then what factors are dominant in axonal pathfinding? The fact that spinal motor pools are organized in a manner bearing loose topographic similarity to the arrangement of limb musculature has led to the hypothesis that an ordered outgrowth of motor axons, together with mechanical constraints and contact guidance, is sufficient to produce myospecificity in the developing limb (Horder, 1978). Evidence against this proposal arises from a study in which lengths of the neural tube were deleted just prior to generation of motor neurons (Lance-Jones and Landmesser, 1980a). As missing segments did not regenerate, distinct gaps were apparent in the spinal cord after further development. Orthograde labeling of adjacent remaining segments revealed that these projected in a normal fashion rather than altering their course to occupy depleted or absent nerve trunks. Electrophysiological analysis further showed that muscles normally innervated by the missing segments did not receive compensatory innervation from remaining motor pools. Retrograde labeling studies provide additional evidence of active guidance. Motor axons bound for a particular muscle are scattered more or less randomly through multiple spinal nerves as they emerge from the spinal cord, but then collect to form discrete bundles as they pass through the plexus (Lance-Jones and Landmesser, 1981a; Tosney and Landmesser, 1985b).

The process of axonal reorganization within the plexus is further demonstrated by studies in which the relationship of the spinal cord and the limb have been

experimentally altered. When sections of the lumbrosacral spinal cord were rotated prior to axonal outgrowth, motor neurons were able to find and innervate their original target muscles despite their new spinal roots of origin, provided that the positional shifts were small enough so that they entered the same plexus (Lance-Jones and Landmesser, 1980b, 1981b). Similarly, following dorsal-ventral rotations of limb buds, motor axons regrouped within the plexus and innervated the appropriate hindlimb muscles despite their new orientation relative to the spinal cord (Ferguson, 1983). In contrast, Summerbell and Stirling (1981) reported that following either dorsal-ventral or anterior-posterior rotations (the latter accomplished by switching left and right limb buds), the dorsal-ventral selectivity of motor neurons was usually although not always lost. Their result has since been attributed to inconsistencies in the level at which donor limb buds were grafted, so that correctly oriented tissue was not always present in the plexus region (Hollyday, 1981). This proposed reconciliation of apparently divergent observations was supported by experiments in which the level of grafting was more carefully controlled: grafting of limb buds distal to the plexus produced dorsal-ventral errors in connectivity beyond the graft (Whitelaw and Hollyday, 1983c). Finally, Tosney and Landmesser (1984) have demonstrated the normal sorting of motor axons in the plexus even after the surgical ablation of more distal tissue.

The topographic relationship between mediolateral position of spinal motor pools and the ventral or dorsal origin of the their target muscles, together with the coalescence of axon families in the plexus regions, provide compelling evidence for molecular labeling of related sets of motor neurons. Studies of both normal and perturbed development strongly suggest that this identifying information governs the sorting of axons into appropriate groupings during early outgrowth. But what about the latter stages of outgrowth, and invasion of the target muscle: Do processes

such as timing and passive guidance suffice to lead ordered groups of axons to their targets, or does molecular recognition, involving either nerve branch points or the target muscles themselves, play any role?

Unfortunately, the experimental evidence does not provide a clear answer. The behavior of motor axons in serial limb segment duplications argues against the presence of specific chemical markers. In these experiments, a second (donor) limb bud is grafted distally onto the tip of the host bud, leading to repeated limb segments. In the normal wing, for example, the inferior brachialis longus nerve separates into three branches at the elbow. One of the branches, the median nerve, continues on to innervate the hand. By constructing wings containing two elbows, Lewis (1978) was able to test the behavior of the median nerve when it encountered the second elbow. If the constituent axons responded solely to specific chemical cues, they should all repeat the choice made at the first elbow. Instead, the nerve again separated into three distinct branches, a behavior more consistent with either mechanical guidance or a gradient of directional markers. In serial hindlimb segment duplications, Whitelaw and Hollyday (1983b) found that the proximal pathway which a nerve trunk followed in the plexus region seemed to confer segmental selectivity. Thus those nerves issuing from the sciatic plexus which normally innervate muscles in the calf would instead innervate a second thigh were this the second segment encountered, even though a calf segment was available distally.

Other observations are more suggestive of the possible presence of molecular markers. At the growing tip of advancing nerve bundles, growth cones viewed in silver stained whole mounts diverge somewhat, as if exploring the local territory (Al-Ghaith and Lewis, 1982). This "frayed" character appears more pronounced in regions where branching occurs. A quantitative analysis of growth cone trajectory

(Tosney and Landmesser, 1985c) indicated substantially greater complexity in regions where pathway decisions occur. At the branches of muscle nerves, axons do not diverge as an orderly group; rather, axons exiting toward the muscle cross over others which choose to continue along the trunk (Tosney and Landmesser, 1985b). Ultrastructural examination of advancing growth cones reveals no preference for extracellular matrix or other oriented substrata which might be expected from a passive guidance model (Al-Ghaith and Lewis, 1982; Tosney and Landmesser, 1985a).

While the experiments described above suggest a role for selective markers during axonal outgrowth, they provide little if any direct evidence that molecular labels are present on muscle fibers and contribute in a meaningful way to target recognition. While these experiments offer interesting and informative pathway choices to growing motor neurons, it is difficult to design an experiment in which motor axons are offered an equal choice between an appropriate and inappropriate target muscle. An alternate paradigm, in which correct and incorrect motor axons are forced to compete for synaptic sites within individual muscles, is more practical. A situation resembling this paradigm occurs in experiments in which a chick hindlimb segment has been selectively deleted prior to axon outgrowth (Whitelaw and Hollyday, 1983a). When either a thigh or a calf segment is missing, axons destined for both segments are effectively restrained to innervate only the remaining one. While both sets of axons reach the available segment and can be retrogradely labeled with HRP, cell death results in the selective depletion of motor pools supplying the inappropriate axons. Unfortunately, although inappropriate axons are observed adjacent to potential target muscle, the result does not conclusively demonstrate that the unsuccessful axons were losers in a direct synaptic competition. The effective phase of the competition may have occurred earlier,

involving the pathway guidance cues which appear so likely to be present.

More commonly, competition between native and foreign axons has been studied in reinnervation experiments. In contrast to the selectivity exhibited by lower vertebrates (Bennett and Raftos, 1977; Dennis and Yip, 1978; Wigston and Kennedy, 1987), mammalian muscle appears to be equally receptive to reinnervation by either native or foreign motor axons. Weiss and Hoag (1946) cut the peroneal and tibial nerves in rat hindlimb, then arranged for the proximal stumps of these two nerves to regenerate through a 'Y'-shaped artery segment and converge upon the distal stump of the tibial nerve. Following reinnervation, the original and foreign nerves were stimulated, and tension generated by the triceps surae recorded. On average, there was no significant difference in the tension measurements. There were, however, substantial differences for individual animals, and the experiment has since been criticized on the grounds that whichever nerve reached the 'Y' first may have effectively limited the access of the other nerve. Gerding *et al.* (1977) performed a similar experiment by implanting the proximal ends of the transected tibial and peroneal nerves into the denervated lateral gastrocnemius muscle. As long as both nerves were allowed equal access to endplate regions, no preference during reinnervation was detected. In a related experiment, Bixby and Van Essen (1979b) positioned a transected foreign nerve on the surface of a fully innervated rat soleus muscle and observed that foreign axons were occasionally able to displace the native innervation.

While competitive reinnervation experiments in intact limb muscles have failed to detect molecular recognition of specific muscles, Wigston and Sanes (1982) have conducted a similar experiment which appears to reveal at least weak positional labeling. They transplanted external intercostal muscles from various levels into the neck, then positioned the severed cervical sympathetic trunk onto the

muscle, thereby allowing cholinergic preganglionic axons originating from different spinal segments to compete for synaptic sites. Subsequent stimulation of ventral roots demonstrated a moderate yet significant competitive advantage for axons originating from or near the segment giving rise to the transplanted intercostal, suggesting that both muscles and nerves may carry labels indicating their segment of origin. Studies using chick-quail chimeras have shown that precursors from individual somites contribute only to certain limb muscles (Beresford, 1983), and that furthermore, the spinal position of motor neurons closely matches the somitic origin of the muscles they innervate (Lance-Jones, 1985). All of these observations lend credence to the idea that recognition of segmental labels may be important in establishing specific muscular innervation.

Alternatively, segmental recognition could play a role in axon navigation: a trail of labeled extracellular matrix or premuscle cells deposited by muscle precursors during their migration into the developing limb might provide the cues necessary for motor neurons to make appropriate choices in the plexus and at other decision regions (Keynes and Stern, 1985). Interestingly, while discounting the role of extracellular matrix, Tosney and Landmesser (1985a) observed a cellular contact unique to pioneering axons in which filipodial processes of growth cones would occasionally penetrate deeply into mesenchymal cells, reminiscent of the contact between pioneering axons and guidepost cells in invertebrates (Bastiani and Goodman, 1984). To investigate this possibility, Keynes *et al.* (1987) first grafted quail somites into chick embryos, altering their positions along the anterior-posterior axis, and found that muscle precursors migrated according to their new position. Next, they performed shifts and reversals of somitic mesoderm in chick embryos and analyzed the subsequent positions of motor neuron pools. If pathfinding growth cones followed segmentally identified trails, they should pursue transplanted muscle

precursors to a new and ectopic position in the limb. The fact that motor pools were instead found in their normal positions despite the altered segmental origin of their target muscle argues that segmental labeling, while it may be present, is not crucial to axon guidance. Relevant to this issue is the earlier finding by Lewis *et al.* (1981) that normal branching of nerve trunks occurs in limbs which lack muscles due to early somite ablation. Muscle nerves, however, do not form in limbs lacking muscles.

Topographic Innervation of Individual Muscles

Given the organization of motor pools within the spinal column and the widespread occurrence of topographic projections in the central nervous system, it is of interest to determine whether individual motor units are spatially localized to limited regions within a muscle, and if so, whether there may be any topographic structure relating a motor neuron's position in its motor pool to the intramuscular location of the fibers it innervates. In various two dimensional sheet-like muscles, including cat diaphragm (Duron *et al.*, 1979), rat intercostal (Dennis *et al.*, 1981) and rat gluteus (Brown and Booth, 1983), it has been possible to roughly identify the boundaries of individual motor units as they contract following stimulation of single motor axons. In each case, motor units were observed to occupy specific subregions within the muscle rather than being spread uniformly throughout. Furthermore, because of the longitudinally elongate character of spinal motor pools, axons innervating mammalian skeletal muscle generally emerge from the cord through more than one ventral root. In experiments where both the spinal root position of a motor axon and the intramuscular location of its motor unit have been recorded, a clear correlation between rostrocaudal position of a motor neuron and the anterior-posterior location of its motor unit has been demonstrated in thin

muscles (Duron *et al.*, 1979; Brown and Booth, 1983; Laskowski and Sanes, 1987a). These electrophysiological findings have been confirmed by retrograde transport of locally injected dyes (Hardman and Brown, 1985; Laskowski and Sanes, 1987a). Topography along another axis has been reported by Hardman and Brown (1985) based on retrograde labeling experiments in rat internal intercostal muscles. Fibers in these thin muscles are distributed along a proximo-distal axis, and the motor neurons supplying their innervation are arranged dorsoventrally within the motor pool such that more dorsal neurons control distally located units. When considered together with the fact, described previously, that medial pools innervate ventrally derived muscles while lateral pools innervate muscles originating from the dorsal premuscle mass, there is evidence for topographic organization, and hence possibly positional markers, along all three axis of the spinal cord (Hardman and Brown, 1985).

Whether topography is present in the innervation of thick non-sheetlike muscles is less clear. Based on visual observation of surface contractions of cat medial gastrocnemius, Swett *et al.* (1970) found evidence for an organized progression of motor unit position as ventral root filaments were stimulated sequentially along the rostrocaudal axis. Sampling surface fibers with an intracellular microelectrode, Bennett and Lavidis found a clear progression of segmental innervation across the rat lateral gastrocnemius (1984a) and biceps brachii (1984b). In contrast, Fladby (1987) was unable to detect similar topography in the innervation of mouse soleus muscle despite a careful search. Glycogen depletion labeling of motor units in rat soleus (Soileau *et al.*, 1988) indicates that fibers belonging to a single motor unit may be widely dispersed in thick muscles. It is relevant to note (Hardman and Brown, 1985) that in those three dimensional muscles where all fibers converge onto a single tendon, a topographic distribution of motor units would make little

difference, while for several of the sheet like muscles studied, spatial segregation of motor units could have practical functional significance.

How might a topographic relationship develop between neurons of a spinal motor pool and the intramuscular position of their target muscle fibers? In large sheet muscles like the diaphragm, the obvious pattern of intramuscular nerve trunks suggest the possibility that axon guidance might play a role, as it clearly does in establishing myospecificity. In some muscles, such as the lateral gastrocnemius and the extensor digitorum longus, primary nerve branches to the muscle are readily accessible. Glycogen depletion and recording of evoked EMG have been used to map the territory innervated by these primary branches. These techniques have revealed the existence of spatially distinct compartments within muscle, each innervated exclusively by axons carried by one of the primary nerve branches (English and Ledbetter, 1982; English and Weeks, 1984; Balice-Gordon and Thompson, 1988; Bennett and Ho, 1988). Such compartments could be significant elements in generating a topographic mapping. Weeks and English (1985) have demonstrated by retrograde HRP labeling that axons in a particular primary branch arise from motor neurons grouped within a restricted region of the motor pool. While the groups supplying different branches overlap, a clear topographic organization is present. Whether subcompartments defined by secondary intramuscular nerve branches also exist, or contribute to topography, remains unknown.

Factors other than branching may mediate the development of topographic innervation. The relative timing of axon ingrowth is a second parameter which might determine motor unit position. A third possibility involves chemospecific recognition: motor neurons which are somehow labeled according to their spinal position might selectively form synapses with muscle fibers bearing compatible labels. Hardman and Brown (1987) have approached this question through

reinnervation experiments in rat intercostal muscles. When muscle nerves were cut in animals aged 10 days postnatal, subsequent reinnervation closely approximated the topographic pattern observed in normal animals. The same procedure applied to animals aged 6–8 weeks, however, led to an apparently random reinnervation. Laskowski and Sanes (1987b) have reported topographically selective reinnervation of rat serratus anterior and diaphragm muscles in both neonates and adults, although selectivity was somewhat greater in younger animals. The finding of topographic reinnervation of younger muscles in each of these cases would appear to rule out timing as a mechanism. The discrepancy between these findings regarding the pattern of mature reinnervation leaves doubt concerning the fate of whatever markers might guide the initial formation of a topographic projection. A possible reconciliation of these differing results might involve two sets of markers: Signals mediating pathway selection at branch points may persist, while positional markers on muscle fibers themselves might disappear or become inaccessible. Differences in the primary branching patterns of the muscles studied could then account for the varying specificity of reinnervation.

Some investigators have reported that synapse elimination also plays a role in establishing topographic projections, although this claim remains controversial. In their study of the rat gluteus, Brown and Booth (1983) found that the topographic arrangement of motor units, while present in polyinnervated neonatal muscle, was considerably enhanced during the episode of synapse elimination. The spatial extent of individual motor units, defined visually, was reduced by about threefold. Fibers were not lost equally at both extremes of a motor unit. Instead, motor units near the edges of the muscle preferentially lost muscle fibers from their border nearest to the center of the muscle, and their midpoints shifted so as to sharpen the rostrocaudal mapping of motor neurons onto the anterior-posterior axis of the muscle. English

(1986) questions the conclusions of this study. Mapping the same muscle using evoked EMG, he finds a compartmentalized organization which remains unchanged during synapse elimination, although he cannot rule out topographic sharpening within compartments.

The surface topography described by Bennett and Lavidis (1984a,b) also developed during synapse elimination; in fact, in these cases, virtually no segmentally derived topographic organization was visible in polyinnervated neonatal muscles. These investigators also examined the fraction of whole muscle tension which could be elicited by stimulation of either of the two ventral roots supplying innervation, and found that the relative contribution measured in this way changed during synapse elimination. Observations of this nature, however, are difficult to interpret. Because the degree of overlap due to polyneuronal innervation may differ for the two roots, it is not safe to conclude that differential synapse loss has occurred. Hence the relation which such changes may bear to the development of topography are unclear. Detailed study of motor unit size in rat and rabbit soleus (Gordon and Van Essen, 1983; Thompson, 1983) have shown that actual synapse loss does not vary segmentally. Interestingly, Callaway *et al.* (1987, 1988) have demonstrated that motor neurons occupying extremal positions in the soleus motor pool in rabbits experience significantly greater synapse loss than those in the central regions of the pool. Whether this difference contributes to topography in the projection is not known. Another problem in analyzing the findings of Bennett and Lavidis (1984a) is that the relationship of their observations to the compartmental organization of the muscle was not considered. Studies in both the rat LG (Donahue and English, 1987) and EDL muscles (Balice-Gordon and Thompson, 1988) indicate that synapse elimination is not involved in the restriction of motor units to individual compartments. In a recent study, however, Bennett

and Ho (1988) report that synapse elimination contributes to the development of topography within an individual compartment.

Innervation of Muscle Fiber Types

As described earlier, all muscle fibers in an adult motor unit display a remarkable similarity in contractile and metabolic properties, probably reflecting neural regulation of these characteristics (Kugelberg, 1973; Nemeth *et al.*, 1981). There is a good deal of evidence indicating that this segregation of fiber types does not arise simply by neuronal specification of fiber type following random innervation. In the transversus abdominus, a one fiber thick muscle of the garter snake, fast twitch, slow twitch and tonic fibers are arrayed in a regular geometric pattern, yet each is incorporated in a motor unit containing exclusively fibers of its own type (Lichtman and Wilkinson, 1987). It is difficult to imagine how random innervation of an array of equally developed fibers could yield such a regular pattern. Similarly, the mosaic of fast and slow fibers in neonatal mammalian muscle does not appear to be a random spatial distribution, but rather to reflect the development of primary and secondary generation myotubes (Kelly and Rubinstein, 1980).

A second and more powerful line of evidence is that the fiber type composition of neonatal motor units in the soleus muscle is strongly biased toward one of the two fiber types, even while a substantial degree of polyinnervation is present in the muscle (Thompson *et al.*, 1984; Gordon and Van Essen, 1985). If fibers were innervated randomly, and then awaited instructions before differentiating, conflicting signals would be commonplace. Electrical coupling of embryonic muscle fibers (Dennis *et al.*, 1981; Schmalbruch, 1982) further complicates the problem of regulation. There remains doubt as to whether embryonic motor neurons exhibit differentiated activity patterns capable of driving fiber type differentiation

(Navarrete and Vrbová, 1983). Also, under experimental conditions, neuron directed fiber type conversion does not occur quickly enough to yield the observed motor unit differentiation.

Alternatively, it is possible that motor neurons randomly innervate muscle fibers without regard for their type, but that during the earliest phase of synapse elimination, occurring prior to ages examined in the studies cited above, inappropriate connections are preferentially lost. Error correction of this sort would presumably require some form of selective recognition and would define an interesting pathway to achieving specificity. This explanation, however, would require an extraordinarily high peak level of polyinnervation, considering the 3–6 fold polyinnervation present among slow motor units in rabbit soleus at an age when motor unit clearly exhibit distinct contractile properties (Gordon and Van Essen, 1985). Glycogen depletion labeling of a small number of motor units before and immediately following the peak observed episode of synapse elimination provides no evidence of a selective loss of inappropriate connections (Thompson *et al.*, 1984). More consistent with the available evidence is the hypothesis that two classes of motor neurons specifically innervate differentiated muscle fibers. The preceding section presented evidence that there is a substantial intrinsic component to the development of muscle fiber type, and that each fiber is in fact committed to the expression of a particular contractile type prior to synaptogenesis.

Two distinct mechanisms have been proposed to explain how specific connections are established during development. The first does not require active recognition of fiber type, but rather relies on timing differences in the developmental program of the two fiber types. As discussed in the previous section, primary myotubes preferentially develop into slow fibers, while secondary myotubes generally become fast fibers (Rubinstein and Kelly, 1981). Primary myotubes

mature first, and begin to receive innervation earlier than secondary myotubes (Kelly and Zacks, 1969). If slow motor axons began to branch and form synapses as soon as primary myofibers were competent to receive them, while fast motor axons experienced a delay in this process, each neuronal type might find the available target heavily biased toward muscle fibers of the appropriate type (Rubinstein and Kelly, 1981). While some inappropriate connections would likely form, such a passive sorting process could produce substantial specificity. The second possible mechanism is chemospecific recognition. Under this scheme, fast and slow motor axons would identify and select muscle fibers of the appropriate type based upon the presence of molecular markers. Recognition need not be of the lock and key variety; differences in adhesivity could suffice. Furthermore, selectivity need not be perfect: fibers of an inappropriate type make up 10–20% of polyinnervated neonatal motor units which have been labeled by glycogen depletion (Thompson *et al.*, 1984). It is noteworthy, however, that while chemospecific recognition has long been considered to account for specificity in various neural projections (Sperry, 1963), specific chemical markers which might mediate such recognition have not yet been identified.

Little information is available regarding the generation of fiber type specificity during the normal developmental process. Given the absence of a marker to differentiate between embryonic fast and slow motor axons, it is difficult to design an experiment to directly probe the role of timing in securing appropriate connections. An alternative approach is to search for evidence of selectivity following reinnervation. Selective reinnervation of twitch and tonic muscle fibers has been demonstrated in frog pyriformis muscle (Elizalde *et al.*, 1983). In an interesting variation of this experiment, Schmidt and Stefani (1976) crushed the sciatic nerve at a greater distance from the muscle. Fast conducting axons, which

normally innervate the twitch fibers, regenerated faster and reached the muscle first, innervating both twitch and tonic fibers and demonstrating that inappropriate innervation is not forbidden. As slow axons arrived, however, these displaced fast axons from tonic fibers, restoring the normal pattern of innervation.

In adult mammalian muscle, experimental evidence strongly suggests that reinnervation is not selective according to fiber type. Histochemical analysis of reinnervated muscles following either nerve crush or section and suture reveals the existence of "type groups," or clumps of fibers exhibiting similar ATPase and metabolic enzyme histochemistry (Karpati and Engel, 1968; Kugelberg *et al.*, 1970; Nemeth and Turk, 1984). This clustering of fiber types contrasts sharply with the normal mosaic arrangement, and is taken to reflect the failure of regenerating axons to selectively reinnervate fibers of the appropriate type. Glycogen depletion of reinnervated units under these conditions confirms that single units tend to observe the type group boundaries (Kugelberg *et al.*, 1970). It remains possible, however, that molecular markers which guide specific innervation during development disappear during maturation. Using glycogen depletion to label reinnervated motor units in neonatal rat soleus, Soileau *et al.* (1987) presented evidence of selective reinnervation of fiber types. Reinnervated units were generally less homogeneous in fiber type composition than normal motor units, and 2 of 12 actually exhibited a fiber mix which was consistent with random reinnervation. Nonetheless, the fiber type mix of each of the remaining 10 motor units analyzed was clearly biased toward one or the other type, and it is highly unlikely that such distributions could arise solely by chance. This result is consistent with the finding of Hardman and Brown (1987) that topographic reinnervation of intercostals, while not possible in adults, indeed occurs in young animals. These latter investigators, however, found evidence of type grouping following reinnervation, casting doubt

upon the presence of fiber type specificity in their experiment.

Summary

Specificity has been examined at three distinct loci in the peripheral motor system: the innervation of appropriate muscles, topographic organization of motor units within certain muscles, and selective innervation of muscle fiber types. During normal development, motor neurons grouped in stereotypically positioned motor pools send axons along predictable routes to consistently innervate the appropriate muscles, making few if any mistakes in the process. Pathway guidance appears to be the dominant factor. Axonal trajectories indicate that routing choices are concentrated in certain "decision regions," such as the plexus and nerve branch points. Molecular cues may influence routing decisions at these points. Neurons are capable of innervating inappropriate muscles following experimental manipulations. Apart from the suggestion of segmental markers, little evidence exists to indicate that motor axons actively recognize specific molecular labels identifying their target muscle. There is good evidence for the existence of topographic mappings from motor pools to fibers within two dimensional sheet-like muscles, and weaker evidence for similar topography in the projections to 3-D muscles. When topography is present, it may be closely related to the existence of compartments within the muscle. Because these compartments are defined by the territory innervated by each of the primary muscle nerve branches, it is possible that topography develops via a guidance mechanism similar to that which generates muscle specificity. Whether synapse elimination plays a role in defining intramuscular topography remains uncertain. Finally, evidence from neonatal animals strongly suggests that motor neurons selectively innervate muscle fibers of the appropriate contractile type.

Developmental timing has been suggested as an explanation for specificity

at all three levels. Limb manipulation experiments in the chick appear to rule out differences in the timing of outgrowth, coupled with passive guidance, as an adequate mechanism to explain the generation of muscular specificity. Similarly, reinnervation experiments suggest that timing does not play a central role in the generation of intramuscular topography. While some experimental evidence favors chemospecificity, the issue of whether timing is involved in generating fiber type specificity is not yet fully resolved.

THESIS EXPERIMENTS

Chapter 2 of this thesis addresses the potential role of chemospecificity in generating the fiber type selectivity observed in neonatal motor units. Reinnervation experiments, conducted soon after birth in a muscle composed of both fast and slow fibers in roughly equal proportion, provide a promising avenue to approach the origin of specificity in the innervation of muscle fiber types. If a form of chemospecific recognition is an essential component in establishing specific connections, then it is possible, although not inevitable, that appropriate connections would again be established during reinnervation. If an ordered developmental sequence, including timing differences in the maturation of fast and slow neurons or muscle fibers, is required to achieve specificity, then it is doubtful that such a pattern could be reestablished following axon regeneration.

The reinnervation study of Soileau *et al.* (1987) appears to provide strong evidence that selective connections reform, and that by inference, muscle fibers are labeled according to their type, allowing motor neurons to recognize and preferentially innervate the appropriate type. Why then is further study of this issue worthwhile? One problem inherent in the glycogen depletion approach was the need to wait for two weeks following reinnervation, to allow synapses to mature sufficiently to withstand the rigorous stimulation protocol required to succesfully deplete active fibers. During this interval, other processes could act to enhance the appearance of specificity. Polyneuronal reinnervation could be followed by selective synapse loss (Soileau *et al.*, 1987), or muscle fiber contractile types could be respecified according to the pattern of neural activity, although steps were taken to control for this latter possibility.

The experiments described in Chapter 2 provide an independent approach to

assessing fiber type selectivity during reinnervation. In the neonatal rabbit soleus muscle, the time required to achieve peak tension during the twitch contraction of an isolated motor unit is a reliable assay for motor unit type (Gordon and Van Essen, 1985). Unlike the situation in rat soleus, there is little overlap in the rise time distributions of fast and slow motor units. Comparing a histogram of twitch tension rise times for single motor units from reinnervated muscles to a histogram derived from control muscles revealed that there was little, if any, selectivity by fiber type during reinnervation at the ages studied. Reconciliation of this finding with the results of Soileau *et al.* (1987) is discussed in Chapter 2.

The first of two experiments presented in Chapter 3 compares the timing of the later stages of synapse elimination from the endplates of fast and slow muscle fibers. Because most muscle fibers belong to motor units of the same contractile type, this study can also be regarded as addressing the relative timing of synapse elimination for fast and slow motor units. While the question is interesting on its own merits, it is also pertinent because of its relationship to the role of timing in achieving type specific innervation. A central feature of the timing hypothesis is that slow motor units begin to form from primary myofibers a day or more before innervation of fast fibers commences. If the two populations of motor units are relatively disjoint, it seems plausible that each might follow a similar but temporally offset program of early synaptic development. To separately monitor synapse elimination among both fast and slow muscle fibers, the following strategy was employed. The innervation state of individual fibers were first determined using *in vitro* intracellular recording with a glass microelectrode. Fibers meeting a particular criterion were labeled by pressure injection of the fluorescent dye lucifer yellow. After sectioning the muscle, the histochemical type of each dye labeled fiber was then determined by staining for alkali stable ATPase activity. Surprisingly, no significant difference was seen in the

fiber type breakdown of multiply innervated or singly innervated fibers at either of two ages studied, indicating that the endpoint of the synapse elimination process is nearly synchronous for the two fiber types.

The second of the experiments of Chapter 3 was motivated by evidence for a fiber type selective reorganization of motor units following the major episode of synapse elimination. By two independent measures, Gordon (1983) observed a increase in the size of slow motor units relative to fast motor units in rabbit soleus muscle between 2 and 5 weeks of age. Because the ratio of fast and slow motor neurons did not appear to change during this interval, he hypothesized that fast muscle fibers were being selectively removed from fast motor units and added to slow motor units. This synaptic reorganization would be fundamentally different in character from the later wholesale conversion of motor units from fast to slow described by Kugelberg (1976) in the rat soleus. A possible anatomical substrate for this synaptic reorganization appeared to be available when Taxt *et al.* (1983) reported finding a small yet significant incidence of polyinnervation in rat muscles aged 3–6 weeks. While this could represent residual polyinnervation not fully removed during the nominal interval of synapse elimination, the fact that one of the synaptic inputs on multiply innervated fibers always appeared to be substantially smaller than the other suggested that each occurrence might be transient, and that the phenomenon therefore represented genuine synaptic plasticity. It thus appeared that transient dual innervation might be an intermediate stage in a process producing a net transfer of muscle fibers from fast to slow motor units. The experiment described in Chapter 3 set out to corroborate the existence of the phenomenon, relate it to the hypothesized secondary synaptic reorganization, and to further determine whether such a process might be overtly type selective, or whether initial differences in motor unit size imposed a dynamic upon an otherwise random process. This latter

question was to be addressed by studying the fiber type distribution of the late stage polyinnervated fibers, using the intracellular lucifer yellow labeling technique to mark multiply innervated fibers for subsequent ATPase processing.

Using the *in vitro* cut muscle technique (Barstad, 1962), which provides high sensitivity while eliminating muscle contraction, compound endplate potentials were in fact observed in 17–23 day rabbit soleus muscles at a low frequency comparable to that reported by Taxt *et al.* (1983). Furthermore, the character of these potentials matched those described by Taxt, consisting of one large component, and one which was much smaller; too small, presumably, to be seen in curarized preparations. The spatial distribution of fibers exhibiting compound e.p.p.'s soon became a cause for concern, however. None of these fibers were found on the surface of the muscle, even though several hundred surface fibers were examined. Compound e.p.p.'s were only observed in deeper fibers, after the electrode had passed through at least one other muscle fiber. By this and several other criteria fully described in Chapter 3, it appears likely that the compound endplate potentials do not in fact represent genuine polyneuronal innervation, but instead are an artifact resulting from electrical coupling of muscle fibers induced by the process of electrode penetration. I conclude that the incidence of genuine polyinnervation in muscle of this age is very low, if any exists at all. This finding is more significant than might first be apparent. First, it constrains the operation of the proposed secondary synaptic reorganization by establishing a stringent upper limit upon transient dual innervation, although transiently denervated fibers remain a viable alternative mechanism through which the process could unfold. Perhaps more importantly, it dampens unwarranted enthusiasm for what appeared to be the first physiological evidence for continuing plasticity in the innervation of healthy skeletal muscle, a topic which has received attention for many years (Barker and Ip, 1966).

The final chapter of this thesis presents a computer model of neuromuscular synapse elimination, and describes a series of modeling experiments intended to study and compare various mechanisms which might play a role in the process. Synapse elimination is a complex phenomenon involving the interplay of many distinct aspects. Among the processes and interactions which have been implicated in synapse elimination are neural induction of endplate specializations, adhesive interactions, competition for space, the dynamics of terminal growth and retraction, competition for trophic support, noncompetitive trophic influences, protease effects, neuronal and muscle activity, and neuronal metabolic capacity. Computer modeling offers a objective framework for exploring ideas regarding how the process might work.

Previous computer models of synapse elimination (Willshaw, 1981; Gouze *et al.*, 1983) can be faulted on several grounds, including an overly analytic approach, a failure to relate intermediate parameters to tangible characteristics, and in the latter instance, questionable mechanistic assumptions. The present model attempts to avoid these pitfalls. The model focuses on terminal dynamics: the growth and retraction of individual presynaptic terminals constitutes the principal outcome of each iteration. Dynamic choices are made stochastically based upon the state of the parameter ensemble. Key parameters, such as terminal size, neuronal and muscular activity, neuronal metabolic loading, and the concentration of hypothesized molecular constituents, are physically identifiable.

Three mechanisms potentially involved in synapse elimination have been implemented in the model. The first of these invokes a synaptic stabilization molecule, termed "scaffolding" (Van Essen, 1982), which anchors a presynaptic terminal to the basal lamina, thereby increasing its bias for growth over retraction. Central to the second mechanism is a hypothesized trophic factor (Jansen *et al.*,

1978), synthesized by muscle fibers as a function of their activity, secreted into the synaptic cleft, and subsequently accumulated by presynaptic terminals. Variants of this mechanism consider the growth enhancing effects of the factor to be confined to individual presynaptic terminals, or to be integrated by axonal transport and act centrally, yielding a coordinated response throughout any particular neuronal arbor. The third mechanism reflects the intrinsic capacity of a motor neuron to support the metabolic demands of its terminal arbor (Brown *et al.*, 1976; Thompson and Jansen, 1977). Within the overall framework of each mechanism, variations are included to compare the avenues by which activity influences the process, or to explore the role of terminal size. The three mechanisms are not mutually incompatible, and may be combined during simulations. Nine experimental observations were selected to evaluate the performance of the model. These describe the behavior of synapse elimination both under normal conditions, and following experimental perturbations, including altered activity and partial denervation. The performance of the model, and its ability to simulate the selected experimental criteria, are described in detail in Chapter 4.

Chapter 2

LACK OF FIBER TYPE SPECIFICITY DURING REINNERVATION OF NEONATAL RABBIT SOLEUS MUSCLE

INTRODUCTION

The neonatal rabbit soleus is a mixed muscle, composed primarily of two distinct muscle fiber types that can be distinguished by differences in their contractile speed and the pH stability of their actomyosin ATPase activity. During the first two weeks after birth, histochemical type I fibers (slow contracting) constitute approximately 30% of the total fiber count, while type II fibers (fast contracting) constitute about 70% (Gordon, 1983). In adult mixed muscles, individual motor units exclusively contain muscle fibers of a single type (Edstrom and Kugelberg, 1968; Kugelberg, 1973; Burke *et al.*, 1973), a pattern consistent with the dependence of fiber type upon the pattern of neural input (Salmons and Sréter, 1976). Considerable specificity of innervation by fiber type is also present during the first week after birth (Gordon and Van Essen, 1985), at a time when all muscle fibers are heavily polyinnervated (Redfern, 1970; Brown *et al.*, 1976; Bixby and Van Essen, 1979). Histograms of twitch tension rise times for single motor units from 1–4 day rabbit soleus muscles are bimodal, indicating substantial homogeneity in the fiber type composition of individual motor units. Glycogen depletion experiments in polyinnervated neonatal rat soleus (Thompson *et al.*, 1984) indicate a similar anatomical specificity (but see Jones *et al.*, 1987).

Several possible mechanisms by which this specificity could be established have been suggested (Thompson *et al.*, 1984; Gordon and Van Essen, 1985). Initial innervation of muscle fibers might actually be random, producing a degree of polyinnervation well in excess of that observed in early postnatal studies. Specific loss of inappropriate connections during an early phase of synapse elimination would then be necessary to yield two largely distinct populations of polyinnervated motor units. A second suggestion derives from the observation that primary and secondary

myotubes are formed at different times (Wirsen and Larsson, 1964; Kelly and Zacks, 1969), and develop preferentially to become the initial complement of slow and fast fibers, respectively (Rubinstein and Kelly, 1981). Specificity of innervation by fiber type might result from the sequential arrival of two sets of motor neurons timed to match the staggered developmental schedule of primary and secondary myotubes (Rubinstein and Kelly, 1981). Sperry's chemoaffinity hypothesis (Sperry, 1963) offers a third possible mechanism. Chemospecific recognition of appropriate muscle fibers by motor neurons during the initial episode of innervation might provide an active process by which individual muscle fibers could become multiply innervated by motor neurons of the same type.

Reinnervation experiments offer an approach for studying the possible role of chemospecificity in the establishment of neuromuscular connections. The alternative hypotheses cited above could not account for fiber type specificity which might be observed at an early stage of reinnervation. While reinnervation is known to be non-specific in adults (Kugelberg *et al.*, 1970; Brooke *et al.*, 1971), it remains possible that recognition molecules which have vanished at this later age might still be present soon after birth. Indeed, Soileau *et al.* (1987) have presented evidence suggestive of fiber type specific reinnervation in neonatal rat soleus, by employing glycogen depletion to label the majority of muscle fibers composing individual reinnervated motor units. We have chosen an alternative approach to assess the specificity of reinnervation in neonatal rabbits, using the distribution of single motor unit twitch tension rise times as an assay of motor unit diversity. Our results indicate that specificity is largely absent during reinnervation in the particular species and developmental age that we examined.

MATERIALS AND METHODS

Pregnant female New Zealand White rabbits were obtained from ABC Rabbitry (Pomona, CA). Experiments were conducted using soleus muscles of immature animals of either sex. Surgical procedures were performed on animals aged 1 day or 4 days postnatal, while *in vitro* analysis of single motor units was performed using animals aged 7–10 days. Ages were calculated from the time of birth. Prior to surgery, animals were anesthetized either with methoxyflurane (Pitman-Moore) followed by ether (1 day rabbits), or with Ketamine HCl by intramuscular injection of the contralateral hindlimb (4 day rabbits). In one series of animals, the soleus muscle nerve was crushed at least three times near its entry to the muscle, using No. 5 forceps. In another series of animals, 1 ng (2 μl of 0.5 μg/ml) of botulinum toxin (BoTx; Type A, Sigma, in 0.2% gelatin and 0.07% phosphate buffer, pH 6.5) was injected superficially over the ventral face of the muscle following surgical exposure and freeing of connective tissue. Full *in vivo* block of reflexive hindfoot flexure and extension was evident by the following day, and continued through the 6 day interval preceding *in vitro* analysis. A third group of unoperated animals was used in control experiments.

For *in vitro* experiments, animals were anesthetized with methoxyflurane followed by ether, and soleus muscles were dissected free, together with their innervation back to contributing spinal roots. A bone fragment including the proximal tendon insertion was pinned to the bottom of a shallow wax-lined dish, and the distal tendon was affixed via 6–0 surgical silk to a piezoresistive tension gauge (Aksjeselskapet MikroElektronikk, Horten, Norway, Model AE 875). Responses were linear up to 9 grams. The preparation was continuously superfused with chilled, oxygenated Ringer's (Gordon and Van Essen, 1985), with flow rate

adjusted as necessary to maintain temperature in the range 18.8–19.2 °C. Following verification of block in BoTx poisoned muscles, transmission was restored (Lundh *et al.*, 1977; Brown *et al.*, 1981) by superfusing with Ringer's containing 0.15 mM 4-aminopyridine (4-AP) and elevated Ca^{2+} (15mM).

Whole muscle twitch contractions were stimulated using pulses of 2 msec duration and 60 V amplitude applied with bipolar electrodes spanning the muscle. The muscle was stretched to a length yielding maximal whole muscle contractions and maintained at this length throughout the experiment. Single motor units were isolated by applying carefully graded stimuli to teased ventral root filaments using a suction electrode. Twitch tension traces were recorded using an IBM PC/XT computer equipped with a Tecmar Labmaster analog input board. Occasionally, multiple units were recorded from single filaments, and off-line computer subtraction was used to estimate single unit twitch responses. Contraction times computed from summed traces are accurate to within approximately 10% (Gordon and Van Essen, 1985).

Following completion of *in vitro* analysis, muscles were frozen by immersing them, stretched, in isopentane cooled by dry ice, and then stored at -70°C. Cross sections from representative muscles selected at random were cut on a cryostat at -20°C and processed for myofibrillar ATPase activity at pH 10.4 following the procedure of Guth and Samaha (1970).

Motor unit twitch tension traces were analyzed off-line to determine rise times, taken to be the interval between stimulus and the moment of peak tension. The timing of peak tension was determined by a computer algorithm following computer smoothing of the digitized tension record. The width of the smoothing window was varied if necessary so that the computed time of peak tension was within

5% of a visually estimated time of peak. Histograms of single motor unit twitch tension rise times were tabulated to compare contractile diversity between different experimental groups. Generally, rise time data were pooled directly within each group. In cases where we were concerned that systematic differences in average rise time between animals in a group might obscure the inherent variability measured in individual muscles, we employed a non-parametric normalization. In this procedure, the rise time of each motor unit was expressed as a percentage of the median rise time value for the muscle of origin before data from individual muscles were pooled. The interquartile ratio (IQR), defined as the ratio of the 75% and 25% points in a cumulative rise time distribution ($t_{.75}/t_{.25}$), provides a non-parametric, scale invariant measure of motor unit contractile diversity within individual muscles or pooled experimental groups.

We conducted computer simulations to establish an upper limit on the degree of fiber type selectivity consistent with the diversity in rise times in our experimental data. The first step in assembling a simulated motor unit was to determine the number of fibers it would contain. The experimental histogram describing the sizes of reinnervated motor units (Fig. 2A) was regarded as a probability distribution, and motor unit sizes were randomly sampled from this distribution. The concept of selectivity presumes that each motor neuron participating in the reinnervation process possesses a type identity, either fast or slow. We assigned each motor unit an inherent type with equal likelihood, reflecting the approximately equal frequency of fast and slow motor units in normal rabbit soleus muscles of this age (Gordon, 1983). Next, each fiber in the simulated unit was randomly assigned a contractile type, based upon a specified level of fiber type selectivity. The probability P_M that the type of any particular fiber matched the inherent type of its motor unit was

taken to be

$$P_M = 0.5 + \frac{S}{200},$$

where S is fiber type selectivity, ranging between 0% and 100%. Twitch rise times of individual fibers were then sampled from rise time probability density functions defined separately for fast and slow fibers. These probability distributions were estimated from a histogram of normal single motor unit rise times from 9 day muscles (Fig. 3A) using two different procedures described in Results. Finally, simulated motor unit rise times were calculated by averaging single fiber rise times. Simulations were conducted for a range of fiber type selectivities. The number of units simulated (162) was equal to the number of experimentally reinnervated units. Histograms were plotted and IQRs calculated for comparison with the experimental distribution of reinnervated motor unit rise times.

RESULTS

The soleus muscle nerve was crushed unilaterally in rabbits aged 1 day or 4 days postnatal at a point just proximal to its insertion into the soleus muscle. Reinnervation was subsequently assessed *in vitro* at 19°C by comparing nerve evoked twitch tension to the tension produced by direct whole muscle stimulation. For animals operated on day 4, the first indication of functional reinnervation appeared 4 days following nerve crush (Fig. 1, circles), but was insufficient to permit reliable tension measurements from single motor units. Reinnervation progressed rapidly to 8% ± 3% (N = 5, mean ± S.E.M.) at 5 days post-crush and 32% ± 4% (N = 9) at 6 days post-crush, and continued to increase thereafter. Animals operated on day 1 (Fig. 1, triangles) displayed essentially the same degree of reinnervation at 6 days post-crush, and thus presumably had a similar time course of reinnervation. We selected 5–6 days post-crush as an appropriate interval for analysis of reinnervated single motor units based upon two considerations. First, a sufficient degree of reinnervation had occurred in these muscles to allow successful isolation of individual motor units and a meaningful analysis of their contractile properties. Second, because individual muscle fibers had been reinnervated for 2 days or less, insufficient time had elapsed for neuron-directed respecification of muscle fiber type to have occurred (Pette *et al.*, 1976; Klug *et al.*, 1983).

Motor unit properties in reinnervated muscles, specifically motor unit size and twitch tension rise time, were analyzed *in vitro* at 19°C (Methods). At 5–6 days following nerve crush, reinnervated muscles clearly contained fewer detectable motor units than normal muscles. Difficulties in recognizing very small units when these were recruited in combination with one or more larger units prevented an exhaustive count. Nevertheless, based upon the average size of teased filaments and the number

Figure 1. Percent reinnervation in experimental muscles examined *in vitro* at various times following crush of the soleus muscle nerve near its entry to the muscle at 1 day (triangles) or 4 days (circles) postnatal. Reinnervation was estimated by dividing maximum nerve evoked twitch tension by the peak tension recorded following direct stimulation of the whole muscle using bipolar electrodes. The interval 5–6 days post-crush was selected for analysis of the contractile diversity of reinnervated motor units. Individual units at this time were large enough for meaningful analysis of twitch tension rise times, yet the interval of functional reinnervation was sufficiently brief to preclude muscle fiber type respecification.

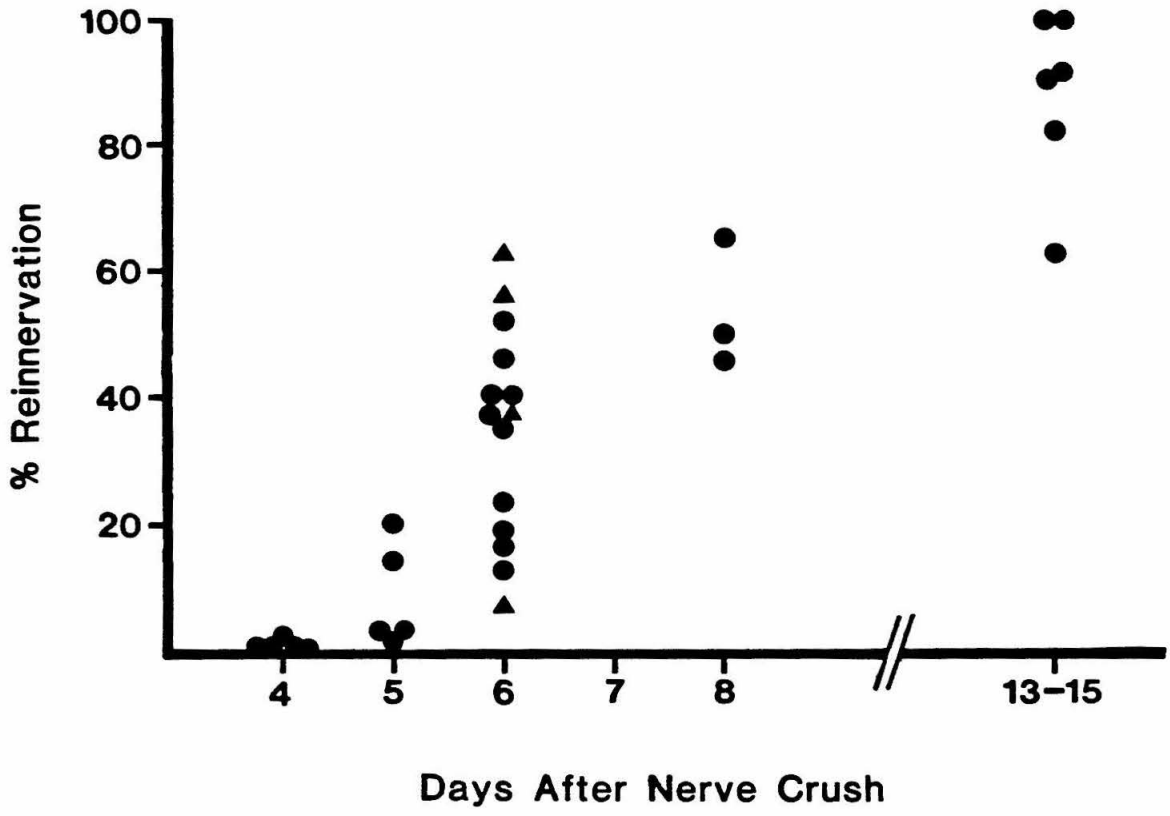
100
80
60
40
20
% Reinnervation
4
5
6
7
8
13–15
Days After Nerve Crush

Figure 1

of units elicited when these were stimulated, we estimate that 6 day reinnervated muscles contained roughly half of the normal complement of 60–70 motor units (Bixby and Van Essen, 1979a; Gordon and Van Essen, 1985).

Motor unit sizes were expressed as a percentage of maximal twitch tension obtained by direct whole muscle stimulation. The distribution of motor unit sizes for reinnervated units estimated according to this procedure is shown in Fig. 2 for muscles examined in normal Ringer's (Fig. 2A) and for muscles examined in Ringer's containing 4-AP and high Ca^{2+} (Fig. 2B). We also estimated the number of muscle fibers per motor unit by assuming that the rabbit soleus consists of 11,000 fibers (Bixby and Van Essen, 1979a) of equal cross-section and specific tension. This information was needed in order to estimate the degree of diversity that would result from purely random reinnervation or from a low level of selectivity. At 5 days after nerve crush, reinnervated units averaged 0.27% of maximal direct tension, corresponding to 30 $\pm$ 5 muscle fibers (n = 19, 1 muscle), while 6 day reinnervated units averaged 0.64% of maximal direct tension , corresponding to 69 $\pm$ 6 muscle fibers (n = 143, 6 muscles). About 13% of reinnervated units analyzed (21 of 162) contained fewer than 10 muscle fibers. Interestingly, in the muscles analyzed in Ringer's containing 4-AP and elevated Ca^{2+}, motor unit sizes averaged 1.58% of maximal direct tension, corresponding to 174 $\pm$ 23 fibers (n=58, 3 muscles). This 2.5-fold increase suggests that many newly formed synapses are subthreshold when tested in normal Ringer's.

A histogram of single motor unit twitch tension rise times recorded *in vitro* in 9 day normal rabbit soleus muscles (Fig. 3A; n = 127, 3 muscles) exhibits roughly a 2-fold diversity in contractile rate (total range 180–450 msec, IQR = 1.61). A population of fast contracting units (180–250 msec) clearly forms a single peak. Whether the slow contracting population consists of one or more distinct

Figure 2. Size distribution of reinnervated motor units analyzed in (A) normal Ringer's solution (5 or 6 days post-crush) or (B) Ringer's containing 4-aminopyridine and elevated Ca^{2+} (6 days post-crush). The larger sizes of units measured under the latter conditions suggests that a substantial degree of normally subthreshold innervation is present during this early stage of reinnervation. Sizes of isolated motor units are expressed as the ratio of their peak twitch tension to maximal whole muscle twitch tension. A rough estimate of motor unit fiber count can be obtained by multiplying horizontal axis values by 110.

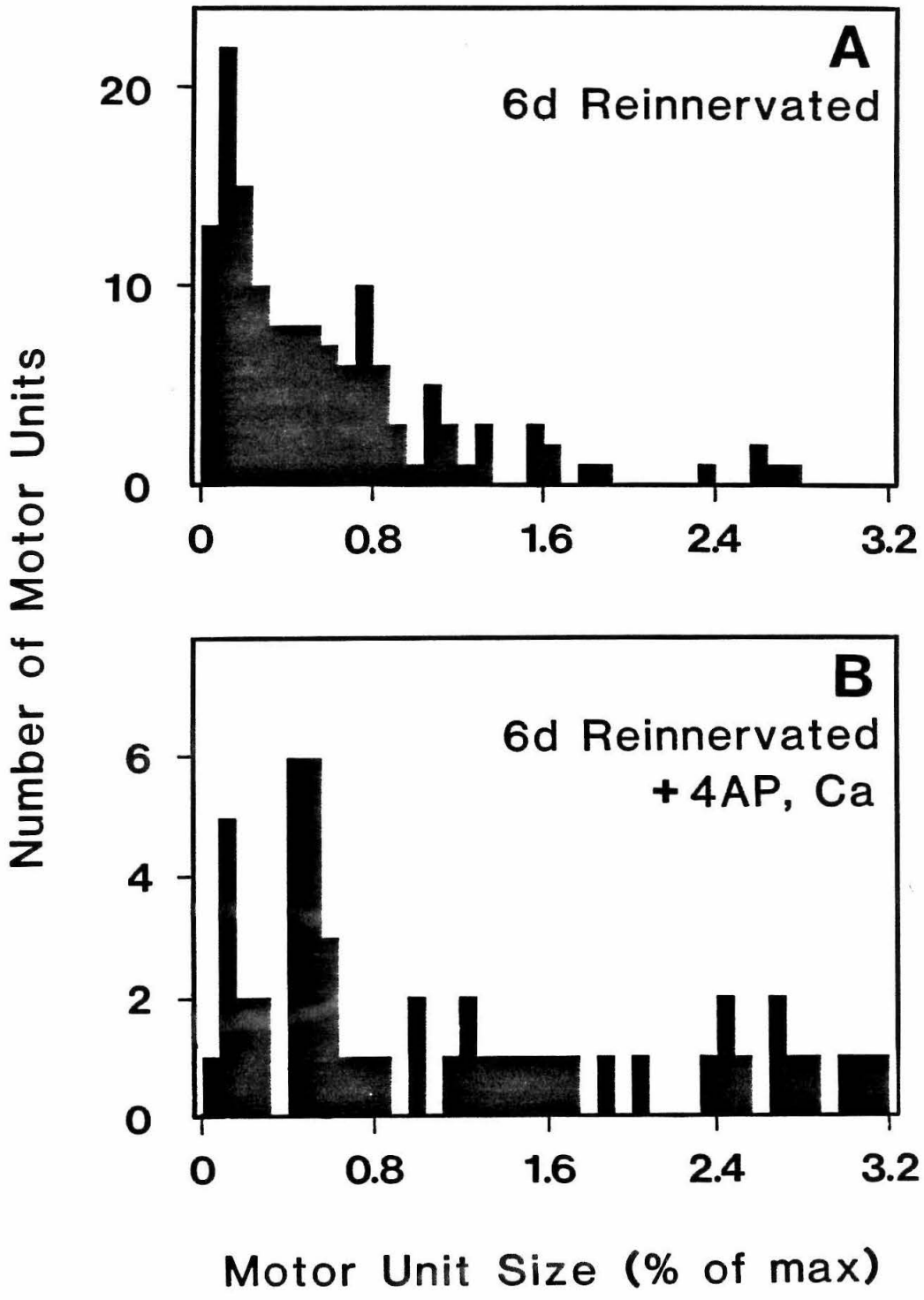
A
6d Reinnervated
20
10
0
0
0.8
1.6
2.4
3.2
B
6d Reinnervated
+4AP, Ca
6
4
2
0
0
0.8
1.6
2.4
3.2
Number of Motor Units
Motor Unit Size (% of max)

Figure 2

Figure 3. The distribution of single motor unit twitch tension rise times in (A) normal control muscles aged 9 days postnatal and (B) reinnervated muscles 5–6 days after nerve crush at postnatal day 4. Normal muscles exhibit a distinctly multimodal distribution of twitch rise times, evidence of substantial homogeneity in the fiber type composition of individual fast or slow neonatal motor units. The arrow suggests a split point for separating fast and slow units. In contrast, reinnervated motor units appear to constitute a single population with intermediate rise times, suggesting that each comprises a similar proportion of fast and slow muscle fibers. A comparable result (C) was obtained following crush of the soleus muscle nerve at the earliest convenient opportunity, during postnatal day 1. Apart from a marginal slowing of all contractions in the less mature muscles, the distribution of rise times is indistinguishable from that observed when nerve crush is performed on postnatal day 4. Because motor unit contractile properties were assayed *in vitro* at 19,°Ctwitch rise times were considerably slower than the normal range *in vivo*.

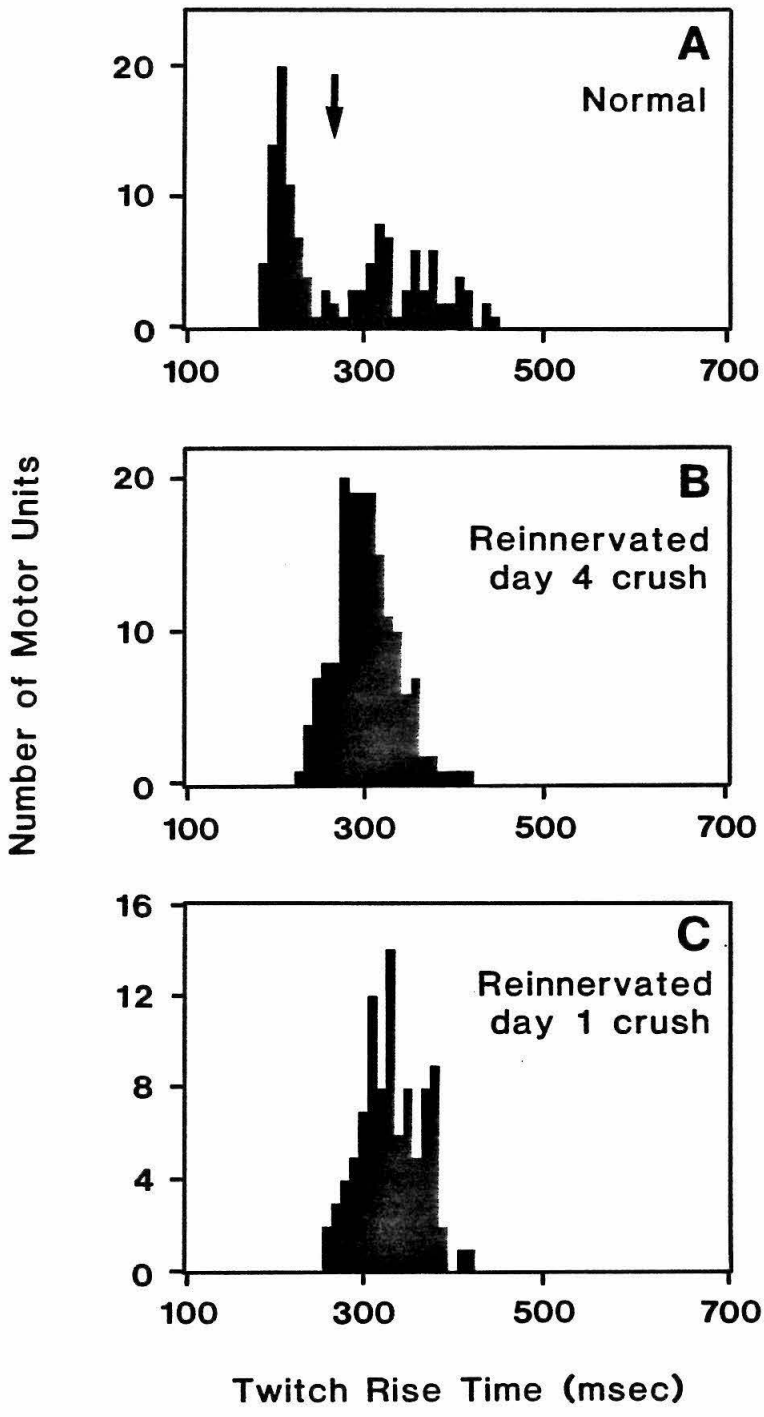
A
Normal
B
Reinnervated
day 4 crush
C
Reinnervated
day 1 crush
Number of Motor Units
Twitch Rise Time (msec)
20
10
0
16
12
8
4
100
300
500
700

Figure 3

peaks is less clear, but is not of critical importance for the present study. This heterogeneity in motor unit contractile speed is present at all ages studied during the first several weeks of life (Gordon and Van Essen, 1985), and suggests strongly that individual neonatal motor units are composed primarily of a single muscle fiber type. In contrast, a similar histogram of twitch tension rise times of 162 motor units from 7 reinnervated muscles 5–6 days following nerve crush at day 4 is narrow (total range 220–420 msec, IQR = 1.16), unimodal, and centered on intermediate speeds (Fig. 3B). These features suggest that reinnervated motor units constitute a relatively uniform population, with most units composed of a similar mixture of fast and slow muscle fibers.

A possibility we considered is that the capacity for specific recognition and reinnervation according to fiber type is lost by postnatal day 4, but is present at earlier ages. We therefore performed soleus nerve crushes in another group of 4 animals at the earliest practical time, during the first postnatal day, and analyzed reinnervation 6 days later. The level of reinnervation in these muscles was similar to that observed following nerve crush at day 4. A histogram of twitch tension rise times of 95 isolated motor units from these muscles is unimodal (Fig. 3C; IQR = 1.17) and similar to that seen when nerve crushes were performed on day 4 (Fig. 3B), again suggesting random reinnervation.

There are, however, alternative explanations whereby these results would be consistent with the specific or preferential reinnervation of muscle fibers by motor neurons of the corresponding type. One possibility is that a de-differentiation of muscle fiber contractile properties occurs during the short interval of denervation following nerve crush. In this event, differences in the twitch tension rise time of motor units composed predominantly of either fast or slow muscle fibers could be substantially reduced. A second alternative is that at the early stage of

reinnervation, only one population of motor neurons had reestablished connections, and that these connections specifically favored the corresponding muscle fiber type.

To investigate the possibility of muscle fiber de-differentiation during a short interval of inactivity, botulinum toxin was applied to soleus muscles in a separate group of animals aged 4 days. Subsequent paralysis of the affected lower hindlimb became apparent within a day of toxin application and remained present throughout the survival period. Transmission blockade continued for 5–6 days, after which muscles were removed for *in vitro* analysis. Following verification of full blockade, synaptic transmission was restored by superfusing muscles with Ringer's containing 4-AP and high Ca^{2+} (Brown *et al.*, 1981). This treatment is thought to act by increasing the duration of presynaptic action potentials, thereby elevating internal Ca^{2+} sufficiently to restore effective transmitter vesicle release (Lundh *et al.*, 1977). A histogram of twitch tension rise times of 175 single motor units from 5 BoTx treated muscles (Fig. 4A) yielded an IQR of 1.53 and a total range of 230–650 msec. This histogram is quite similar in shape to the distribution of rise times in untreated muscles (Fig. 3A), indicating that heterogeneity of motor unit contractile properties was maintained during the period of inactivity. The overall lengthening of twitch rise times apparent in toxin treated muscles may derive from events pursuant to a doubling in the duration of muscle fiber action potentials due to the presence of 4-AP (Lundh *et al.*, 1977). Preservation of motor unit properties during the interval of transmission blockade is further confirmed by a two dimensional plot of motor unit size vs. twitch rise time of isolated motor units from a single muscle (Fig. 5). Separation of clusters representing fast and slow motor units is comparable to that seen with normal muscles (Burke, 1967; Gordon and Van Essen, 1985).

Additional evidence that muscle fibers maintained their contractile identity during the interval of functional denervation was obtained by examining muscle

Figure 4. Motor units from muscles in which transmission blockade was induced by administration of botulinum toxin exhibit a multimodal distribution of twitch rise times (A) following 5–6 days of inactivity *in vivo*. 4-AP and elevated Ca^{2+} were included in the bathing medium to restore synaptic transmission during the *in vitro* assay, leading to a general slowing of all contractions. Otherwise, the distribution of rise times is not readily distinguishable from that of normal muscles. Reinnervated muscles analyzed 5–6 days post-crush in the same bath yield a unimodal distribution of twitch rise times (B) intermediate to those of toxin treated motor units, but slower than motor units assayed in normal Ringer's.

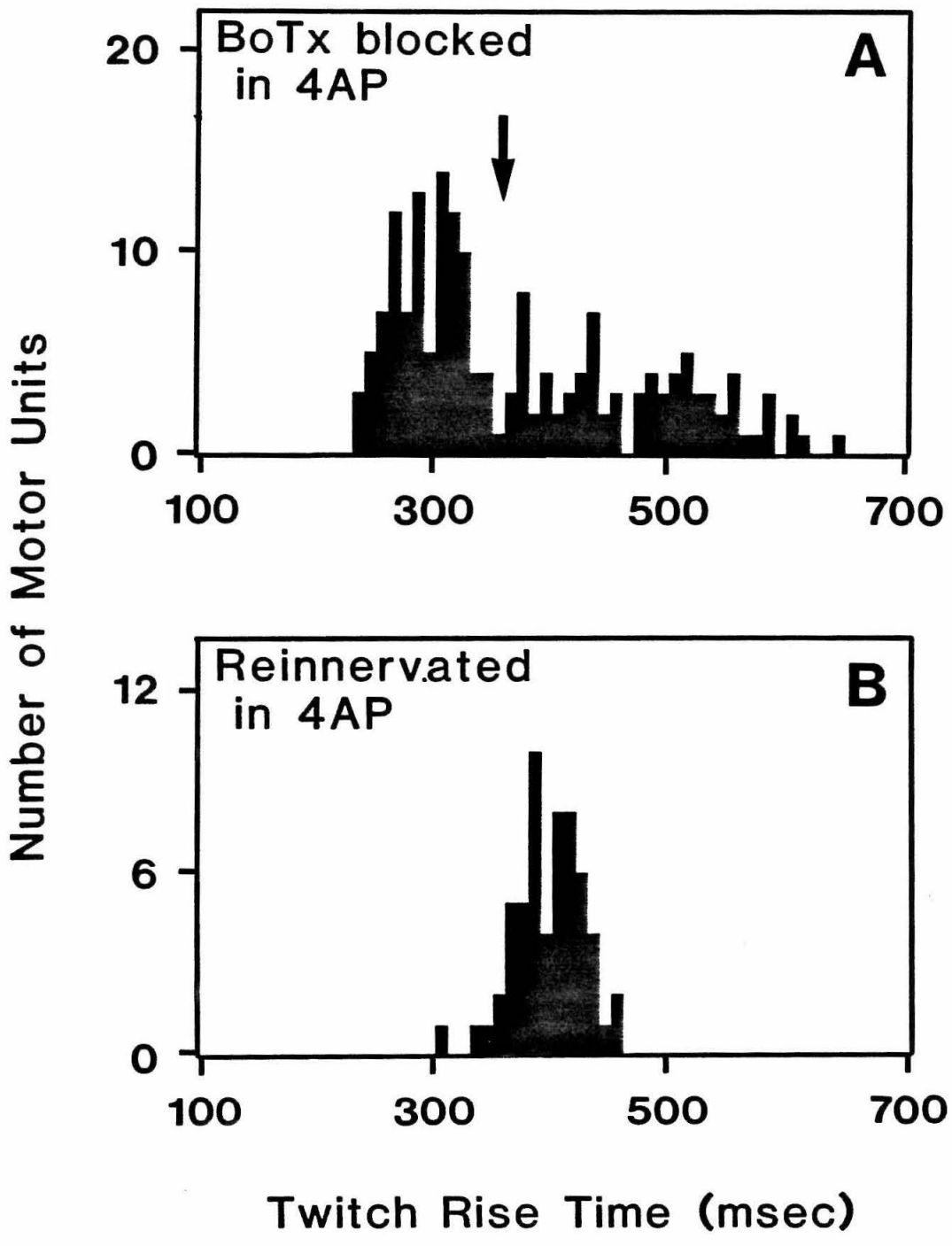
BoTx blocked
in 4AP
A
20
10
0
100
300
500
700
Reinnervated
in 4AP
B
12
6
0
100
300
500
700
Number of Motor Units
Twitch Rise Time (msec)

Figure 4

Figure 5. A two dimensional plot of motor unit size vs. twitch rise time for isolated motor units (circles) from a single muscle following blockade of synaptic transmission with BoTx for 6 days *in vivo* demonstrates that fast and slow motor units maintain differentiated contractile properties during the interval of inactivity. Transmission was restored for assay using 4-AP and high Ca^{2+} in the bathing medium.

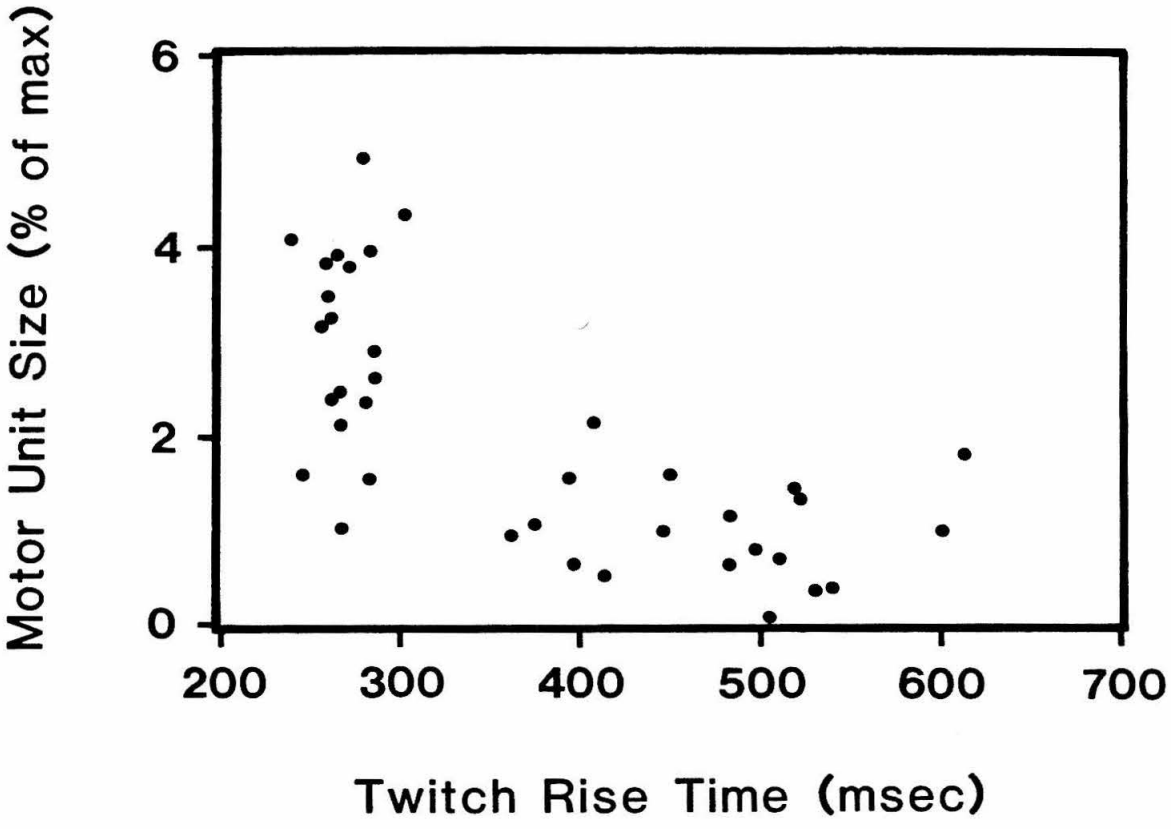
Motor Unit Size (% of max)
6
4
2
0
200
300
400
500
600
700
Twitch Rise Time (msec)

Figure 5

cross-sections stained for alkali stable ATPase activity. Contrast in fiber type staining in reinnervated muscles appears to be equivalent to that of normal muscles (Fig. 6), suggesting that substantial changes in the distribution of contractile isoforms did not occur. Also, the spatial distribution of fiber types lacks the clumping or type grouping characteristic of reinnervated transformed muscle (Kugelberg *et al.*, 1970).

Rise times for reinnervated motor units were intermediate to those of fast and slow units from normal muscles (Fig. 3), suggesting that reinnervated units contained both fast and slow muscle fibers in comparable numbers. However, the period of denervation might have affected the contraction rate of all muscle fibers, thereby altering the rise times of reinnervated units. Comparison of reinnervated units with motor units from animals treated with BoTx is more appropriate for approaching this issue. Thus we analyzed 3 additional 6 day reinnervated muscles in a bath containing 4-AP and elevated Ca^{2+}. Contraction times of reinnervated units ($n = 58$) were lengthened when 4-AP was present, and in fact were intermediate to those of fast and slow units from BoTx treated muscles analyzed in an identical solution (Fig. 4). This finding is consistent with the idea that reinnervated units contain a similar combination of fast and slow muscle fibers.

An independent way to approach the issue of motor unit fiber type composition is to compare contractile diversity at early and later stages of reinnervation. If early reinnervation were specific, but consisted exclusively of fast (or slow) motor units, then a second population of units would likely appear as later arriving slow (or fast) axons reestablished functional connections. We therefore analyzed twitch tension rise times in another group of 109 motor units from 3 muscles 14 days after soleus muscle nerve crush at postnatal day 4. Reinnervation averaged 84% at this later time, and there appeared to be approximately 50% more motor units than

Figure 6. Sections from (A) a reinnervated muscle analyzed 6 days after soleus nerve crush on postnatal day 4, and (B) a soleus muscle from a 9 day normal animal, each stained to demonstrate alkali stable actomyosin ATPase activity. Type II (fast contracting) fibers are darkly stained, while type I (slow contracting) fibers remain largely unstained. Contrast between the two fiber types in the reinnervated muscle is similar to that of the normal muscle, indicating that histochemical differentiation of fibers types is maintained during early reinnervation. Type II fibers appear relatively less mature in the reinnervated muscle. Scale bar = 100 μm.

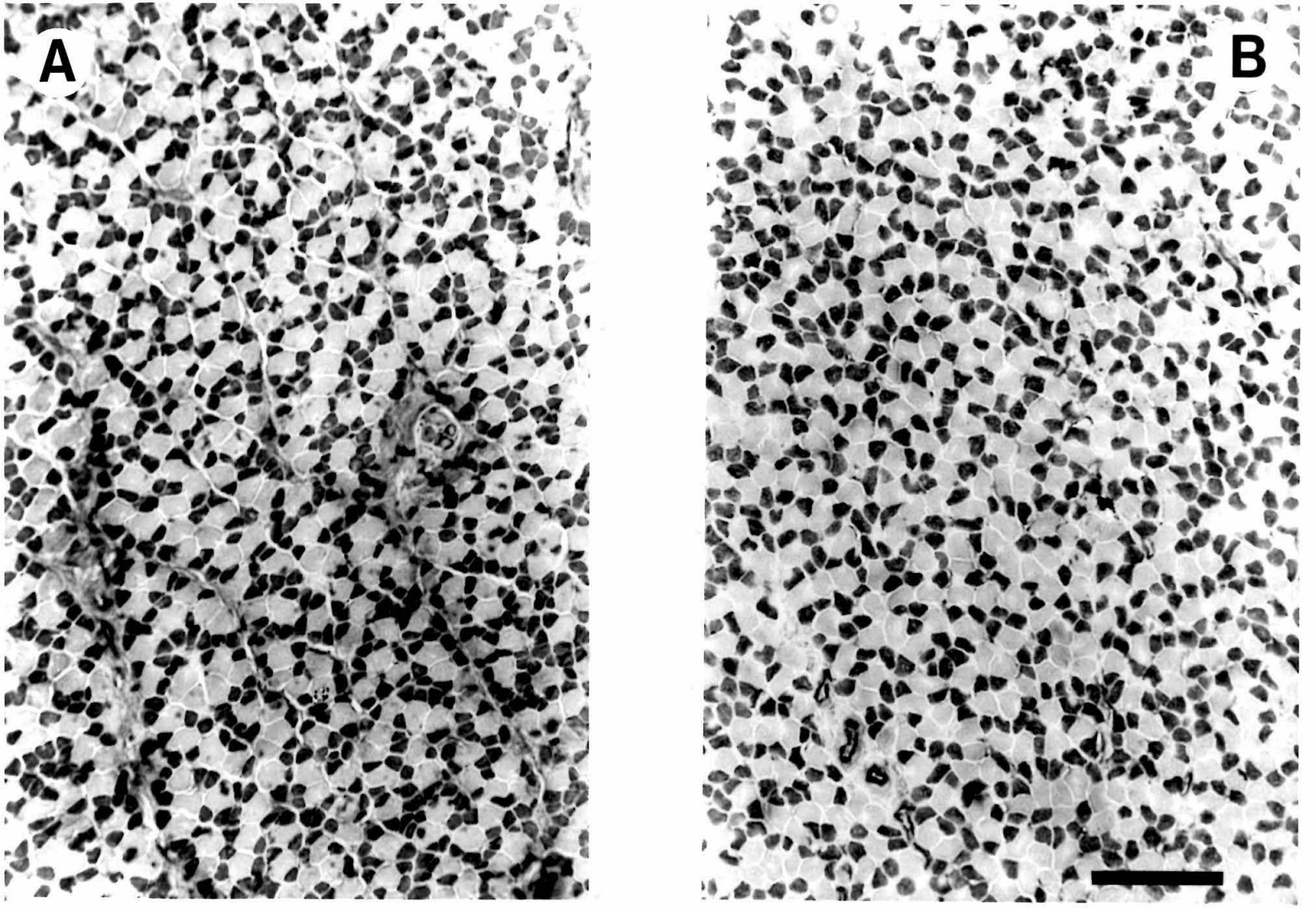
A
B

in 5–6 day reinnervated muscles, although once again an exhaustive count was not feasible. The rise time diversity found within individual 14 day reinnervated muscles was virtually identical to that present after 5–6 days of reinnervation (average IQR = 1.15 ± 0.01 S. E. M. for 14 day vs. 1.15 ± 0.02 for 5–6 day). While the rise time distribution for each of these older muscles was narrow, there were systematic differences in median rise times in different muscles (range 275–330 msec). To prevent a misleading broadening of the distribution when the rise times of all motor units are pooled, we first scaled individual distributions to the median value for each muscle. The similarity in rise time diversity is readily seen when distributions from individual animals are pooled in this manner (Fig. 7), suggesting that motor units continue to represent a single population at the later age.

The close similarity in twitch rise time diversity between the two age groups further argues that no appreciable respecification of fiber types by motor neurons occurred during the extended interval following early reinnervation. Whether the additional 8 days of functional activity would be sufficient to produce phenotypic changes in muscle fibers is uncertain. Significant changes in the activity of the sarcoplasmic Ca^{2+} pump first become apparent after 6 days of chronic stimulation (Klug *et al.*, 1983). Considerably more time may be required to produce changes in contractile rate (Salmons and Vrbová, 1969) or myosin expression (Pette *et al.*, 1976). Finally, it is possible that the differentiation of activity into tonic and phasic patterns has not yet occurred among neonatal motor neurons (Navarrete and Vrbová, 1983).

While rise time histograms are narrow for both 5–6 day and 14 day reinnervated motor units, some diversity is apparent. But does this diversity reflect a low level of selectivity in the reinnervation process, or does it merely reflect random fluctuations in the composition of motor units in which there is no inherent specificity? To

Figure 7. Single motor unit twitch tension rise times from reinnervated muscles 5–6 days (A; 7 muscles, 162 units) and 14 days (B; 3 muscles, 109 units) following crush of the soleus muscle nerve at postnatal day 4. To remove systematic differences in contractile speed between muscles, motor unit rise times were expressed as a percentage of the median rise time for the muscle of origin before data from individual animals were pooled. The similarity of the within animal variation in rise times for the two intervals of reinnervation suggest that little if any muscle fiber type respecification occurs in the first two weeks following nerve crush. Three additional 13–15 day reinnervated muscles (n = 107) were examined using a less sensitive tension gauge. Rise time distributions from these muscles were somewhat broader (reflecting the decreased signal to noise ratio), yielding an average quartile ratio of 1.25 $\pm$ 0.02, but were nonetheless substantially narrower than either the 9 day normal distribution of Fig. 3A (IQR = 1.61) or the distribution of BoTx treated units (Fig. 4A, IQR = 1.53).

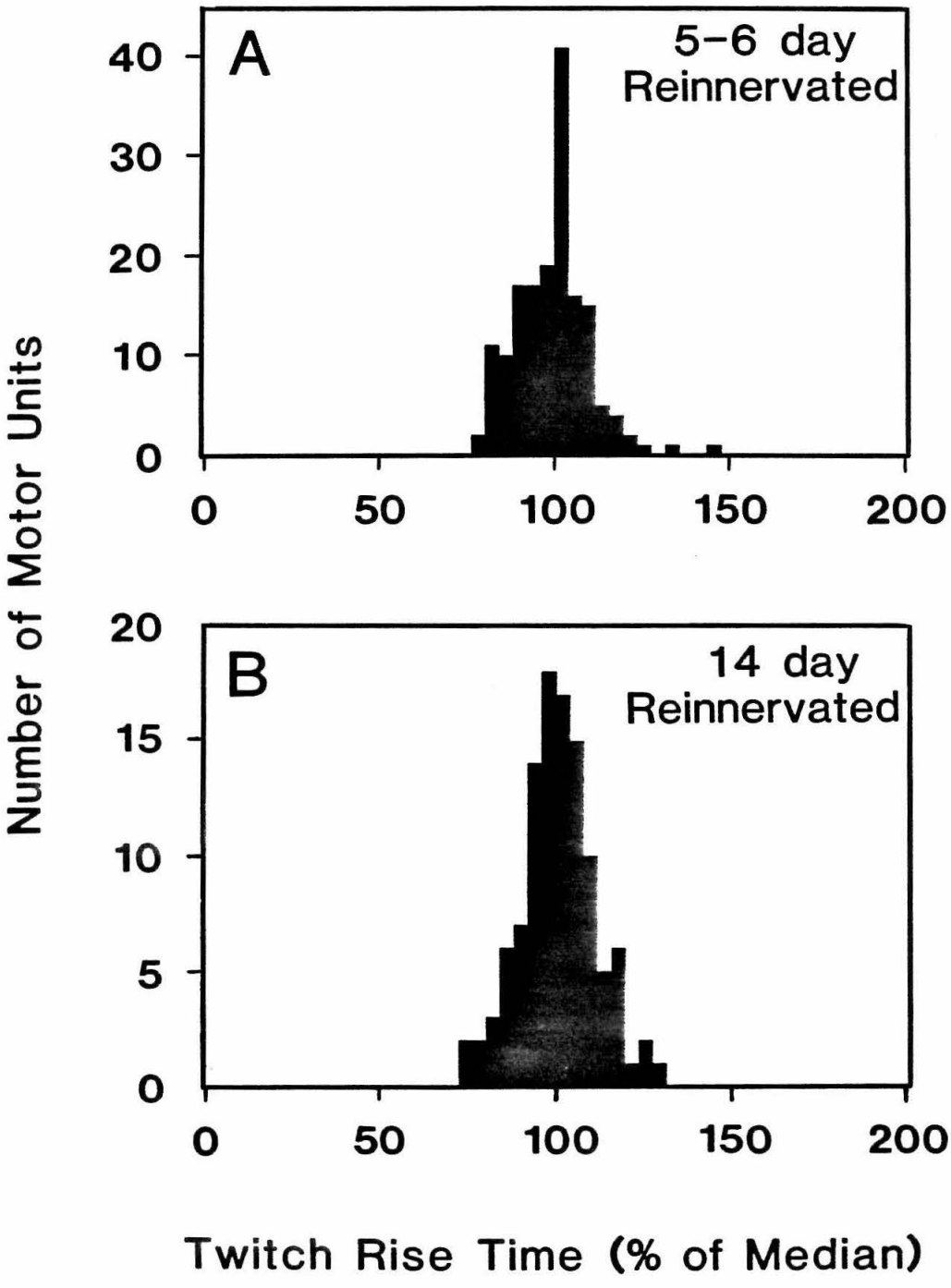
A
5–6 day
Reinnervated
40
30
20
10
0
0
50
100
150
200
B
14 day
Reinnervated
20
15
10
5
0
0
50
100
150
200
Number of Motor Units
Twitch Rise Time (% of Median)

Figure 7

help distinguish between these possibilities, we conducted computer simulations to estimate the motor unit rise time diversity which would be expected to follow from various levels of fiber type selectivity, ranging from 0% (completely random) to 100% (perfect homogeneity).

Simulations were predicated on the assumption that the rise time of motor unit tension during a twitch contraction can reasonably be estimated by averaging the individual rise times of all of the fibers in the unit, were these to be stimulated one at a time. Simulated units were assigned varying numbers of muscle fibers selected at random to satisfy two criteria: The distribution of motor unit sizes matched that of actual 5–6 day reinnervated units (Fig. 2A), while the distribution of fibers types within individual units reflected a specified degree of selectivity. Each fiber within a motor unit was assigned a twitch rise time selected randomly from fast and slow distributions derived from the histogram of rise times for normal 9 day motor units (Fig. 3A). The twitch rise time of the full motor unit was then estimated by averaging the individual rise times of its constituent fibers (see Materials and Methods for additional details).

A key consideration in this analysis is the assignment of rise times to individual fibers. In particular, what are the appropriate single fiber rise time distributions for fast and slow fibers? Two different strategies were employed to estimate these distributions. In adult muscles, there is little variability in a variety of metabolic and contractile properties among individual fibers of a single motor unit (Kugelberg, 1976; Nemeth *et al.*, 1981). If this uniformity were also characteristic of neonatal motor units, then the distribution of single fiber rise times would be virtually the same as the distribution of motor unit rise times, so that fast and slow distributions could be obtained by splitting the histogram of Fig. 3A into its fast and slow components. Using this strategy, rise time histograms describing simulated

reinnervated motor units were produced for a range of fiber type selectivities and compared with the observed rise time distribution of experimentally reinnervated motor units (Fig. 3B). As fiber type selectivity was increased, the breadth of the simulated rise time histogram expanded monotonically, as shown in Fig. 8 (open squares). Histograms of width equal to the experimental data (as measured by IQR) resulted from fiber type selectivity of about 30%, suggesting that this value is an upper bound for the degree of fiber type selectivity present during our reinnervation experiments. Interestingly, the rise time histogram of simulated units obtained when selectivity was set at 30% is bimodal, exhibiting small yet distinctive fast and slow peaks (Fig. 9A).

Because the experimental histogram is unimodal (Fig. 3B), this finding argues that either actual selectivity was not as great as 30%, or the estimated distributions of fast and slow single muscle fiber rise times were not appropriate.

An alternative possibility is that there might be substantial diversity in the contractile speeds of fibers within individual neonatal motor units, even though they consist predominantly (ca. 90%) of the same fiber type (Thompson *et al.*, 1984). This seems particularly likely considering that the polyinnervation present in neonatal muscles would prevent all fibers in a unit from receiving identical patterns of activation. In this case, the distribution of motor unit rise times (Fig. 3A) would not provide an accurate estimate of either the fast or slow rise time distributions for single fibers. Motor units at the extremes of this distribution would themselves contain fibers exhibiting a range of contraction times. Hence the distribution of single fiber contraction times would be substantially broader. To simulate this alternative, we developed estimates of the applicable fast and slow single fiber rise time distributions by adding extra random variation to the full unit distributions defined by separating the fast and slow components of Fig. 3A. The magnitude of

Figure 8. Expected motor unit rise time diversity as a function of fiber type selectivity during reinnervation, as estimated by computer simulation. Rise times of units whose size distribution was consistent with experimental units (Fig. 2A) were computed by averaging the individual rise times of constituent fibers, sampled from fast and slow distributions derived from a histogram of the rise times of normal motor units (Fig. 3A). Two distinct strategies for selecting the fast and slow fiber distributions provide upper and lower bounds for the expected rise time diversity. If the normal neonatal units of Fig. 3A are composed of fibers having very similar contractile rates, narrower single fiber rise time distributions and hence less rise time diversity would be expected among reinnervated units (open squares) than if normal neonatal units are instead formed of muscle fibers whose contractile rates vary across the available range (filled diamonds). Points are mean $\pm$ sd of three simulations. Horizontal line illustrates IQR of experimentally reinnervated units (Fig. 3B).

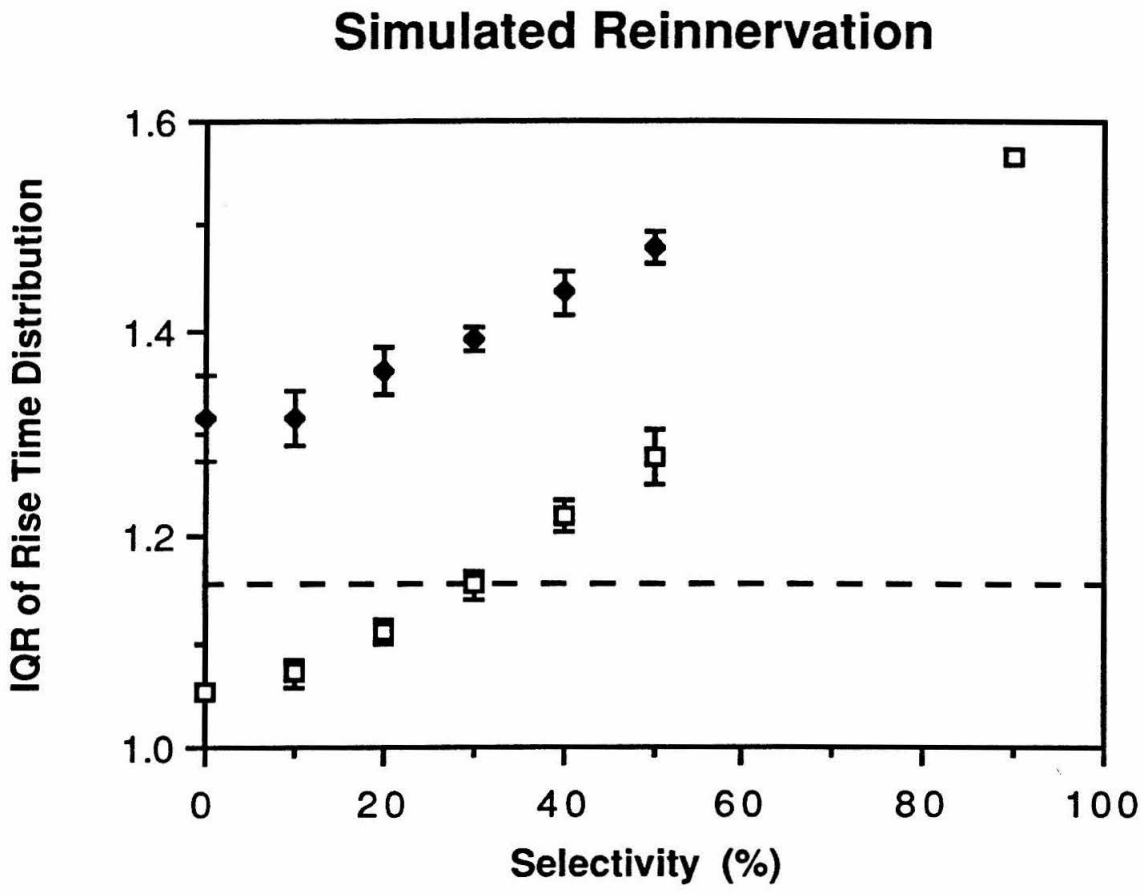
Simulated Reinnervation
IQR of Rise Time Distribution
1.6
1.4
1.2
1.0
0
20
40
60
80
100
Selectivity (%)

Figure 8

Figure 9. Rise time histograms of simulated reinnervated motor units. If single fiber rise time distributions are identical to the fast and slow modes of Fig. 3A, fiber type selectivity of about 30% is required to yield a rise time histogram equal in breadth to the experimental histogram (A). The fact that this simulated histogram is bimodal while the experimental histogram (Fig. 3B) is not suggests that actual selectivity is not this great. If single fiber rise times are estimated by a second procedure which is also consistent with the rise time diversity of normal units, a histogram of simulated units is broader than the experimental distribution even in the absence of fiber type selectivity (B).

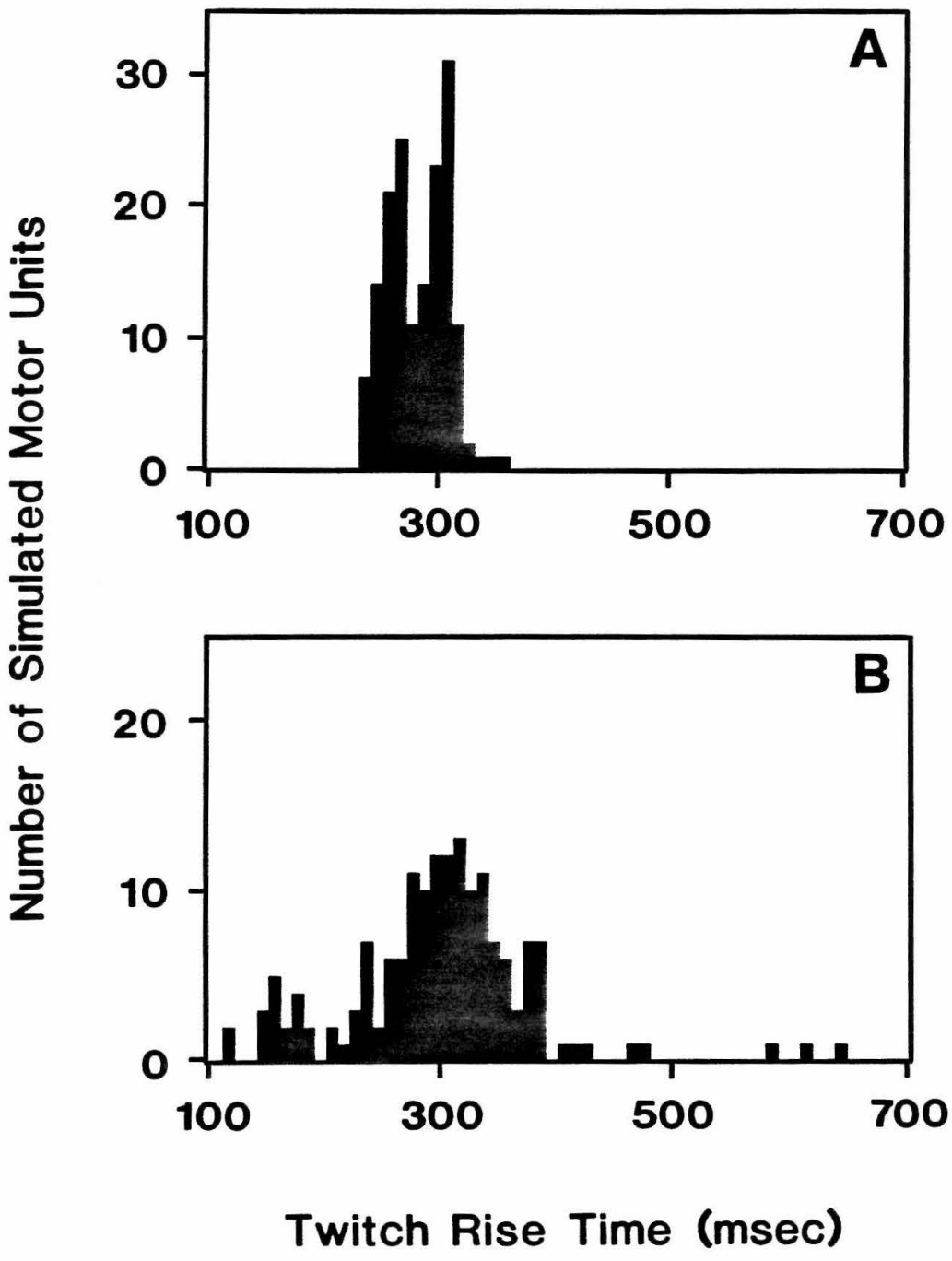
A
B
30
20
10
0
20
10
0
100
300
500
700
100
300
500
700
Number of Simulated Motor Units
Twitch Rise Time (msec)

Figure 9

this additional variance was chosen so that use of the simulation algorithm for units of normal size (200 ± 70 fibers) with a selectivity of 90% yielded a distribution of rise times similar to Fig. 3A. When the alternative fast and slow single unit rise time distributions were used to simulate reinnervated units equivalent in size to the 5–6 day experimental units, the breadth of the simulated rise time histograms again increased with increasing fiber type selectivity (Fig. 8, filled diamonds), but was always greater than the width of the histogram determined by experimentally reinnervated units (Fig. 3B). The histogram generated when selectivity was set to zero is illustrated in Fig. 9B. This result implies that there was little or no fiber type selectivity present during actual reinnervation.

The two alternatives examined above represent extremes in the spectrum of possible fast and slow fiber rise time distributions. Real muscle fibers may form distributions intermediate to these two cases. In any event, the simulations suggest that the degree of fiber type selectivity indicated by our experimental observations was probably less than 30%, and that in fact, selectivity may have been totally absent.

DISCUSSION

The development of specificity in the innervation of skeletal muscles has received considerable experimental attention. Several studies address the issue of whether positional markers may be present within muscle and play a role in establishing the correct pattern of connectivity during normal development. During original axon outgrowth in the chick limb, motor neurons prefer their correct target muscles, even when normal ordering in the spinal column has been disrupted (Lance-Jones and Landmesser, 1980a,b). This process is largely dependent upon axonal sorting within the appropriate plexus and nerve branching regions, and hence appears to represent pathway selection and guidance (Lance-Jones and Landmesser, 1981a; Tosney and Landmesser, 1985b,c). While these experiments suggest that motor neurons bear molecular labels based upon their position, or are able to selectively react to positional signals encountered during outgrowth, they provide no indication of specific molecular markers on muscle fibers.

Other indirect experimental evidence suggests that such positional markers may be present. In the competitive environment created by embryonic limb segment deletion experiments, Whitelaw and Hollyday (1983a) showed that motor neurons deprived of their normal target preferentially succumbed to cell death, whereas neurons normally innervating the remaining segment survived and innervated appropriate target muscles. This finding points to positional markers, but does not fully constrain their location to target muscles as opposed to distal growth pathways. The apparent peripheral specification of transplanted dorsal root ganglion sensory neurons in bullfrog (Frank and Westerfield, 1982; Smith and Frank, 1987) could reflect common markers shared by muscles and spinal motor neurons. In mammals, preganglionic axons of the rat cervical sympathetic trunk reinnervate transplanted

intercostal muscle in a segmentally selective manner, suggesting the presence of positional labels which vary along the rostrocaudal axis (Wigston and Sanes, 1985). Experiments using chick-quail chimeras have shown that individual limb muscles are populated by myogenic precursors deriving from particular somites (Beresford, 1983), and that motor axons from a given spinal segment preferentially innervate muscles of matched segmental origin (Lance-Jones, 1985). However, Keynes *et al.*, (1987) observed that following shifts and reversals of embryonic somitic mesoderm, myogenic precursors migrate according to their new segmental position, but motor neurons continue to find and innervate their normal target muscles rather than following the segmentally labeled muscle fibers to their new positions. This finding casts doubt on the idea that segmental markers are a major factor in the origin of specific innervation.

Topographic ordering of motor projections to a given muscle based upon rostrocaudal position within the spinal motor pool has been reported in several cases (Brown and Booth, 1983; Bennett and Lavidis, 1984a; Hardman and Brown, 1985; Bennett *et al.*, 1986; Laskowski and Sanes, 1987a). Such patterns might reflect differential labeling of muscle fibers or motor neurons according to their position. Neonatal synapse elimination has been proposed to strengthen an initially weaker topographic gradient (Brown and Booth, 1983; Hardman and Brown, 1985; Bennett and Ho, 1988; but see English, 1986). The fact that topographic accuracy can be reestablished during reinnervation (Hardman and Brown, 1987; Laskowski and Sanes, 1987b) indicates that timing differences in outgrowth and synapse formation are not required to establish the pattern, thereby strengthening the proposition that molecular markers are involved. In at least some muscles, however, axons entering through different primary nerve branches innervate contiguous but spatially distinct compartments within the muscle (English and Weeks, 1984; Balice-

Gordon and Thompson, 1988). Synapse elimination does not contribute to this pattern (Donahue and English, 1987; Balice-Gordon and Thompson, 1988). The compartmental innervation itself is topographically represented in the spinal motor pool (Weeks and English, 1985). Hence while synapse elimination might serve to further refine topography within compartments (Bennett and Ho, 1988), axonal guidance mechanisms may be largely responsible for the initial development of this intramuscular organization.

Reinnervation studies afford a convenient paradigm for analysis of specificity in a competitive environment, particularly because a positive finding implicates molecular markers. A clear preference for muscles to be reinnervated by their original motor neurons has been demonstrated in leech (Van Essen and Jansen, 1977) and axolotl (Wigston and Kennedy, 1987). In adult mammalian muscle, specific recognition of appropriate muscles does not appear to occur during reinnervation (Weiss and Hoag, 1946; Bernstein and Guth, 1961; Gerding *et al.*, 1977; but see Hoh, 1975). Similarly, specific reinnervation of muscle fiber types is not found in mature animals (Karpati and Engel, 1968; Miledi and Stefani, 1969; Kugelberg *et al.*, 1970). Whether type selective reinnervation could occur in neonates remains an interesting question. The topographic reinnervation of intercostal muscle in neonatal rats contrasts with the situation in adults, where the pattern of reinnervation was random (Hardman and Brown, 1987). In two other muscles, Laskowski and Sanes (1987b) report topographic reinnervation at both ages, although they observed greater selectivity in neonates. Interestingly, a study by Hoh (1975) conducted on younger (3 week) rats suggested specificity of reinnervation when soleus and extensor digitorum longus (EDL) muscle nerves competed to reinnervate the EDL or soleus muscles. The finding that the EDL was preferentially reinnervated by the EDL nerve, while both muscle nerves competed

equally within the soleus muscle, is consistent with fiber type selectivity. In the present study, we have examined single motor unit contractile properties following reinnervation in newborn rabbits, which we feel offers a more direct approach to the issue of fiber type specificity during reinnervation.

The two- to threefold range of single motor unit twitch tension rise times in normal neonatal rabbit soleus muscles analyzed *in vitro* at 19°C offers a convenient assay for possible fiber type specificity in reinnervation. While a measure of the breadth of the rise time distribution would be adequate, the distribution is in fact multimodal, exhibiting a well defined peak of fast contracting motor units, and a broader band of slow contracting motor units possibly encompassing two distinct peaks. Early glycogen depletion studies in adult animals (Kugelberg, 1973, 1976; Burke *et al.*, 1973) together with direct evidence concerning the fiber type composition of neonatal motor units (Thompson *et al.*, 1984) support the inference that fast contracting units are composed primarily of type II muscle fibers, while slow contracting units comprise mostly type I muscle fibers. The distributions of twitch rise times of reinnervated units which we obtain following nerve crush at either postnatal day 1 or 4 are substantially narrower than the normal control distribution, are unimodal in appearance, and are intermediate in timing to the normal fast and slow populations. Computer simulations indicate an upper bound of 30% for fiber type selectivity during reinnervation, but also suggest that selectivity is probably less, and may be absent altogether. A reasonable conclusion to draw from these results is that returning motor axons reinnervate muscle fibers largely at random, independent of their type, and that reinnervated units consist of combinations of fast and slow muscle fibers which fluctuate around the average frequency of occurrence within the muscle.

To support this conclusion, it was essential to establish that during the brief

interval of denervation following nerve crush, muscle fibers had not de-differentiated in a manner which would either prevent recognition of their type by ingrowing motor axons or hinder the detection of specific reinnervation by our assay. The approach we adopted was to emulate the denervation episode by inducing a transmission blockade, using BoTx, for an equal interval. Both neurally evoked and spontaneous transmitter release are drastically reduced but not completely eliminated by BoTx (Cull-Candy *et al.*, 1976). This approach would not be effective in duplicating the possible loss of trophic influences which might be present due to physical proximity, but not involving neural activity. However, changes in any of a wide array of fiber type related characteristics, including contractile rate and ATPase histochemistry (Salmons and Sréter, 1976), and metabolic properties and contractile protein isoforms (Pette *et al.*, 1976; Klug *et al.*, 1983) are dependent upon the character of neural activity, and most likely, of muscle fiber activity (Lømo and Rosenthal, 1972; Lømo *et al.*, 1974). Hence a treatment which blocks activity should provide an adequate control for denervation effects. We find that a nearly normal distribution of twitch rise times is maintained during a 6 day interval of transmission blockade, indicating that loss of muscle fiber differentiation is not likely to be a factor in our results. Thus we conclude that chemospecific recognition leading to selective reinnervation according to muscle fiber type was not present to any substantial degree in our experiment. We cannot rule out the possibility that recognition molecules present at the moment of surgery were lost due to the disruption of connectivity. More significantly, our results leave open the possibility that chemospecific recognition is important in establishing the initial specificity of innervation. Markers present during ingrowth and synaptogenesis could disappear early in development.

Soileau *et al.* (1987) have reported results from reinnervation studies in neonatal

rat soleus which appear to be in conflict with our own. Using glycogen depletion to label muscle fibers in individual motor units, they found that the fiber type composition of reinnervated units was distinctly non-random for 10 of the 12 units studied, although it varied almost continuously across the available spectrum. A key difference in their paradigm is that they waited 10 days or more following reinnervation for synaptic connections to strengthen sufficiently to support the long term tetanic stimulation required to achieve depletion. Thus one formal possibility is that random reinnervation is followed by fiber type respecification deriving from the subsequent pattern of neural activity. They offered plausible controls to rule out this possibility, and in any event, we saw no indication of an increase in reinnervated motor unit contractile diversity in rabbit soleus analyzed 2 weeks post-crush. Differences in the ability of appropriate vs. inappropriate synaptic connections to maintain transmission during the rigorous glycogen depletion process is also possible (Soileau *et al.*, 1987). Such a difference would reflect small yet interesting variations in selectivity which may not be detectable using an assay based on twitch contractions. Another possibility (Soileau *et al.*, 1987) is that an initially random polyneuronal reinnervation is followed by loss of inappropriate connections. Once again, our histogram of reinnervated units at two weeks following crush does not support this explanation. It is interesting to note that gestation in rabbit is 10 days longer than in rat, and at least one early developmental event, the episode of neonatal synapse elimination, is completed at a significantly earlier postnatal age (by 4–7 days) in rabbits (Bixby and Van Essen, 1979a) than in rat (Brown *et al.*, 1976). Hence, a particularly interesting alternative for reconciling the two results is that the rat experiments were conducted just prior to the loss of markers necessary for selective reinnervation, while our study on rabbits involved reinnervation just after this milestone.

Defining the roles which positional or type specific markers may play in the development of motor specificity remains a challenging problem. If molecular markers are in fact significant in the generation of fiber type specificity during normal development, it will be interesting to understand the expression and regulation of these markers, and the process by which they are lost or rendered inaccessible near the age of birth. Our results suggest, however, that further consideration of alternative mechanisms, perhaps including differences in developmental timing, remains worthwhile.

Chapter 3

SYNAPSE ELIMINATION BY FIBER TYPE AND MATURATIONAL STATE IN RABBIT SOLEUS MUSCLE

INTRODUCTION

The soleus muscle at birth consists of a matrix of distinct muscle fiber types differing in metabolic and contractile properties as well as enzyme immunoreactivity and histochemistry. Of the two predominant fiber types, type II (fast contracting) are roughly twice as common as type I (slow contracting) in neonatal rabbit soleus (Gordon, 1983). Muscle fibers are extensively polyinnervated at birth, but soon experience an episode of synapse elimination during which they attain their mature configuration of a single neural input (Redfern, 1970; Brown *et al.*, 1976; Van Essen, 1982). In mature animals, motor units (each consisting of a motorneuron together with the muscle fibers it innervates) are composed almost exclusively of a single fiber type (Edstrom and Kugelberg, 1968; Kugelberg, 1973; Burke *et al.*, 1973). Recently, glycogen depletion experiments in rat (Thompson *et al.*, 1984) and twitch tension measurements in rabbits (Gordon and Van Essen, 1985) have demonstrated that a similar pattern of specific innervation by fiber type exists in neonatal muscles well before synapse elimination is completed. While less homogeneous than in the adult, the composition of individual motor units is heavily biased toward one or the other of the two major fiber types. In the rabbit soleus, two largely distinct populations of motor units exist even at a time of fourfold polyinnervation.

In the present study, we have utilized the technique of intracellular labeling of particular muscle fibers with the fluorescent dye Lucifer Yellow to investigate two issues involving the relative development of the two classes of motor units. The first issue concerns whether there are differences in the timing of synapse loss for fast and slow motor neurons. Consideration of this possibility is motivated by the observations that primary and secondary myotubes are formed at different times (Wirsen and Larsson, 1964; Kelly and Zacks, 1969), and develop preferentially

to become the initial complement of slow and fast muscle fibers, respectively (Rubinstein and Kelly, 1981). This leads to the suggestion that the specificity of innervation by fiber type in early muscles might involve the sequential arrival of two sets of motorneurons timed to match the staggered developmental schedule of primary and secondary myotubes (Rubinstein and Kelly, 1981), thereby producing two largely independent sets of motor units. If there is indeed a significant temporal difference in the initial formation of fast and slow motor units, a corresponding timing difference might persist through subsequent developmental events. Relevant to this hypothesis is the report by Riley (1977b) that, in the rat soleus, the last fibers to lose their polyneuronal innervation are predominantly of the fast histochemical type. To study more directly the relative time course of synapse elimination in the two fiber populations, we injected Lucifer Yellow into individual muscle fibers whose innervation state was first clearly identified by recording single or compound intracellular end plate potentials. The histochemical type of each labeled fiber was then determined in muscle cross sections.

The second issue deals with the state of innervation in juvenile animals, well after the bulk of synapse elimination is completed. A significant incidence of residual polyinnervation has been reported in the soleus and lumbrical muscles of rats aged 3–6 weeks (Taxt *et al.*, 1983; Taxt, 1983), whereas the peak period of synapse elimination occurs during the first two postnatal weeks (Brown *et al.*, 1976; Betz *et al.*, 1979). This finding was of particular interest owing to other evidence for a synaptic reorganization at a late developmental stage. Gordon (1983) has found changes in the relative sizes of motor units, as measured by twitch tension, between 2 and 5 weeks of age in rabbit soleus. His evidence suggests that slow motor units expand in size relative to fast motor units. This could imply a secondary stage of synaptic reorganization well after the initial period of

heavy polyneuronal innervation. Transient dual innervation of some muscle fibers could be an intermediate state in such a reorganization, reflecting the capture of histochemically fast muscle fibers by slow motorneurons. In this scenario, histochemical type conversion of the newly captured muscle fibers (Buller *et al.*, 1960; Kugelberg *et al.*, 1970; Salmons and Sréter, 1976) would lag the onset of dual innervation by at least several days (Pette *et al.*, 1976; Klug *et al.*, 1983). Our initial intent was to identify polyinnervated fibers in the soleus of juvenile rabbits, and to determine their histochemical type by using the Lucifer Yellow labeling technique. While we replicated the basic observations of apparent compound endplate potentials in soleus muscles of the appropriate age, a more detailed analysis suggests that the multicomponent responses are artifactual and do not represent genuine polyneuronal innervation.

MATERIALS AND METHODS

Pregnant female New Zealand White rabbits were obtained from ABC Rabbitry (Pomona, CA), and a pregnant female Sprague-Dawley rat was obtained from Simonsen (Gilroy, CA). Experiments were conducted using soleus muscles of immature animals of either sex. Relative time course studies (Experiment 1) were performed using rabbits aged from 7 to 11 days, while late stage polyinnervation experiments (Experiment 2) utilized rabbits aged from 17 to 23 days and rats aged from 22 to 30 days. Animals were aged from the time of birth, even though the gestation period in rabbits varied by as much as three days. Previous evidence from this laboratory (Bixby and Van Essen, 1979a; Gordon and Van Essen, 1985) has indicated that intra-litter variation in size, weight, and muscle fiber differentiation is comparable to the variability between litters of the same age as calculated by this method. Physiological measurements (see Results) confirmed the separability of the two age groups (7–8 days and 10–11 days) used for Experiment 1 in terms of the overall degree of polyneuronal innervation.

***In Vitro* Physiology and Dye Labeling.** For the relative time course experiment, the soleus muscle along with several mm of its nerve was isolated under ether anesthesia, freed of excess connective tissue, and pinned out in a plexiglass chamber. The muscle was continuously superfused with oxygenated Ringer's (Gordon and Van Essen, 1985) at room temperature, to which was added D-tubocurarine (Sigma; 1–2 mg/liter) to prevent nerve evoked muscle contraction. Graded stimuli were applied to the muscle nerve using a suction electrode, and endplate potentials (e.p.p.'s) were monitored with an intracellular glass microelectrode. While e.p.p.'s often fluctuated considerably in magnitude (Bixby and Van Essen, 1979a), the presence or absence of multicomponent e.p.p.'s,

indicative of polyneuronal innervation of the muscle fiber, could be reliably assessed in nearly all fibers having responses greater than about 2 mV.

Glass microelectrodes, produced using a Brown-Flaming P77 micropipette puller, were filled with a 12% solution of Lucifer Yellow CH (Sigma) in 1 M lithium chloride. When a muscle fiber exhibiting the desired response (single- or multi-component e.p.p.) was unequivocally identified, Lucifer Yellow was pressure injected into the fiber. Applied air pressure was gradually increased from zero to 20 psi and maintained at that level for 2–3 minutes. Pressure injection was chosen over iontophoresis both for convenience and to allow a greater salt concentration within the micropipette, which in turn permitted reduced resistance values and hence lower noise levels. A drop in electrode resistance resulting from electrolyte flow was also useful in monitoring dye injection. Electrodes having a resistance of about 20 MΩ proved most effective. Resistance above 25 MΩ permitted little if any dye flow, while resistance values below 16 MΩ often resulted in leakage of Lucifer Yellow into all fibers penetrated. Generally between 10 and 30 muscle fibers were examined in each muscle analyzed, while between 1 and 6 of these fibers were labeled by dye injection. Following examination and dye labeling, surface fibers of the muscle were lightly fixed for 40 seconds in 0.5% paraformaldehyde in 0.1 M phosphate buffer (pH = 7.3). Fixed muscles were rinsed twice in 30% sucrose, then stretched and frozen in isopentane cooled to dry ice temperature, and stored at -70°C.

For the residual polyinnervation analysis (Experiment 2), the cut muscle preparation (Barstad, 1962) was employed to prevent muscle contraction while preserving larger stimulus evoked endplate responses. As shown by Taxt *et al.* (1983), this procedure gave a better signal to noise ratio, making it easier to detect tiny e.p.p. components than the conventional curarized preparation. For the rabbit, because of the more proximal nerve insertion, the proximal end must

be cut obliquely, between (and parallel to) the tendon and the major intramuscular nerve trunk. The distal end was also removed, and the central muscle fragment was pinned in the Sylgard (Dow Corning) coated lid of a small plastic petri dish. The geometry of the nerve insertion, together with the need to occasionally trim the muscle further to maintain appropriate resting potentials, made recording from the ventral surface of the muscle difficult. Thus we examined the dorsal surface, even though the majority of postnatal fiber conversion takes place in the ventral half of the muscle (Gordon, 1983). The more central nerve insertion in the rat soleus allowed the muscle to first be pinned tightly and then trimmed squarely at each end. The Sylgard filled dish was anchored in the aforementioned plexiglas chamber and superfused with oxygenated Ringer's.

Electrophysiology with the cut muscle preparation was performed using Lucifer Yellow filled electrodes, as described above, for rabbit experiments. The rat experiments, aimed at repeating the observations of Taxt *et al.* (1983), were performed using electrodes filled with 5 M potassium acetate (without Lucifer Yellow). On average, 26 fibers per muscle were examined. Resting potentials in the cut muscle preparations ranged between -50 mV and -20mV, while e.p.p.'s were generally 3–12 mV. Labeled muscles were briefly fixed as above, then frozen while still pinned by dropping the entire Sylgard coated petri dish into cold isopentane. The central section of the muscle was cut away from the pins and stored at -70°C.

Fiber Type Identification. Muscle cross sections were cut at 10 μm in a cryostat (-20°C), and approximately 1 in 5 was saved in the region of dye injection. We adopted a strategy of both identifying fluorescent fibers and then determining their histochemical type using the same sections, as we found that small variations in geometry near the muscle margin often made correlation difficult in serial sections. Sections were air dried, then inspected for the presence of fluorescent

dye-filled fibers using a Leitz microscope. To reduce the likelihood of scoring fibers labeled by inadvertant dye leakage, two criteria were adopted. First, the geometry and order of initial appearance of labeled fibers must match that of rough maps sketched during physiology sessions. Second, dye labeling must persist through a series of sections extending at least 0.5–1.0 mm of muscle length. Following initial visual characterization of labeling, short wavelength illumination was discontinued and representative sections were photographed using Polaroid 55 P/N film and transmitted white light. Photography of the unstained, uncoverslipped sections was necessary since Lucifer Yellow fluorescence does not survive ATPase staining. After photographing a section, labeled fibers were identified and marked on the print by alternating between fluorescence and normal viewing. Generally, each labeled fiber was located and marked on photos of at least 5 sections.

Sections were stained for myofibrillar ATPase activity following pre-incubation at pH 10.4 according to the method of Guth and Samaha (1970). Stained sections were moistened with a drop of distilled water and again photographed with Polaroid film. Corresponding photos before and after staining were compared to identify the histochemical fiber types of the previously marked dye labeled fibers. In every section in which a labeled fiber was identified, an assignment was made to one of five descriptive categories: definite Type I, probable Type I, uncertain, probable Type II, or definite Type II. A clear consensus classification was apparent for each fiber. About 6% (29 of 480) of all sections were scored as uncertain, while only 2.9% (14 of 480 sections) were scored contrary to the ultimate consensus type, and these appeared as isolated single occurrences scattered among the 97 labeled fibers. Incorrect identification of the injected fiber when matching the fluorescence and ATPase photographs, due primarily to minor geometric distortions during processing, is the most likely source of these occasional inconsistencies in fiber type

determination.

Data Analysis. For the time course experiment, statistical comparison of the degree of polyinnervation by fiber type for a given age group was made using the raw observational data of Fig. 3. The relative number of Type I and Type II fibers in the singly innervated group was compared directly to the fiber type distribution of the multiply innervated group, using the χ^2 test. We also estimated the percentage of fibers of either histochemical type which were polyinnervated at a given age by applying Bayes' theorem (e.g., Papoulis, 1965). The probability $P(M_A|T_I)$ of finding multiple innervation at age A, conditioned upon the assumption that only Type I fibers are sampled, is:

$$P(M_A|T_I) = \frac{P(T_I|M_A)P(M_A)}{P(T_I|M_A)P(M_A) + P(T_I|S_A)P(S_A)}$$

Estimates of the conditional probability $P(T_I|M_A)$, that a multiply innervated fiber is also Type I, and $P(T_I|S_A)$, that a singly innervated fiber is also Type I, were provided directly by the type distributions of dye-labeled fibers (Fig. 3). The probability of a fiber being multiply innervated, $P(M_A)$, or singly innervated, $P(S_A)$, at age A was taken to be the average prevalence of polyinnervation in all muscles from that age group (Fig. 1).

To determine the sensitivity of the time course experiment, we calculated, for each age group, hypothetical experimental outcomes corresponding to the minimum difference in the distributions of Type I and Type II fibers which would be significant at the 1% level, using the χ^2 test. First, the experimental data from the singly innervated group was taken to define the "expected" outcome, and hypothetical fiber type distributions were calculated for the multiply innervated group to satisfy the significance constraint. The relevant quadratic equation yields two such distributions. The total number of hypothetical observations was forced

to equal the actual total of labeled, multiply innervated fibers, and fractional fibers were permitted. Next, the multiply innervated group was taken to define the expected outcome, and the calculation was repeated, yielding a total of 4 hypothetical outcomes for each age group. For each hypothetical outcome, the corresponding frequency of polyinnervation for each fiber type was calculated using Bayes' theorem, as described above. The resulting differences between Type I and Type II fibers in percent polyinnervation provide estimates of the minimum detectable difference inherent in our experiment. The four estimates for each age group were averaged, and then converted to a timing difference by dividing by the average rate of synapse elimination defined by the slope of Fig. 1.

RESULTS

Experiment 1. Polyinnervation by Fiber Type

Neonatal rabbit soleus muscles were examined in a curarized, *in vitro* preparation, using intracellular recordings to determine the innervation state of individual muscle fibers. Particular muscle fibers were classed as either singly innervated or multiply innervated depending upon whether one or more distinct components of the endplate potentials were distinguishable during careful gradations of nerve stimuli. To avoid incorrect identifications within the small population to be analyzed, fibers having any hint of ambiguous classification were not injected. Fibers having the desired innervation pattern were labeled by pressure injection of the fluorescent dye Lucifer Yellow. For one series of muscles, only singly innervated fibers were labeled; multiply innervated fibers were labeled in a second set of muscles.

Two age groups, 7–8 days and 10–11 days postnatal, were selected for study. These ages correspond to the early and late stages of the appearance of singly innervated fibers (Fig. 1). In 7 day and 8 day rabbits, the mean incidence ($\pm$ standard deviation) of polyinnervation was 81% $\pm$ 10% and 69% $\pm$ 13% respectively. By days 10 and 11, the percentage of multiply innervated fibers had declined to 20% $\pm$ 13% and 15% $\pm$ 10% respectively. From these data we estimate the rate of synapse elimination in the intervening period (7.5–10.5 day) to be 19% per day; synapse loss occurred on more than half of the muscle fibers between these two time windows.

Labeled fibers were subsequently identified and their histochemical types determined in a series of cryostat sections (see Methods). Two multiply innervated

Figure 1. Percentage of muscle fibers remaining polyneuronally innervated in each of the muscles examined in the time course experiment. The two age groups chosen for study, 7–8 days and 10–11 days postnatal, were selected as defining the extremes of the steep sloping region of the synapse elimination curve. Muscles in which only singly innervated fibers were injected (circles) are distinguished from those in which only multiply innervated fibers were injected (triangles) to highlight any detection bias. A few 9 and 13 day muscles are included to more fully delineate the shape of the curve.

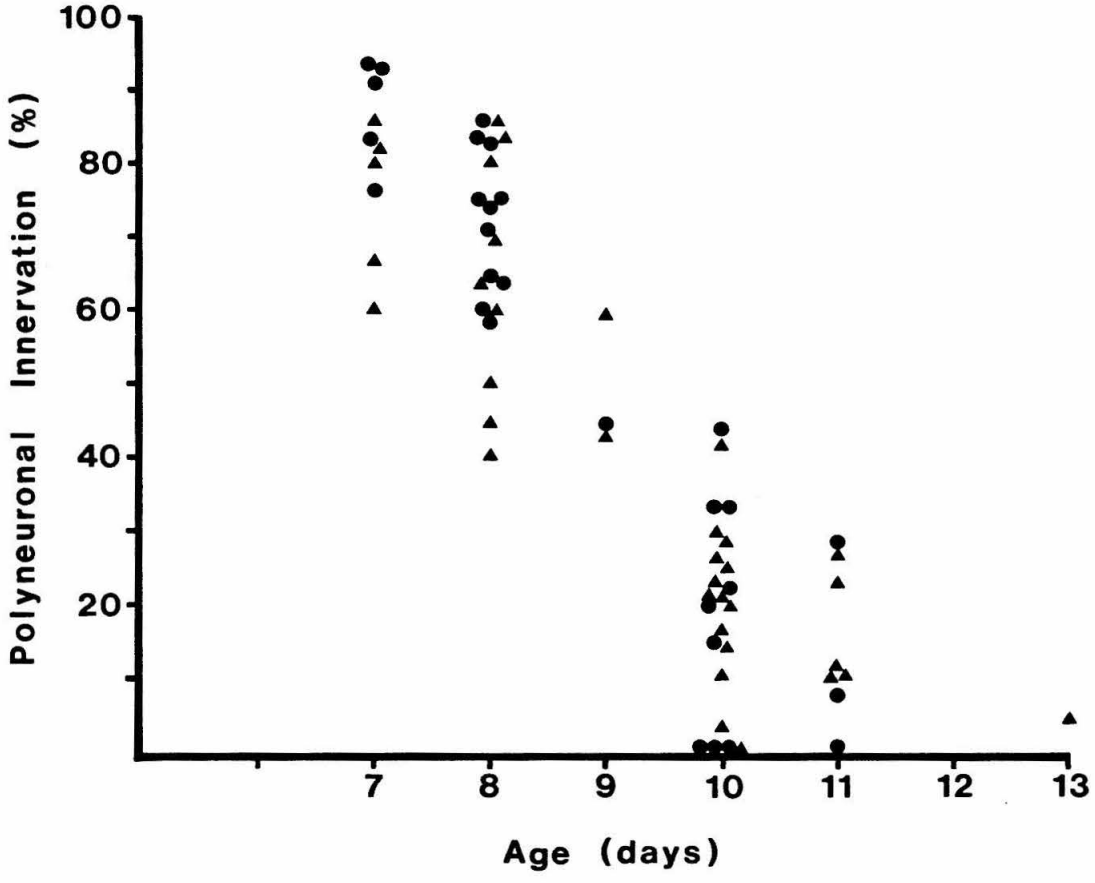
100
80
60
40
20
Polyneuronal Innervation (%)
7
8
9
10
11
12
13
Age (days)

Figure 1

fibers appearing at the surface of an 11 day soleus are shown in Fig. 2. Both fibers were pale staining and identified as Type I.

Comparative time course results are summarized in Fig. 3. For the 7–8 day group, the incidence of Type I fibers was 59% (13 of 22) among the singly innervated fibers and 53% (14 of 26) among multiply innervated fibers. This difference is not significant ($p > 0.5$, χ^2 test). Among the 10–11 day age group, the incidence of Type I fibers was 70% (16 of 23) among singly innervated fibers and 81% (21 of 26) among multiply innervated fibers. This difference is also not statistically significant ($p > 0.2$). Despite the 2-fold greater prevalence of type II fibers, a sampling bias favoring type I fibers is apparent, presumably owing to their larger size: the cross-sectional area of the slow fiber type averages twice that of fast fibers at these ages (Gordon, 1983). The fact that this sampling bias is greater for the older group is puzzling. The two age groups were examined sequentially; hence, one possibility is that there were systematic changes in any of several factors involved in successful dye labeling, such as electrode properties or details of pressure application. In any event, because analysis of the two age groups is independent, a change in sampling bias is not critical to our major findings.

While the experimental observations reflect the distribution of fiber types for a given innervation state, it is also of interest to reverse this ordering and express the degree of polyinnervation as a function of fiber type. Because singly and multiply innervated fibers were labeled in separate sets of muscles, the relative number in each category identified in this study (Fig. 3) does not reflect their actual frequency of occurrence in muscles of the appropriate age (Fig. 1). Hence polyinnervation by fiber type cannot simply be determined by regrouping the data of Fig. 3. However, Bayes' theorem can be applied to obtain the desired transformation, as described in Methods. Essentially, this procedure weights the observations of Fig. 3 in a manner

Figure 2. Two dye labeled, multiply innervated fibers from an 11 day muscle. Both fibers were located on the dorsal surface of the muscle. (A) Fluorescent fibers (arrows) are readily detected against faintly illuminated background in unstained cross sections. (B) The same section stained for alkali stable ATPase activity. Both fibers were Type I (slow). Just under half of the fibers labeled appeared at the surface in at least one section. The artifacts encountered in cut muscles (see Experiment 2) would not be expected in the less sensitive curarized preparation, and indeed there was no significant difference between singly and multiply innervated fibers regarding the percentage appearing at the surface. Scale bar = 100 μm.

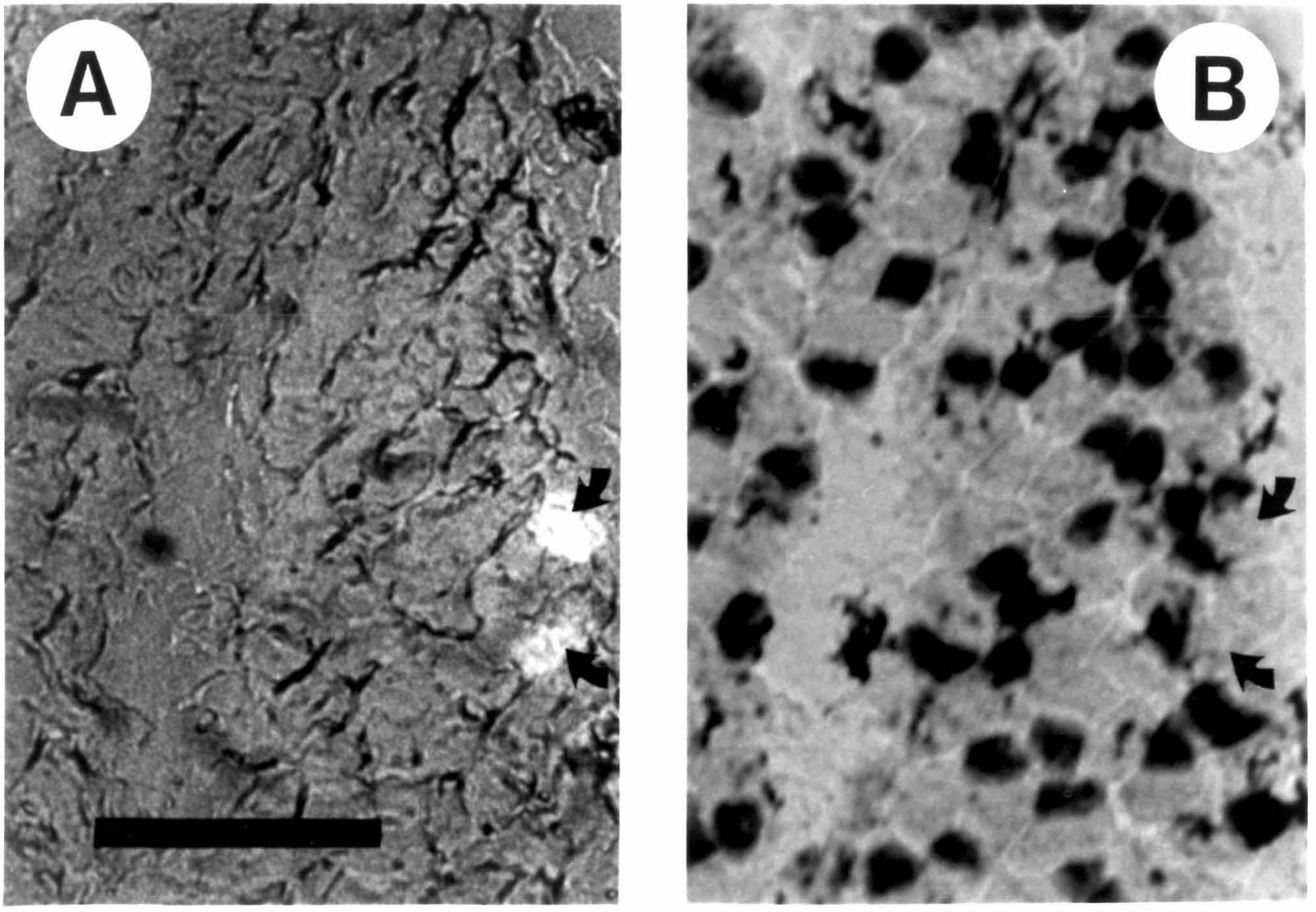
A
B

Figure 3. Distributions of histochemical fiber types for singly innervated and multiply innervated fibers in each age group. Height of bars normalized to Type I frequency for each pair. Total number of fibers appears above each bar. The difference in percent polyinnervation between fiber types is not statistically signficant at either age. A moderate sampling bias for slow fibers is apparent, probably owing to their larger size. It should be noted that 3 of the 5 type II fibers in the 10–11 day multiply innervated group were found in a single muscle. Three other labeled fibers in this muscle were type I. Omitting this muscle from the scoring would result in a difference which, while still not significant at the 1% level, would suggest a tendency of type I fibers to retain their polyinnervation slightly longer. There is no evidence that this particular rabbit lagged developmentally, however, as the percentage of polyneuronally innervated fibers in this muscle (21%) was well within the normal range for a 10 day muscle.

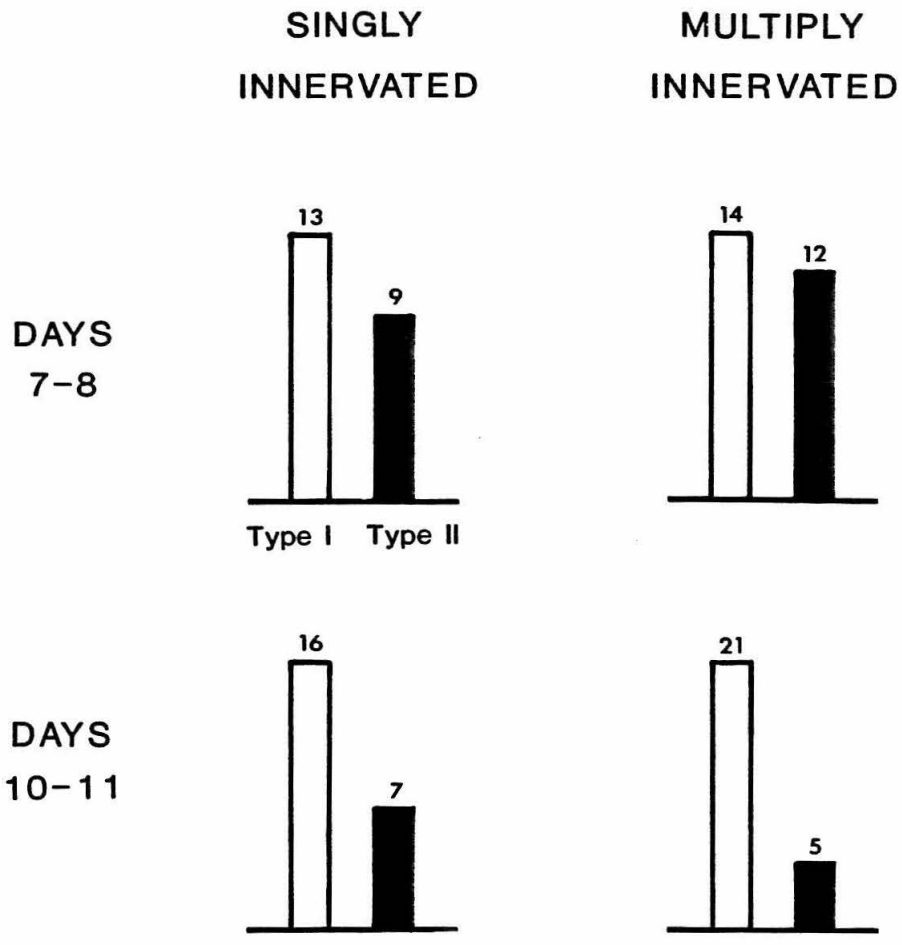
SINGLY INNERVATED
MULTIPLY INNERVATED
DAYS 7–8
13
9
14
12
Type I
Type II
DAYS 10–11
16
7
21
5

Figure 3

consistent with the actual overall frequency of polyinnervation (Fig. 1) prior to regrouping. The estimates thus obtained suggest that in the 7–8 day age group, the incidence of polyinnervation was 73% for Type I fibers and 77% for Type II fibers; in the 10–11 day group, 19% of Type I fibers and 12% of Type II fibers were multiply innervated.

The ability of our approach to detect any small differences there might be in timing between the fast and slow types is limited by the actual numbers of fibers labeled. To estimate the sensitivity of this analysis, we first ascertained what difference in the incidence of the two fiber types between the singly and multiply innervated populations would just be significant at the $p = .01$ level (see Methods). This numerical difference was converted into a minimum detectable difference in the percentage of polyinnervation for fast and slow fibers, again using Bayes' theorem. The percentage differences, 23% at days 7–8 and 15% at days 10–11, can be transformed to a time difference using the appropriate average rate of synapse elimination. Using the rate of 19% per day loss in polyinnervation from Fig. 1, this translates to a timing difference of about 1 day that would be detectable given our particular sample size. The detectable difference would be somewhat larger if one used the lower rates associated with early and late parts of the sigmoidal curve of Fig. 1; on the other hand, it would be smaller if one used a less stringent ($p < .05$) criterion.

Experiment 2. A Test for Residual Polyinnervation in Older Muscles

Based upon observations in curarized muscles, the bulk of synapse elimination in the rabbit soleus muscle is completed by day 13 postnatal (Fig. 1; see also Bixby and Van Essen, 1979a). Using the cut muscle preparation (Barstad, 1962), we observed a low incidence of compound e.p.p.'s in response to graded nerve stimulus

in muscles from rabbits aged 17–23 days. These closely resembled the compound e.p.p.'s originally described by Taxt *et al.* (1983) at a comparable stage in rat soleus (25–31 days postnatal). One component was consistently much smaller, with a peak amplitude rarely exceeding 10% of the larger component. Occasionally, but not always, a distinct latency difference existed in the onset of the two components. We observed such compound e.p.p.'s in 2.8% of fibers tested (24 of 863 fibers in 32 muscles). Our original intention was to test whether multiply innervated fibers at this age would consist predominantly of a single histochemical type. Using the Lucifer Yellow labeling technique, 4 of the first 7 fibers labeled were Type II. However, this part of the analysis was discontinued when it became apparent that the compound e.p.p.'s were unlikely to represent genuine polyneuronal innervation of the monitored fibers.

Several observations support the view that the compound e.p.p.'s reflect an electrical coupling between muscle fibers that was artifactually induced by the process of electrode penetration (Fig. 4). The first indication of this came from the biased distribution of compound e.p.p.'s with respect to fiber depth. In order to maximize the number of fibers sampled in a situation where we were looking for a rarely occurring event, we routinely recorded from both surface and deeper fibers in succession. After each surface fiber was characterized, the electrode was advanced until resting potential was lost. If a second stable resting potential with a large e.p.p. was encountered within a reasonable distance, the recording was accepted as a "deep" fiber. Interestingly, compound e.p.p.'s were *never* observed in recordings from the 450 fibers noted at the time of the recording to be on the muscle surface. Instead, 20 of the 24 compound e.p.p.'s encountered could be assigned to a deep fiber. Seventeen of these were based on depth assignments made at the time of the recording and came from a population of 208 deep fibers, an 8.2% incidence.

Figure 4. Example of a compound endplate potential occurring under circumstances consistent with a coupling artifact. The first response of each set of superimposed traces is to test stimuli varied gradually in strength. The second peak is the response to supramaximal stimuli delivered 20 msec later. (A) The surface fiber penetrated initially was singly innervated, as were all surface fibers examined. (B) Advancing the electrode into a deeper fiber yielded a compound response. The smaller component had a threshold indistinguishable from that of surface fiber (A).

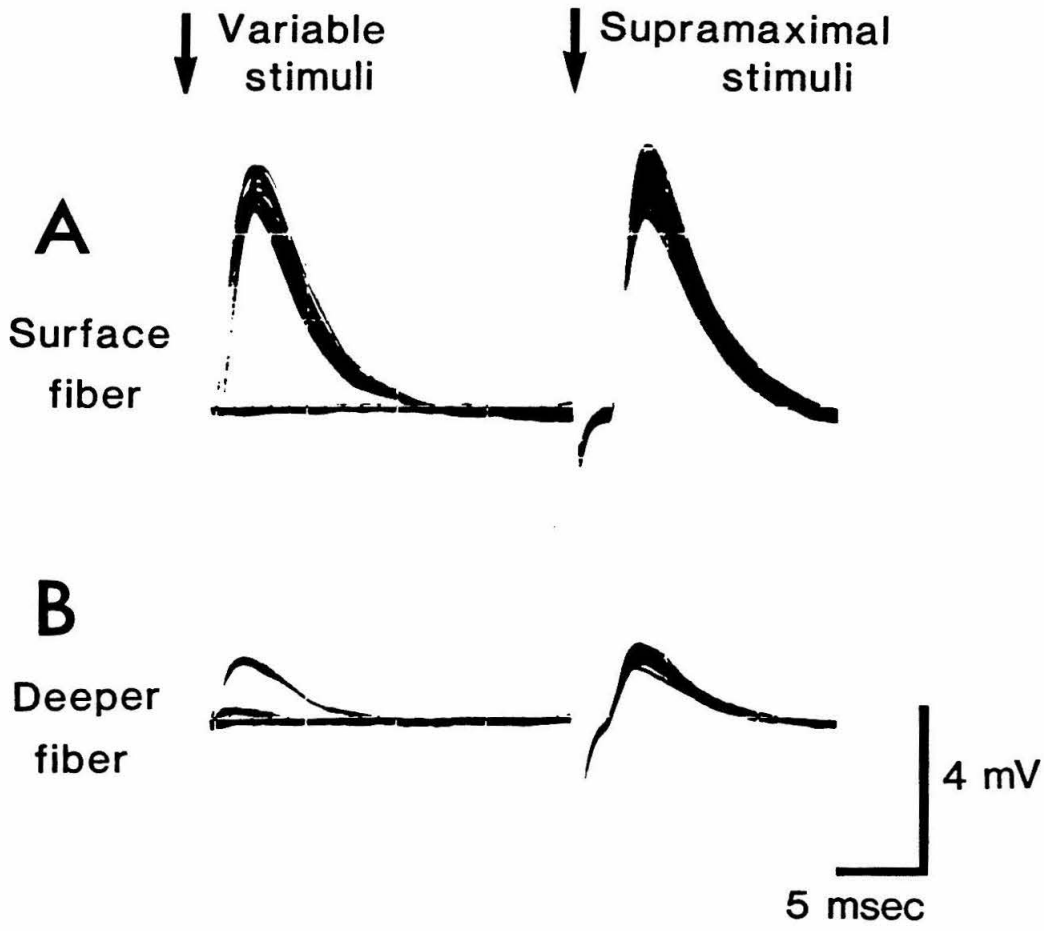
Variable stimuli
Supramaximal stimuli
A
Surface fiber
B
Deeper fiber
4 mV
5 msec

Figure 4

Three additional cases were based on dye-labeled fibers identified in histological sections. No depth information is available concerning the remaining 4 compound responses, which were observed before we began routine monitoring of fiber depth. The total absence of any surface polyinnervation is highly significant ($p < .005$) when compared with the overall frequency of compound e.p.p.'s of 2.8%, and even more significant ($p < .001$) when compared with the rate of compound e.p.p.'s in deep fibers.

After noticing this segregation by recording depth, we began to carefully monitor and record the stimulus threshold at which e.p.p. components were observed, in order to assess whether the minor input to deeper fibers was distinct from the main input to overlying fibers. For all 6 fibers appropriately tested, the threshold of the small component was indistinguishable (within 1–2%, or 0.05 V out of 3–5 V) from that of the overlying fiber previously penetrated (Fig. 4). In contrast, for only 15 of the 82 instances in which adjacent pairs were examined did the thresholds of the upper and lower fibers differ by 0.05 V or less, implying that the chance occurrence of such minimal threshold differences in 6 of 6 cases is extremely unlikely ($p < .001$).

Additional evidence suggestive of transient induced coupling arises from comparison of the peak amplitude of the two components during the course of individual penetrations. We often observed the large component change in size independently of the small one during the course of a single observation, for example when the resting potential slowly declined. In a genuinely polyinnervated fiber, reductions in e.p.p. magnitude resulting from loss of resting potential would be expected to affect both components proportionally. Similarly, the smaller component sometimes shrank visibly, and occasionally vanished, in a manner apparently independent of the larger component, probably resulting from a weakening in the electrical continuity with the overlying fiber.

One final observation was particularly suggestive of coupling artifacts. Occasionally, apparent compound e.p.p.'s were induced by slowly withdrawing the recording electrode after verifying single innervation of a deeper layer fiber. In two of the five examples observed, the electrode remained within the deeper fiber while apparent electrical continuity with the surface fiber, previously determined to be singly innervated, was reestablished (Fig. 5). In these cases, the smaller component of the compound response appeared at the stimulus threshold of the surface fiber, which was lower than that of the deeper fiber. In another case, the electrode appeared to have returned to the surface fiber, based upon the higher stimulus threshold originally observed in the surface fiber, while leaving a low resistance pathway to the deeper fiber along its track. In the remaining two cases, the e.p.p. threshold of the surface and underlying fibers were too similar to distinguish between these possibilities. Although the precise sequence of events was not always the same, the important point is that multicomponent responses were induced in fibers previously determined to be free of compound e.p.p.'s.

Pursuant to these observations in rabbit soleus, we attempted to replicate the observations of Taxt *et al.* (1983) in rat soleus in order to analyze the character of any compound e.p.p.'s. In tightly pinned cut muscles from animals aged 22–30 days (see Methods), we failed to observe any compound potentials in 160 fibers from 7 muscles in which the amplitude of observed responses was at least 4 mV. Such a result is highly unlikely ($p < .005$, χ^2 test) if multiply innervated endplates occurred at the 5% frequency suggested by Taxt *et al.* (1983). We then analyzed two muscles which were pinned loosely (a situation prevelant in cut rabbit muscles due to the less favorable nerve insertion), and observed two fibers demonstrating compound potentials from among 45 tested. Each of these fibers was found beneath the surface layer and yielded responses which resembled the artifacts encountered in

Figure 5. Example of apparent compound endplate potential established by slow electrode withdrawal. (A) Singly innervated surface fiber. (B) Deeper fiber was also singly innervated, with response appearing at higher stimulus threshold. (C) Slow electrode withdrawal yielded a compound response. The electrode remained in deeper fiber, as the smaller component appeared at the threshold of the surface fiber response, while the upper trace continued at the threshold of the deeper fiber. In other cases, repositioning of the electrode into the surface fiber apparently occurred.

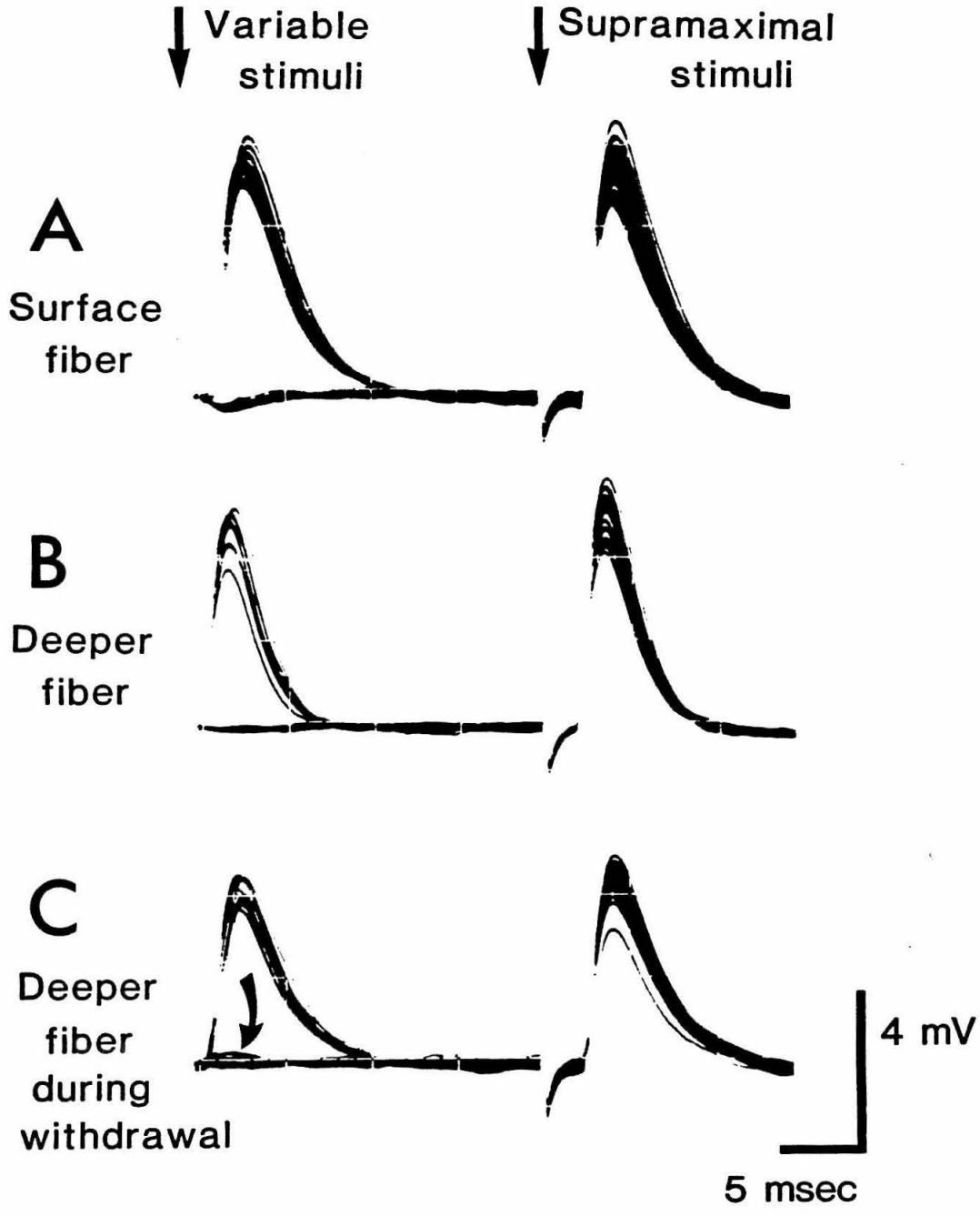
Variable stimuli
Supramaximal stimuli
A
Surface fiber
B
Deeper fiber
C
Deeper fiber during withdrawal
4 mV
5 msec

Figure 5

the rabbit: one small component appeared at the voltage threshold of the overlying fiber, with the major component at a higher threshold.

DISCUSSION

Polyinnervation by Fiber Type

From the first experiment in this study, we conclude that there is no discernible difference in the degree of polyinnervation of fast vs. slow muscle fibers in the rabbit soleus during the interval of 7–11 days postnatal. While a substantial majority of fibers remain polyinnervated at day 7, the interval studied constitutes the late phase of synapse elimination. It is useful to discuss our finding in relation to what else is known about the timing and extent of synapse formation and elimination. In particular, there have been several suggestions of significant differences in maturation of the fast and slow motor units, which contrast with the nearly synchronous endpoint indicated by our results.

The earliest indication of a timing differential occurs with the formation of primary and secondary myotubes in two relatively distinct waves separated by about a day in the rat (Wirsen and Larsson, 1964; Kelly and Zacks, 1969). Innervation that is distinguishable by ultrastructural criteria first occurs on primary myotubes, which subsequently differentiate into Type I fibers, and about a day later on the secondary myotubes that become Type II fibers (Rubinstein and Kelly, 1981).

Gordon, (1983) has suggested that the degree of polyinnervation at an early stage in the rabbit may be substantially greater on slow fibers than on fast fibers (6-fold vs. 3-fold on average). This inference, which is based on comparison of motor unit twitch tensions at early (1–4 day) and late (11–16 day) ages, is critically dependent on an unproven assumption that any changes in the specific tension of muscle fibers during this period occur in parallel for fast and slow fibers. (A second crucial parameter, the relative cross-sectional areas of the two fiber types,

changes little during this interval.) Using the same method, Callaway *et al.* (1987) found a similar pattern at days 4–5 (4-fold polyinnervation on slow fibers vs. 2-fold on fast fibers). Based upon the trend established by these two observations, the peak level of polyinnervation in rabbit soleus apparently occurs sometime before day 2 postnatal. Glycogen depletion experiments in rat soleus by Thompson *et al.* (1984) are also consistent with a greater early degree of polyinnervation on slow compared to fast fibers (3.5-fold vs. 2-fold at 8 days, based upon comparison to motor units sizes at 16 days), although their sample size was too small for statistical significance in this respect. The peak degree of polyinnervation occurs within 4–5 days following the initial appearance of functional innervation in rat diaphragm (Bennett and Pettigrew, 1974) and intercostal muscle (Dennis *et al.*, 1981), and hence probably occurs near the date of birth in rat soleus, based on the first appearance of neuromuscular contacts (Rubinstein and Kelly, 1981). To obtain a greater degree of polyinnervation on slow fibers during the early phase of synapse elimination, either the peak polyinnervation of slow fibers must be greater, or the onset of synapse elimination must occur earlier on fast fibers.

For the apparently greater degree of early polyinnervation on slow fibers to be consistent with similarity in polyinnervation at days 7–11, a steeper initial rate of synapse elimination on slow fibers is required. That the rate of synapse elimination is susceptible to modulation is now well documented. In particular, experimental perturbations that increase or decrease nerve and/or muscle activity cause corresponding changes in the overall rate of synapse elimination (Thompson, 1985). If the greater mean activity of slow motor units in adult muscle (Hennig and Lømo, 1985) is also characteristic of the pattern of neonatal activity, then activity differences might contribute to a greater rate of synapse elimination among slow muscle fibers. EMG studies of neonatal rabbit and rat soleus and EDL

muscles (Navarrete and Vrbová, 1983) suggest, however, that the substantially greater activity characteristic of adult slow muscles may not be present before the completion of synapse elimination.

Another piece of evidence suggestive of differential maturation comes from the report by Riley (1977b) that in the rat soleus, the last fibers to lose their polyinnervation are predominantly fast. He observed that, at 15 days, the few remaining muscle fibers with more than one terminal branch in longitudinal silver stained sections were among the smallest diameter fibers; in ATPase cross-sections, most such small fibers were type II. Because there is overlap in both the size histograms of Type I and Type II fibers and the size histograms of multiply innervated and singly innervated fibers, this inference cannot be regarded as conclusive, however.

In view of the complex interplay of factors leading to the concluding phase of synapse elimination, it is noteworthy that we see little difference in polyinnervation by fiber type at either of the ages studied. Several aspects of the process, including the timing of synaptogenesis, the peak level of polyinnervation or the onset of synapse elimination, and the initial rate of synapse loss, appear to differ for the two fiber types. A systemic factor controlling the timing of synapse elimination is unlikely, as there are clear regional differences in the timing of synapse elimination in the rabbit (Bixby and Van Essen, 1979a). It would be of interest to know whether the nearly synchronous conclusion of synapse elimination in the fast and slow populations is merely coincidental, or is a necessary consequence of certain aspects of the process.

Innervation State of Juvenile Muscles

Based upon two independent, but indirect, measures of motor unit size, Gordon, (1983) has suggested a stage of synaptic reorganization in juvenile (3–5 week) muscles, involving the capture and conversion of originally fast muscle fibers by slow motor neurons. This hypothesis invokes synaptic remodeling, and thus differs from that described by Kugelberg (1976), in which fast motor units in maturing rat soleus (5–34 weeks) undergo gradual wholesale conversion to the slow type. The recent report by Taxt *et al.* (1983) describing a low level of residual polyinnervation in rat soleus following the nominal completion of synapse elimination appeared to offer an anatomical substrate for the proposed juvenile stage of reorganization. Transient dual innervation of fibers undergoing conversion would be a likely intermediate in a reorganization process. We sought to confirm the existence of multiply innervated fibers in 3 week rabbit soleus and to determine the distribution of their histochemical types.

While we have in fact observed compound e.p.p.'s, we attribute these to artifactual electrical coupling between fibers. Taxt *et al.* (1983) acknowledged the possibility of naturally occurring electrical coupling, which is common in embryonic muscles (Dennis *et al.*, 1981); however, this phenomenon appears to have disappeared by birth (Brown *et al.*, 1976). The fact that we never observed compound e.p.p.'s in surface fibers argues against electrical coupling being a normal event. Instead, the relationship of the stimulus thresholds of observed multiple e.p.p. components to the response threshold of the overlying surface fiber, together with the occasional ability during electrode withdrawal to generate these in fibers previously characterized as singly innervated, suggest that the electrical coupling is induced by the actual electrode penetration of a series of muscle fibers. Presumably this reflects electrical continuity associated with leaks around the electrode shaft.

Our failure to observe compound e.p.p.'s in rat soleus except when the muscle was loosely pinned leads us to suspect that the artifact is most likely to occur when the cut muscle fibers are not stretched sufficiently.

While we failed to detect late stage polyinnervation, we cannot rule it out categorically. It might occur at a very low rate or in different regions of the muscle. For technical reasons (see Methods), we examined the dorsal aspect of the muscle, where fiber type conversion is substantial, rather than the ventral aspect, where fiber type conversion is even more prominent (Gordon, 1983). Thus, these findings constrain, but do not invalidate, the hypothesis of a juvenile stage of synaptic reorganization, which might also proceed via the intermediate of transiently denervated fibers.

Chapter 4

A COMPUTER MODEL OF NEUROMUSCULAR SYNAPSE ELIMINATION

INTRODUCTION

For a brief interval following birth, mammalian skeletal muscle is innervated substantially in excess of the normal adult configuration, in which each muscle fiber receives its entire synaptic input from a single motor nerve terminal. This phenomenon of transient polyneuronal innervation has been observed and characterized in several mammalian species, including rat (Redfern, 1970; Bennett and Pettigrew, 1974; Brown *et al.*, 1976; Betz *et al.*, 1979), mouse (Fladby, 1987), cat (Bagust *et al.*, 1973), and rabbit (Bixby and Van Essen, 1979a; Gordon and Van Essen, 1985). In the focal polyinnervation characteristic of mammalian muscle, all presynaptic motor terminals innervating a particular muscle fiber share a single endplate region. Multiple terminal profiles often appear in close apposition in electron micrographs (Korneliussen and Jansen, 1976). Beginning near the time of birth and continuing for about two weeks thereafter, excess synaptic inputs gradually disappear. This process of synapse elimination is largely distinct from the separate episode of motor neuron cell death (Brown *et al.*, 1976; Dennis *et al.*, 1981, Oppenheim, 1986), and is an orderly one in that denervated endplates are not observed under normal conditions (Brown *et al.*, 1976). The behavior of a particular motor nerve terminal is dependent on the presence of other terminals at the endplate, implying that the process is competitive (Van Essen, 1982). Elucidating the logic and the mechanisms underlying this competitive interaction is a fundamental problem in the study of synaptic development.

While a substantial body of experimental evidence pertinent to neuromuscular synapse elimination has been accumulated, many aspects of the process remain unclear. Current evidence suggests that synapse elimination is likely to be a richly complex process involving the interplay of multiple, and fundamentally differing,

mechanisms and factors. It is often difficult to design experiments which isolate specific aspects of the phenomenon. Because of this complexity, applying inductive reasoning to the established data base in an attempt to formulate a mechanistic description of the process is a hazardous undertaking. For these reasons, we have chosen to develop a computer model of neuromuscular synapse elimination to provide an objective framework for assessing the ability of proposed mechanisms to account for observed behavior.

Previous theoretical consideration of polyneuronal innervation and synapse elimination has ranged from conceptual analysis (Jansen *et al.*, 1976; Jansen *et al.*, 1978; O'Brien *et al.*, 1978, 1984; Van Essen, 1982; Smalheiser and Crane, 1984) to mathematical formulations amenable to computer simulation (Willshaw, 1981; Gouzé *et al.*, 1983). Each of the earlier computer models relied on an analytic approach in which a descriptive set of equations was solved iteratively to reveal a fully deterministic course of development. The progressive status of individual terminals was not tied to a clearly identifiable physical characteristic such as terminal size, but instead expressed in terms of a more nebulous overall property such as "survival strength" (Willshaw, 1981), or an idealized molecule termed "stabilization factor" (Gouzé *et al.*, 1983). Our approach differs significantly from these previous modeling efforts in both respects. First, our model is highly dynamic in nature, tracking each step in the growth and retraction of individual presynaptic terminals. Nerve terminal extent is the principal outcome of each iteration of the model. Limited endplate space provides the primary basis for competition in the current implementation. While we regard this as a plausible mechanism, worthy of detailed exploration, it is certainly not the only possibility (see Discussion). Second, rather than iteratively solving a set of analytically formulated equations, our model is stochastic in character. Terminal size changes are determined according

to probabilities of growth or retraction which are recalculated for all terminals at each iteration. Anatomical studies support the dynamic emphasis of our approach. Closely apposed multiple terminal profiles have been traced through serial sections to distinct preterminal axons (Bixby, 1981), consistent with short range competitive interaction. While terminal morphology is relatively static at adult mammalian endplates (Lichtman *et al.*, 1987), observations suggesting a higher rate of sprouting and regression have been reported for younger animals (Bixby, 1981; Robbins and Polak, 1987). Finally, vanquished terminals appear to withdraw through a process of orderly retraction rather than by wholesale degeneration (Korneliussen and Jansen, 1976; Riley, 1977a, 1981; Bixby, 1981; but see Rosenthal and Taraskevich, 1977).

Synapse elimination cannot be explained by a strictly random loss of connections, as this would unavoidably lead to the appearance of denervated endplates and some residual longer term polyinnervation (Brown *et al.*, 1976). Some additional mechanism must be operating to ensure that the last presynaptic terminal is stably retained. The fact that postsynaptic activity is required for normal synapse loss argues that some sort of feedback relationship between nerve terminals and muscle fibers is involved. Several mechanisms have been proposed to account for various aspects of the synapse elimination process. We offer no additional novel mechanisms, but instead seek to clarify the details of existing hypotheses, and evaluate and compare their performance in a quantitative simulation.

One of our primary interests has been to study the possible role of a hypothesized synaptic stabilization molecule (Van Essen, 1982). By anchoring the presynaptic terminal to the synaptic basal lamina, this "scaffolding" molecule would act to stabilize terminals by increasing their preference for growth over retraction. If muscle fibers synthesize scaffolding in an activity regulated manner, then this

mechanism would establish a positive feedback relationship between muscle fibers and nerve terminals. Regeneration experiments in amphibians have provided clear evidence for the presence of basal lamina constituents which are capable of inducing synaptic specializations in either pre- or postsynaptic cells in the absence of the other member of the pair (Sanes *et al.*, 1978; Burden *et al.*, 1979). The neuronal adhesion molecule N-CAM is concentrated at both pre- and postsynaptic components of mammalian neuromuscular junctions at later stages of synaptic development (Covault and Sanes, 1986), and further accumulates following either denervation or paralysis (Covault and Sanes, 1985). Whether one of these or a distinct molecule serves as scaffolding, the presence of a synaptic stabilization molecule would appear highly plausible.

A second mechanism simulated in our model is a proposed intrinsic tendency of motor neurons to reduce their arborization following synaptogenesis (Brown *et al.*, 1976; Thompson and Jansen, 1977). The principal evidence supportive of this conjecture derives from partial denervation experiments in newborn rats. In neonatal animals in which very few motor axons remain intact following the surgical partial denervation procedure, motor units appear to have the opportunity to nearly maintain their peak size. In fact, there is a substantial reduction in the number of fibers in each unit, even though this produces many additional denervated endplates. In contrast, motor units in adult animals can expand by sprouting to as large as five times their normal adult size following partial denervation (Thompson and Jansen, 1977; Brown and Ironton, 1978). At either age, there appears to be a definite limit to the maximum arbor size which can be supported by a motor neuron. While it may appear that the metabolic output of a motor neuron is actually programmed to contract during the period of synapse elimination, it is important to keep in mind that while some terminals are retracting, others are growing to occupy most or all

of the available endplate territory. Endplate specializations themselves increase in size during this period of muscle growth (Hopkins *et al.*, 1985). Thus total terminal length or volume supported by individual motor neurons is likely to increase during synapse elimination. Any of several parameters relating to arbor size (e.g., number of terminals, terminal complexity, or integrated terminal length), as well as activity, are potentially important in determining metabolic load.

Another proposal, that motor nerve terminals compete for a trophic factor released by muscle fibers (Jansen *et al.*, 1978), arises by analogy to nerve growth factor (Purves and Lichtman, 1980), whose stimulatory effects upon sympathetic and sensory neurons are familiar (Levi-Montalcini and Angeletti, 1968; Greene and Shooter, 1980). Evidence of factors which are secreted by denervated muscle and promote survival and neurite outgrowth among cultured motor neurons (Nurcombe *et al.*, 1984) or sprouting of motor terminals *in vivo* (Gurney, 1984) has been reported. There is as yet no evidence that these particular molecules are involved in competitive synapse elimination. It is not difficult to imagine such molecules acting as a neural attractant during synaptogenesis, then declining abruptly in concentration to a level inadequate to support extensive polyinnervation and large motor units (Jansen *et al.*, 1978). Just as nerve growth factor affects both neurite behavior (Campenot, 1977; Gunderson and Barrett, 1979) and neuronal vigor (Levi-Montalcini and Angeletti, 1963; Chun and Patterson, 1977), a muscle derived trophic factor could act either locally, by stimulating growth of individual presynaptic terminals, or via a cumulative effect on an entire motor neuron resulting from the combined uptake and transport from all of its terminals. A muscle derived trophic factor is a centerpiece of a previous mathematical model of synapse elimination (Gouzé *et al.*, 1983).

While each of the mechanisms described above differs in character from the

others, they are not mutually incompatible. It may be that no single mechanism is capable of explaining the entire range of observational data. Limits imposed by arbor size do not appear likely to explain why long term polyinnervation does not routinely occur, but may be essential to account for the outcome of partial denervation experiments. The model has been designed so that two or more mechanisms can be combined in a single simulation, and so that the relative weighting of each mechanism can be freely varied. In the present study, however, we focus on exploring the mechanisms one at a time.

Certain issues are common to more than one of the simulated mechanisms. A critical factor in each of the models is the relevance of terminal size. It would be surprising if there were not systematic differences in strength or vigor between smaller and larger terminals. Any growth advantage accruing to larger terminals would go far in explaining the rapid and complete attainment of a singly innervated state. To investigate this matter, we have incorporated the potential for a selective size advantage into each of the mechanisms simulated. Each mechanism also offers some means by which activity could influence the course of synapse elimination. The models afford an opportunity to compare the importance of presynaptic and postsynaptic events in accounting for experimental observations. Computer modeling offers a reasonable approach for analyzing these and other basic issues affecting the course of synaptic maturation. The goal of this type of modeling is neither to prove nor disprove particular mechanisms, but to better understand the dynamics of each, and the constraints within which they might successfully operate.

EXPERIMENTAL FRAMEWORK

A substantial body of experimental observations concerning neuromuscular synapse elimination has been accumulated, descriptive both of the normal developmental process and of responses of the system to various experimental perturbations. Taken together, these influence the design of a computer model, establish initial conditions, and provide the reference against which performance of the model should be judged. As would be expected in a biological system, details vary between species, or even between different muscles in the same species. Nevertheless, several general characteristics of the process can be readily discerned.

Terminal Interactions at the Endplate

It is important to consider observational evidence relating to terminal interactions within an endplate, and the nature of terminal growth and retraction. Our interpretation of this evidence forms the heart of our modeling strategy. When neonatal endplates are viewed in cross-section in electron micrographs, multiple terminal profiles are often seen in close apposition in a gap between the muscle fiber sarcolemma and an overlying Schwann cell (Korneliussen and Jansen, 1976; Bixby, 1981; Riley, 1981). By following profiles in serial sections, Bixby (1981) observed that closely apposed terminals often originated from distinct axons. Interestingly, some terminal profiles are not immediately adjacent to the muscle fiber. The orthographic view of multiply innervated endplates available in light micrographs of silver or zinc iodide-osmium stained longitudinal sections (e.g. Jansen *et al.*, 1976; Brown *et al.*, 1981) is useful in completing a three dimensional impression of endplate structure. Considerable branching complexity is evident, and while the terminal processes associated with separate axons cannot be distinctly resolved, close contact appears probable. Although there is no direct evidence of competition

for synaptic space, the apparent proximity of distinct terminals lends credibility to the concept.

Only sketchy and indirect evidence is available concerning terminal dynamics at polyinnervated endplates. It seems clear that at least some terminals increase in size substantially during development: integrated terminal length and branching complexity continues to increase steadily, paralleling muscle fiber growth, in the several weeks following the peak episode of synapse elimination (Hopkins *et al.*, 1985). Evidence suggesting continuing sprouting and regression of terminals at amphibian neuromuscular junctions has been reported (Wernig *et al.*, 1980), and recently, clear differences have been observed in the configuration of identified endplates in living frogs at two different time points using fluorescent dyes (Herrera *et al.*, 1987). The same technique applied to the mouse sternomastoid muscle (Lichtman *et al.*, 1987), and a related technique involving fluorescent labeling of acetylcholine receptors in mouse soleus (Wigston, 1987), both indicate that there are only limited changes in terminal morphology at mature endplates over intervals as long as several months. It is possible, however, that this relatively static picture of the adult mammalian neuromuscular junction may not apply to rapidly developing polyinnervated endplates. Staining of terminals with dye-coupled tetanus toxin fragments has revealed filipodial and lamellipodial structures suggestive of sprouting which are transient in nature and more prevalent in younger animals (Robbins and Polak, 1987; Hill and Robbins, 1987). In his ultrastructural study of immature endplates, Bixby (1981) frequently observed both extrasynaptic protrusions from presynaptic terminals and regions of postsynaptic specialization in the absence of terminals. Hence, whether individual terminals alternate between growth and retraction in a short term dynamic equilibrium during the competitive phase of synapse elimination remains an open question.

A final significant issue concerns the means by which terminals are eliminated. Specifically, are they lost through wholesale degeneration, or do they withdraw from the endplate in a more continuous and orderly process? Despite one study indicating degeneration (Rosenthal and Taraskevich, 1977), a preponderance of experimental evidence favors the mechanism of orderly retraction. In three ultrastructural studies (Korneliussen and Jansen, 1976; Bixby, 1981; Riley, 1981), no signs of terminal degeneration were detected. In the latter two instances, a parallel study of denervated muscles was conducted to define the likelihood of finding products of degeneration if these were indeed present. In silver stained sections of polyinnervated muscle, Riley (1977a) also found swellings at the distal tips of axons terminating in extrasynaptic regions which he interpreted to be retraction bulbs, and subsequently described similar structures in electron micrographs (Riley, 1981). In view of the evidence cited above, it seems reasonable to suppose that terminals at multiply innervated endplates experience both growth and retraction, and that all but one of the terminals ultimately are removed from the endplate in an orderly process of withdrawal.

Experimental Criteria

Initial Conditions. The degree of polyinnervation at any particular time can be assessed by any of three independent techniques. *In vitro* intracellular recording of compound endplate potentials (e.p.p.'s) elicited by graded stumulation of the muscle nerve in curarized preparations indicates that peak polyinnervation occurs near birth and averages about 3 $\pm$ 1 synaptic inputs per muscle fiber in rat diaphragm (Bennett and Pettigrew, 1974), soleus (Brown *et al.*, 1976), and intercostal muscle (Dennis *et al.*, 1981). The number of preterminal axons entering a cholinesterase positive endplate region can be counted in silver or zinc

iodide/osmium stained sections, yielding similar estimates. Because the difficulty of accurately counting compound e.p.p.'s or the number of preterminal axons increases with number, a more reliable estimate can be obtained by comparing motor unit sizes at their peak with those at maturity. This approach indicates an average of 5 inputs per muscle fiber in rat soleus (Brown *et al.*, 1976) and fourfold polyinnervation in rabbit soleus (Gordon, 1983). Variance in the degree of polyinnervation cannot be directly estimated by this method. The mean and variance of the distribution of motor unit sizes before and after synapse elimination have been estimated for several muscles, including both rat and rabbit soleus. In the soleus muscle of one rat strain, for example, the range of motor unit sizes at days 2–3 postnatal is 700 ± 300 (mean ± std. dev.) vs. 150 ± 65 in adults (Thompson and Jansen 1977). Callaway *et al.* (1988) estimated motor unit sizes separately for fast and slow motor units in rabbit soleus. Fast units declined from 480 ± 170 fibers at days 4–5 to 225 ± 115 fibers at days 11–15, while slow units contracted from 250 ± 115 to 70 ± 35 fibers.

Normal synapse elimination. The time course of synapse loss has been described in several muscles. When the percentage of muscle fibers which are polyneuronally innervated are plotted vs. time, a characteristic sigmoidal curve is obtained (Brown *et al.*, 1976). This curve is similar in shape but shifted in time for muscles from different regions of the body (Bixby and Van Essen, 1979a), indicating that synapse elimination is not regulated by a systemic factor. Denervated muscle fibers have not been demonstrated either during or following synapse elimination, although it is difficult to completely rule out the possible occasional presence of transiently denervated fibers. Diversity in motor unit size is maintained virtually unchanged during synapse elimination (Gordon, 1983; Callaway *et al.*, 1988), contradicting an earlier speculation that larger motor units

might suffer a competitive disadvantage (Brown *et al.*, 1976). Interestingly, in the mixed rabbit soleus muscle, while slow muscle fibers are polyinnervated at about twice the level of fast fibers (Gordon, 1983; Callaway *et al.*, 1987), the endpoint of the synapse elimination process appears to occur at nearly the same time for both of the fiber populations (Soha *et al.*, 1987). Apparently, a substantially greater rate of synapse loss among slow fibers early in the process can compensate for the disparity in initial innervation.

Activity. Experimental perturbations have revealed that neuromuscular activity is an important factor influencing the rate of synapse elimination (Thompson, 1985). Application of the sodium channel blocker tetrodotoxin in a timed release fashion to the sciatic nerve of neonatal rats severely retards or halts synapse loss in the soleus muscle (Thompson *et al.*, 1979). Following restoration of neural transmission, synapse elimination resumes and proceeds to completion (Thompson, 1985). Botulinum toxin, which blocks synaptic transmission, also retards synapse elimination (Brown *et al.*, 1982), as does α-bungarotoxin, a post-synaptic blocker (Duxson, 1982). Callaway and Van Essen (1988) observed regional differences in the degree to which synapse elimination was retarded by superficially applied α-bungarotoxin which appeared correlated with the degree of transmission block, suggesting that the rate of synapse elimination may respond to activity in a continuous, monotonic fashion. Consistent with this idea, an increase in activity due to stimulation of nerve or muscle hastens synapse elimination (O'Brien *et al.*, 1978; Thompson, 1983b). The relative importance of pre-synaptic and post-synaptic activity in mediating this effect remains uncertain.

In addition to the effect of activity on the overall rate of synapse elimination, activity differences among nerve terminals at the same endplate affect their relative competitive ability. When a small fraction of the axons innervating the rabbit

soleus muscle are blocked using TTX, while the vast majority remain active (as do all muscle fibers), the inactive motor neurons exhibit a distinct competitive advantage: motor units whose activity was blocked remain about 50% larger than under normal conditions (Callaway *et al.*, 1987; but see Ridge and Betz, 1984).

Partial denervation. Another developmental perturbation which has proven informative is partial denervation. In this procedure, a large fraction of the axons innervating a particular muscle are severed at a time when polyinnervation is extensive, thereby altering the competitive equation. Interestingly, following partial denervation, synapses continue to be lost and motor units still shrink in size even though many muscle fibers lose their last synaptic input as a result (Brown *et al.*, 1976; Thompson and Jansen, 1977; Fladby and Jansen, 1987). The remaining motor units do end up about 50% larger than those in normal muscles, reflecting either reduced competitive pressure or the stimulative effects of inactive muscle fibers. Furthermore, synapse elimination is delayed in those muscle fibers which remain multiply innervated.

MODEL FORMULATION AND PERFORMANCE

Muscle fibers, motor neurons, endplates and presynaptic terminals form the basic structural components of the model. Each muscle fiber possesses a single endplate specialization where motor nerve terminals make synaptic contact. For simplicity, endplates in the current model are one-dimensional, although we eventually hope to simulate more realistic two-dimensional endplates. They are divided into a discrete number of positions (generally 100), and remain constant in size throughout a run. Presynaptic terminals each occupy a continuous patch of endplate territory, and hence contact at most two other terminals. Unoccupied space between terminals or at endplate boundaries is permitted. Sprouting into vacant territory beyond the endplate is not allowed. Motor neurons branch to innervate multiple muscle fibers, but contact a given fiber only once. There is no differentiation of muscle fibers into fast or slow contracting, nor of motor neurons into tonic and phasic types.

A starting configuration is established by wiring motor neurons to muscle fibers using a procedure that makes the distributions of motor unit sizes and number of terminals per endplate each conform to a Gaussian distribution of specified width. First, the number of terminals initially present at each endplate is chosen according to the selected probability distribution. This could result in a few endplates starting the simulation with fewer than two terminals. Because we wish to start with 100% polyinnervation, we force these endplates to begin with two terminals. Next, the motor unit allegiance of each terminal is randomly selected to reflect the specified probability distribution of motor unit sizes. Finally, the starting boundaries of each terminal are established. The percentage of available endplate space which is occupied at the outset can be varied. Because the model simulates synapse

elimination rather than synapse formation, we generally assign starting terminal lengths so that 90% of all endplate positions are initially occupied. At each endplate, initial terminal lengths (l_i) are selected to approximate a specified relative dispersion in size (σ_{l_i}/μ_{l_i}); accordingly there are greater initial differences in absolute size at endplates with fewer terminals. Unless otherwise indicated, simulations were conducted assuming a hypothetical muscle containing 800 fibers and innervated by 10 motor neurons, and began with 3 $\pm$ 0.5 -fold polyinnervation and motor units containing 240 $\pm$ 40 muscle fibers.

Because 3 of the 9 experimental criteria of Table 1 involve activity, it is essential to define this parameter for both motor neurons and muscle fibers. Rather than attempt to track short term fluctuations in neural activity, we assign a single numerical value, in arbitrary units, to represent the time-averaged activity of an individual motor neuron. This value in turn defines the activity of all presynaptic terminals associated with that neuron. Each muscle fiber also has a numerical activity level that is recalculated at each iteration from the activity levels of the presynaptic terminals occupying its endplate. Postsynaptic activity may be specified to be the sum of presynaptic activities, or a correction for temporal overlap of presynaptic activity can be applied. The contribution of an individual presynaptic terminal to the activity level of its target muscle fiber is further adjusted according to the size of the terminal: terminals that are shorter than a specified length l_1 are considered subthreshold and hence do not contribute to postsynaptic activity; terminals longer than a second specified value l_2 contribute their full activity; terminals intermediate in length contribute proportionately. Motor neuron activity levels are sampled randomly from a specified normal distribution at the outset of a simulation.

Terminal Growth and Retraction

Change in the size of presynaptic terminals with time, as represented by model iterations, forms the dynamic focus of the model. At each iteration an individual terminal may grow by one endplate unit, retract by one unit, or remain unchanged, at either of its two boundaries. By this process, terminals compete for the limited synaptic space available at each endplate.

Certain general principles were adopted to govern terminal dynamics. The size changes of individual presynaptic terminals are stochastic; there is always a non-zero probability of both growth and retraction at any iteration. Throughout the course of the model, terminals may vary in their relative preference to grow or retract. This growth-retraction bias is represented by the state variable b, ranging from -1 to 1; a more positive value of b indicates a greater probability of growth. Terminals may also vary in their tendency to do anything at all. The dynamic state d, ranging from 0 to 1, defines the probability that a terminal will seek to change its size (either by growth or retraction) at any iteration, and effectively regulates the overall rate of development. Together, these two state variables define the probability that the terminal will seek to grow (P_G), that it will seek to retract (P_R), or that it will be satisfied to remain unchanged (P_N). The preference for growth increases linearly from 0 to its maximum value of d as the bias b increases from -1 to 1, as illustrated in Fig. 1, while the preference for retraction decreases in a complementary fashion. The preference for no change is independent of the growth-retraction bias. In the present simulations, we chose $d = 1$ to reflect our view that the neonatal situation is highly dynamic. In the future, this state variable will permit consideration of how factors such as presynaptic activity might affect synapse elimination by modulating the dynamic vigor of individual terminals.

Figure 1 Terminal dynamics are governed by two state variables, the growth-retraction bias (b) and the dynamic state (d), according to simple linear relationships. The preference for growth (P_G) and the preference for retraction (P_R) range between 0 and their maximum value d in a complementary fashion. Actual size changes are determined stochastically, guided by these preferences. Hence, even when the bias is near unity and the preference for growth is high, there remains a non-zero probability that the terminal will actually retract. If $d \leq 1$, then there is also a non-zero probability that there will be no size change at all.

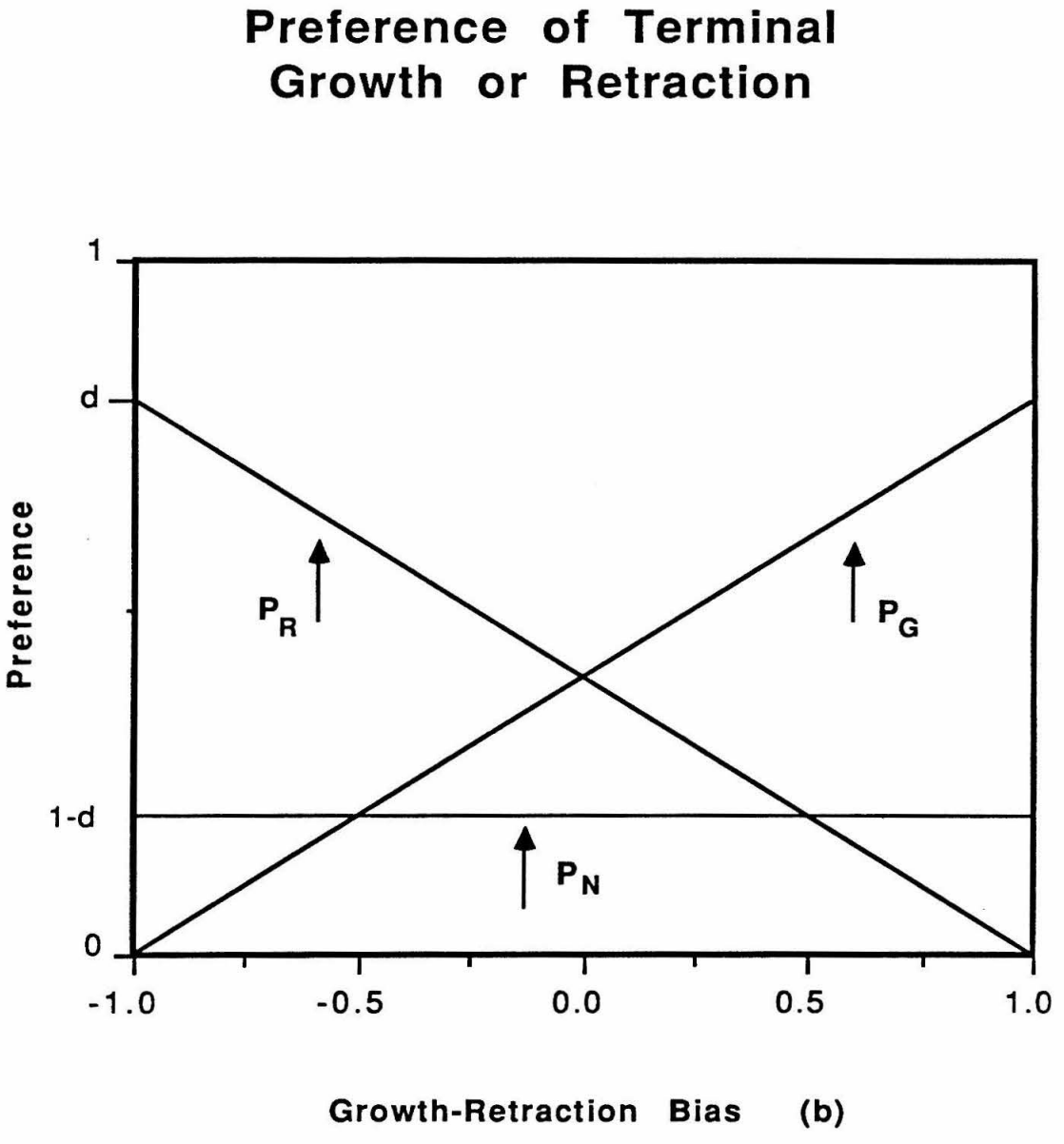
Preference of Terminal
Growth or Retraction
1
d
1-d
0
Preference
P_R
P_G
P_N
-1.0
-0.5
0.0
0.5
1.0
Growth-Retraction Bias (b)

Figure 1.

The growth-retraction bias b is itself a deterministic function of various other parameters representing the state of the muscle, terminal, or motor neuron, whose identity depends upon which of the putative synapse elimination mechanisms are being simulated. For each of the mechanisms, there is one key variable, such as the available quantity of scaffolding or trophic factor, which dominates the calculation of the bias. A general sigmoidal function, shown in Fig. 2, was selected to describe the dependence of the bias upon this key mechanism-specific variable. This functional form has two principal advantages. First, because it asymptotically approaches but never achieves the values $b = \pm 1$, it satisfies our criterion that there must always be a non-zero probability for both growth and retraction, regardless of how much scaffolding or trophic factor may accumulate. Second, the steeper central region concentrates most of the variation into a smaller, biologically relevant region. Where other secondary variables enter into the calculation of the bias, they can be considered to offset the entire sigmoidal curve to the left or right.

Because of the competition for space, actual terminal size changes at each iteration may differ on average from the innate preferences. Actual changes are determined according to the following sequence. First, the bias function b is evaluated for each boundary of every terminal at a given endplate. Then the developmental preference of each terminal boundary, i.e., whether to grow, retract, or remain unchanged, is determined stochastically based on the calculated value of b. All retractions are implemented first. Subsequently, terminals are allowed to grow, but only into vacant positions. If two terminals seek to occupy the same vacant position, neither is permitted to grow. Alternative strategies for resolving encounters between terminals can be readily devised (e.g., probabilistic selection of a victor or allowing "stronger" terminals to dislodge their weaker rivals), but in the absence of experimental evidence, we prefer a simple algorithm. The mutual

Figure 2. The bias for growth or retraction depends on the momentary state of the system. Relevant parameters differ for the different mechanisms, but in each case there is a key mechanism-specific variable which exerts the dominant influence. A sigmoidal form was adopted for the bias function for two reasons. First, because the function only approaches but never achieves its limits of $b = \pm 1$, it satisfies our criterion that there should always be a non-zero probability of both growth and retraction. Second, the steep central portion of the curve defines a narrower region where the biologically relevant interactions can take place.

Bias Functions

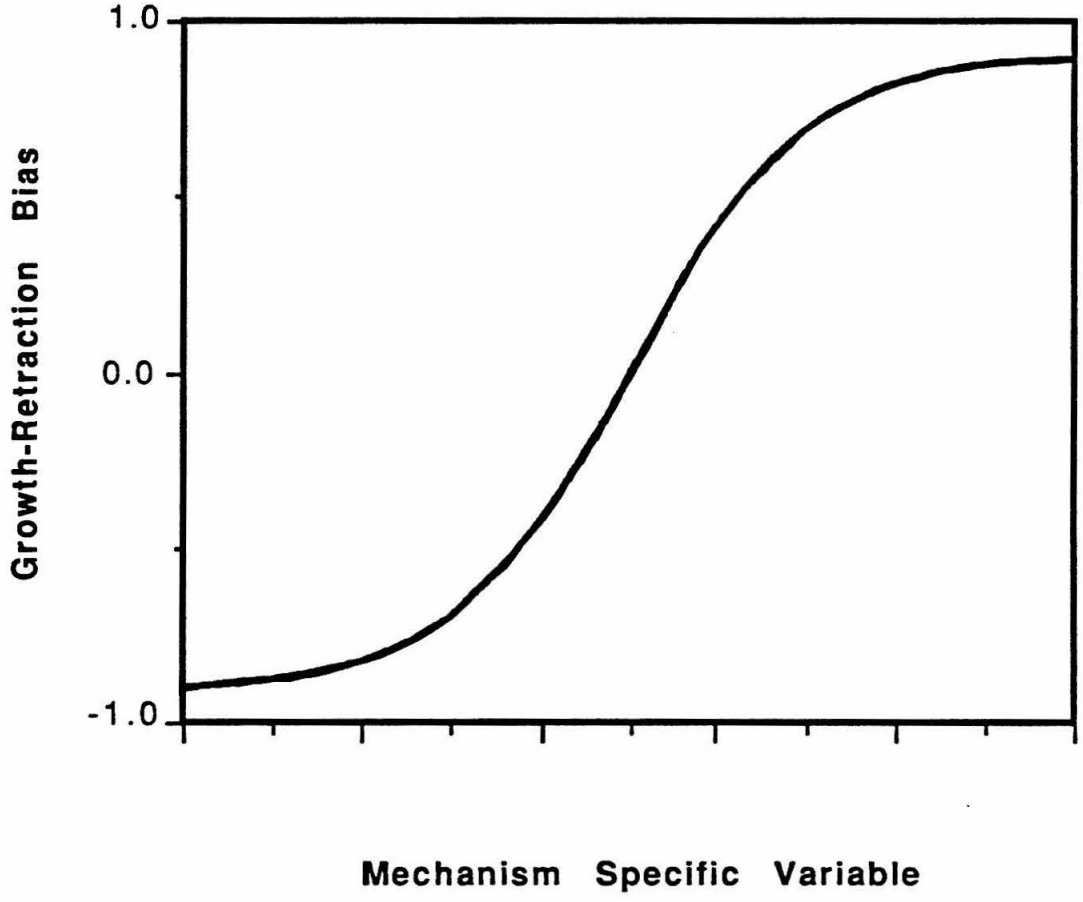

Figure 2

hindrance of growth due to competition causes the effective probability of growth to be less than the preference for growth (P_G) calculated from the growth-retraction bias, and the likelihood of no size change to be correspondingly greater than P_N. This effect becomes important in the performance of the model in certain situations, notably during an experimentally applied wholesale block of neural activity.

In the model, time is measured by iterations (the time required for a terminal to grow or retract by one endplate position). Because little is known about the actual dynamics of terminal growth and retraction at endplates, it is difficult to relate this artificial unit to a physically meaningful interval. A rough estimate of this interval can be obtained by considering the rate of neurite extension *in vivo*. If the length of a neonatal endplate is roughly 10 μm, then each of the 100 positions at a model endplate is about 0.1 μm in dimension. If presynaptic terminals matched a typical neurite growth rate of 30 μm per hour (Bray, 1970), then a terminal could expand by one position in about 10 seconds. Because terminals are not growing steadily, it would seem likely that the actual rate of growth or retraction is considerably slower. Nonetheless, a time scale of the order of minutes for each iteration seems plausible.

The Scaffolding Model

Basic operation. How the model works can be illustrated by first considering a series of simulations employing the scaffolding mechanism. Other mechanisms employ the same basic principles; the respects in which they differ will be discussed in subsequent paragraphs. In the scaffolding model, the growth-retraction bias applicable to either boundary of a terminal is regulated by the local concentration of a hypothesized synaptic stabilization molecule, termed scaffolding, which can be visualized as anchoring presynaptic terminals to the synaptic basal lamina. Scaffolding is synthesized by muscle fibers and accumulates to form a pool

of available scaffolding, presumably within the muscle fiber. In the simplest circumstance, scaffolding synthesis is presumed to proceed at a constant rate, independent of activity. The presence of a presynaptic terminal is required to induce secretion of scaffolding into the synaptic cleft, and its subsequent insertion into the synaptic basal lamina. Accordingly, at each iteration of the model, a percentage of the available pool of scaffolding is incorporated into the basal lamina at each occupied endplate position and bound by the resident presynaptic terminal. Balancing the process of synthesis, insertion and binding are decay rates that are applied to scaffolding in both the basal lamina and the available free pool. Because of its association with the basal lamina, scaffolding is immobile and remains at an unoccupied endplate position when a terminal retracts; it can then be bound again when that position is reoccupied by the same or another terminal. Unbound scaffolding is presumed to decay at a higher rate than bound scaffolding. An estimate of the average equilibrium value of bound scaffolding at an occupied endplate position, S_{eq}, can be readily calculated from the rates of scaffolding synthesis, binding and decay. Following the random wiring which establishes the starting configuration, scaffolding at each occupied endplate position is initialized randomly from a normal distribution having mean S_{eq}.

The activity of scaffolding in promoting terminal growth is presumed to be localized to terminal boundaries. Nevertheless, the effect must occur over a finite range. Hence we compute a weighted average of bound scaffolding S for each boundary region of every terminal, and it is this local scaffolding value which is presumed to regulate terminal growth by determining the value of the growth-retraction bias applicable to that terminal boundary. Simulations have demonstrated that the length of the region over which average bound scaffolding is computed does not have a strong impact on the performance of the model. The

bias b is then determined from S according to the sigmoidal function of Fig. 2. The mathematical details of this relationship are given in the Appendix. The biologically relevant consideration is whether the shape or scale of this curve, together with its offset to the left or right, are significant in determining how synapse elimination proceeds. Two parameters control the shape and location of this curve under the simplest circumstances. The offset S_0 locates the horizontal (S-axis) intercept, which corresponds to the quantity of terminal boundary scaffolding that leads to an equal preference for growth or retraction. A scale factor determines the steepness of the curve; when this factor is set to unity and $S_0 = 0$, numbers typical of our simulations, then local scaffolding values which are near the average equilibrium value S_{eq} yield bias values of 0.4–0.5 (see Appendix), comfortably within the steeply rising portion of the curve. Performance of the model generally does not appear to be critically dependent on the precise position or slope of the bias curve, provided that most bias values are greater than zero.

When the scaffolding model is run using these parameters, terminals are gradually withdrawn, and synapse elimination proceeds without the appearance of denervated endplates. While motor units gradually shrink in size, the diversity in the distribution of motor unit sizes shows little change. A plot of the percentage of muscle fibers remaining polyinnervated vs. time (in iterations) yields a curve (Fig. 3) similar to that seen during actual synapse elimination, By these criteria, the model appears to adequately simulate several of the features of normal synapse elimination. The rate of convergence toward the singly innervated state appears slow, however. About 3400 model iterations are required to progress from 80% to 50% polyinnervation, a transition that requires two days in neonatal rabbit soleus (Soha *et al.*, 1987). Thus each iteration (the time required for a size change of about 0.1 μm) is equivalent to less than a minute of actual time. While this is within the

Figure 3. In the simplest version of the scaffolding model, synapse elimination follows a generally appropriate time course without causing denervated endplates to appear. Measured in iterations, however, convergence toward single innervation progresses slowly. If this curve is to be reconciled with experimental data from rabbit soleus muscle, then one iteration must correspond to just under a minute of actual time. During this interval, a terminal must be capable of growing one endplate unit, or roughly 0.1 μm.

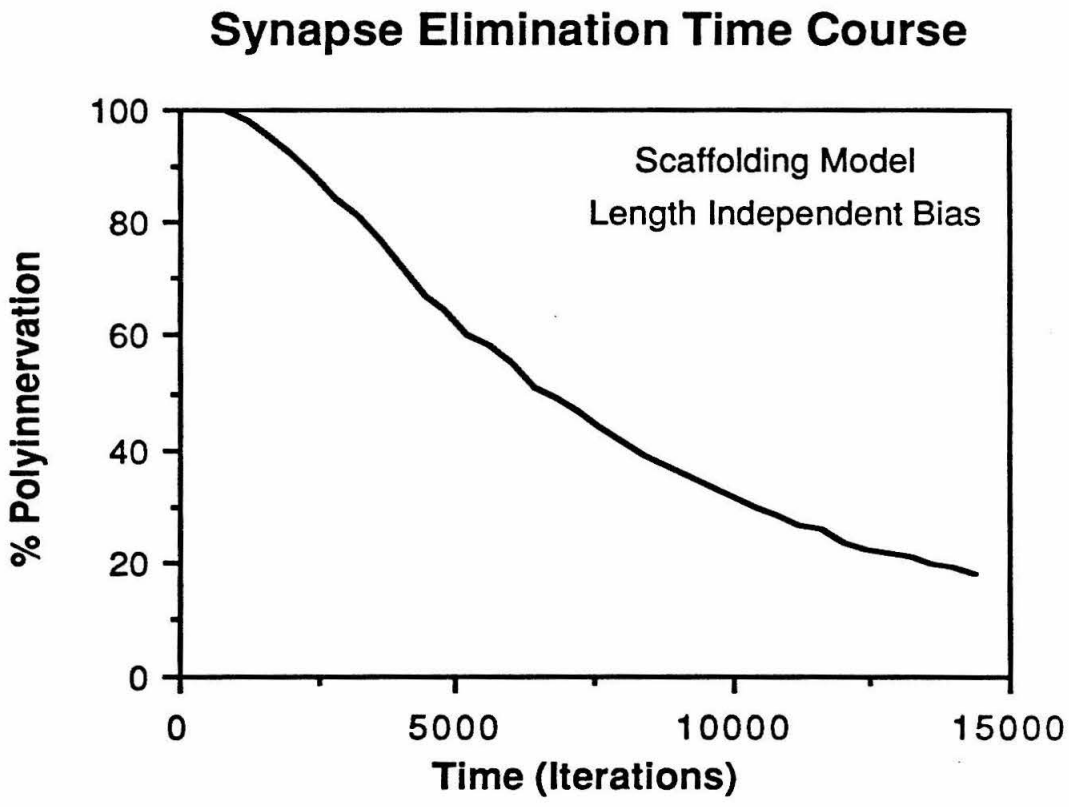
Synapse Elimination Time Course
Scaffolding Model
Length Independent Bias
% Polyinnervation
100
80
60
40
20
0
0
5000
10000
15000
Time (Iterations)

Figure 3

range defined by the average rate of neurite elongation in culture, it in fact requires a disturbingly high rate of growth. Observing the movement of terminal boundaries at a single endplate as a function of time suggests an explanation: their behavior is reminiscent of a random walk (Fig. 4A), and consequently, during the competitive phase, no single terminal ever clearly gains the upper hand.

The role of terminal size. A potentially critical factor influencing the rate of synapse elimination involves consideration of terminal size. The model as described to this point assumes that a change in terminal size has no consequences for the probability of growth, and hence does not affect competitive ability. Even when a terminal reaches the smallest possible size, it is neither more nor less likely to grow. While this is the simplest formulation, it is arguably not the most reasonable one in biological terms. As a terminal changes in size, there will be changes in the surface to volume ratio, the extent of active zones, the percentage of volume readily competent to support growth, and several other factors which are likely to perturb the kinetics of terminal growth. These factors would have to balance out perfectly in order for terminal size to be irrelevant. To address this issue, we introduced an explicit term into the bias function whereby terminal size may influence the likelihood of growth. When this approach is used to confer a competitive advantage upon larger terminals, the bias function is shifted to the left (for larger terminals) or to the right (for smaller terminals) by an amount linearly proportional to terminal length before each calculation of a growth-retraction bias value (see Appendix for details). The effect of this shift is that an equivalent quantity of bound scaffold will produce a greater bias toward growth in a larger terminal. Invoking this strategy accelerates the synapse elimination process considerably, as illustrated in Fig. 5. Subsequent simulations assume a degree of terminal length dependence signified by the arrow in Fig. 5, near the inflection point of the rate curve. The movements of

Figure 4. Following the movements of individual terminal boundaries with time at a single endplate illustrates the competition for synaptic space and the stochastic character of our model. On average, terminals must maintain a bias that favors growth; otherwise at some endplates, all terminals will shrink and disappear. One consequence of this bias toward growth is that boundaries of adjacent terminals are generally in close contact. Another result is that the winning terminal generally maintains occupancy of virtually the entire endplate. When the bias does not depend upon terminal length (A), the process proceeds slowly, and the movement of individual terminal boundaries resembles a random walk. Conferring a selective advantage onto larger terminals (B), accelerates the process.

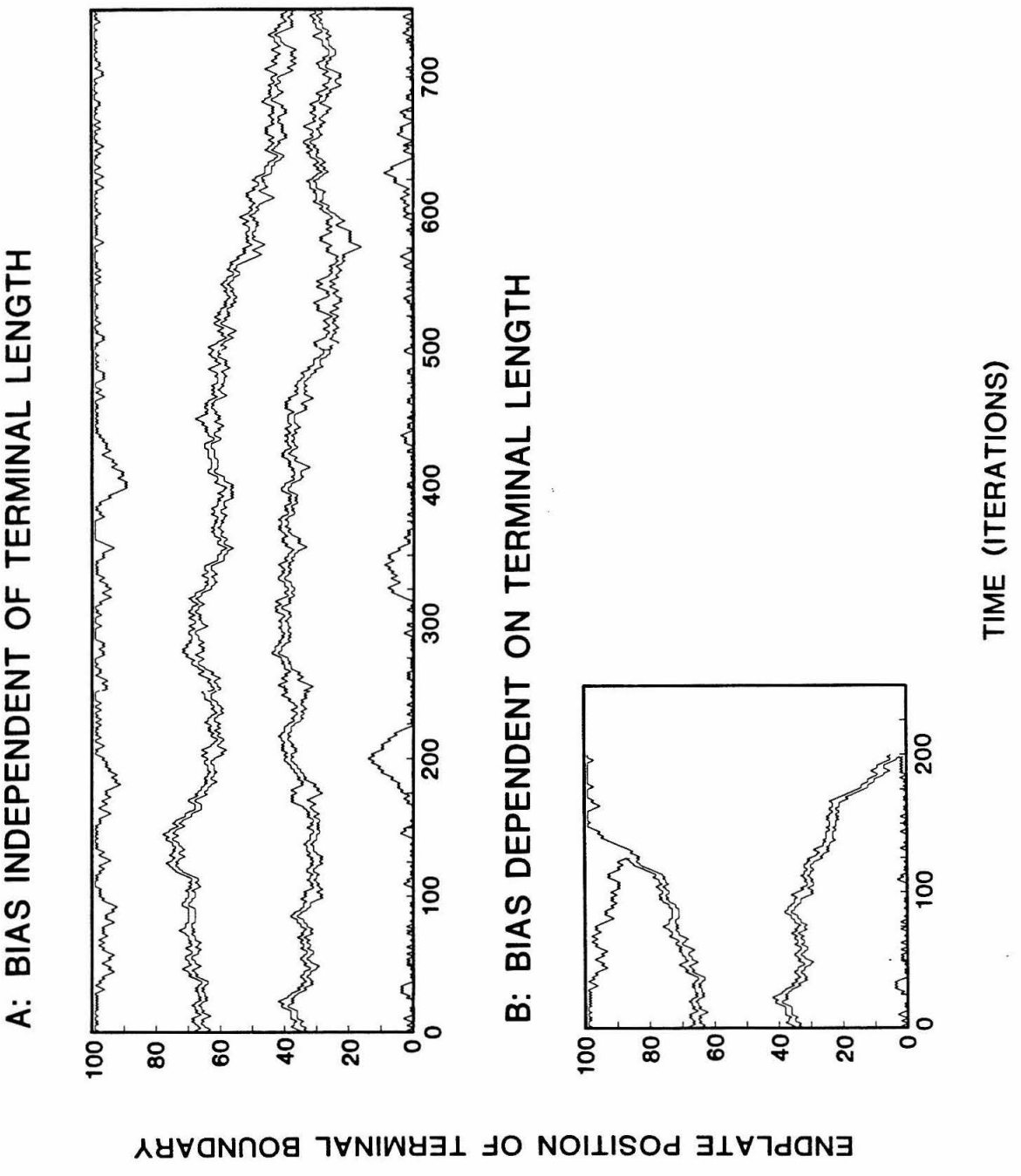
A: BIAS INDEPENDENT OF TERMINAL LENGTH
B: BIAS DEPENDENT ON TERMINAL LENGTH
ENDPLATE POSITION OF TERMINAL BOUNDARY
TIME (ITERATIONS)
0
20
40
60
80
100
0
100
200
300
400
500
600
700
0
100
200

Figure 4

Figure 5. It is reasonable to expect that the growth-retraction bias of a terminal might depend upon its size. The consequences of this possibility can be analyzed by the model. As an increasing advantage is conferred upon longer terminals, the rate of synapse elimination accelerates. In most simulations using the scaffolding model, we used a degree of length dependence signified by the arrow. This action accelerated the rate of synapse loss by about 10-fold. To facilitate comparison with other models, the coefficient describing length dependence (see Appendix) is measured in units related to the width (or slope) of the bias function.

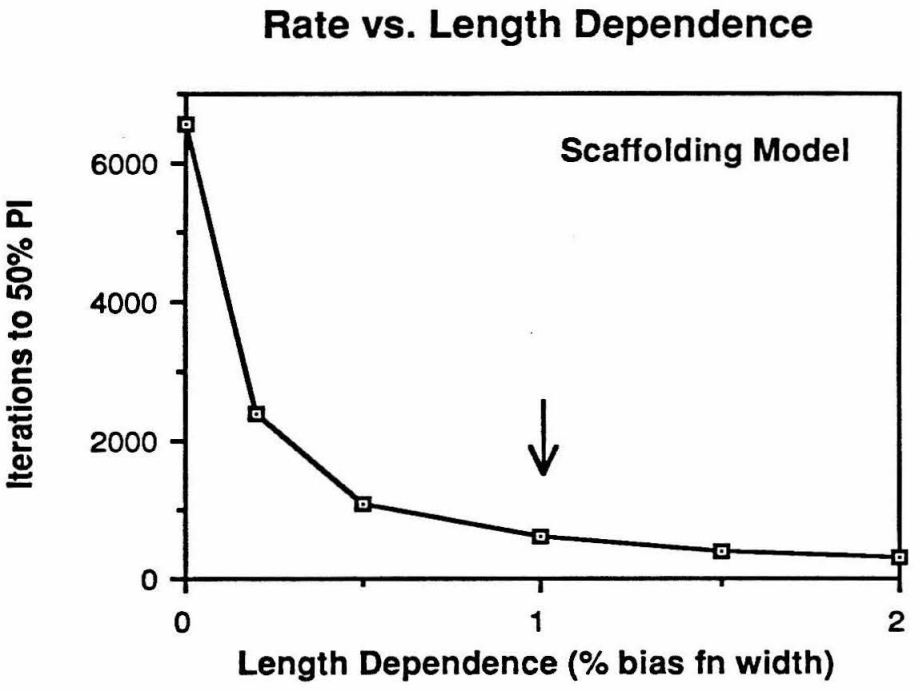
Rate vs. Length Dependence
Scaffolding Model
Iterations to 50% PI
6000
4000
2000
0
0
1
2
Length Dependence (% bias fn width)

Figure 5

terminal boundaries at individual endplates during simulations now appear more directed and display obvious convergence toward a singly innervated state (Fig. 4B). The length dependent simulations emphasized a finding which is also true to a lesser extent in the length independent case. Unless the majority of bias values calculated during the simulation are greater than zero (i.e. biased toward growth), denervated endplates will occasionally arise (data not shown).

One approach to assessing the importance of terminal length dependence in the operation of the scaffolding model is to examine its sensitivity to changes in the size of the incremental step (i.e., the fraction of endplate length which can be occupied in a single iteration). While we generally take this step size to be 1% of total endplate length, it may be varied in the model. In a one dimensional random walk, the mean square displacement x of a terminal boundary would depend upon the step size δ and the number of iterations n according to $x^2 = \delta^2 n$ (e.g., Berg, 1983). Hence the number of iterations required on average for a terminal to randomly retract a distance equal to it length l is inversely proportional to the square of incremental step size, i.e., $n \propto l^2/\delta^2$. In the model, variations in boundary scaffolding prevent the process from being identical to a random walk, even when bias is independent of terminal length. Nonetheless, this reasoning suggests that the number of iterations, and hence the time, required to reach single innervation should increase dramatically as the step size decreases, at least in the length independent case. To study this matter, we conducted a series of simulations, with and without length dependence, in which the effective step size was varied across a 4-fold range by altering the number of endplate positions. Plotting the rate of synapse elimination vs. step size yields a relatively shallow slope when a competitive advantage based on terminal size is present (Fig. 6A). In contrast, removing length dependence yields a curve suggestive of the inverse quadratic relationship predicted by the analogy to a random

Figure 6. Plotting the rate of synapse elimination as a function of the step size of incremental growth or retraction (expressed as a percentage of total endplate length) illustrates a fundamental difference in behavior between length dependent and length independent versions of the model. As iterations are related to time (in particular, the length of time required for an average terminal to grow by one position), the curves define a range of growth rates which are compatible with the normal course of synapse elimination. For both the scaffolding model (A) and the neural energy model (B), length independent simulations exhibit much greater sensitivity to incremental step size than is apparent in length dependent simulations. The length independent models can only function accurately if actual growth rates are sufficiently high. The neuronal energy model converges over a somewhat braoder range of incremental step sizes. The curves in each plot have been normalized to their values at a step size equal to 2% of total endplate length.

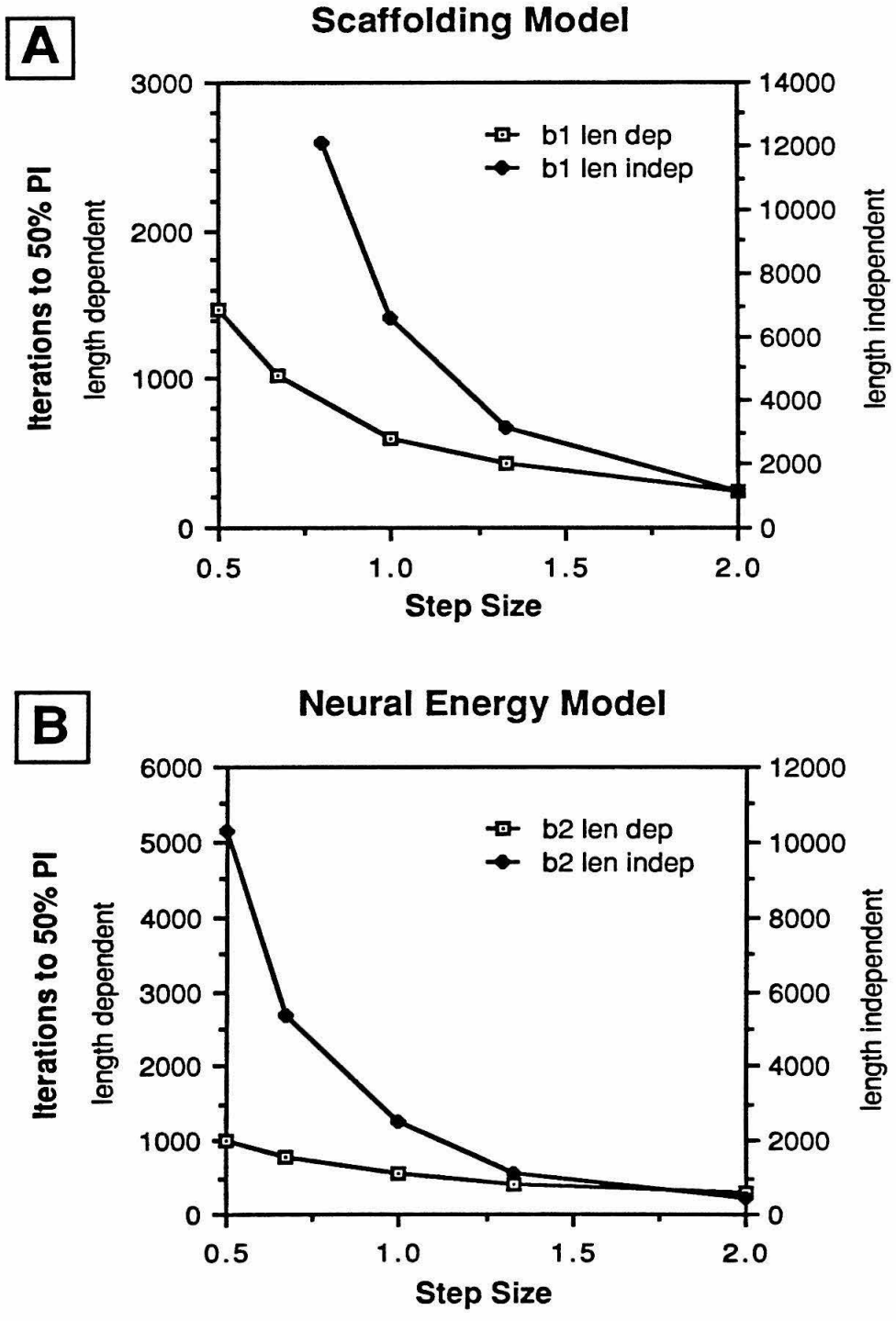
A
Scaffolding Model
Iterations to 50% PI
length dependent
length independent
b1 len dep
b1 len indep
3000
2000
1000
0
14000
12000
10000
8000
6000
4000
2000
0
0.5
1.0
1.5
2.0
Step Size
B
Neural Energy Model
Iterations to 50% PI
length dependent
length independent
b2 len dep
b2 len indep
6000
5000
4000
3000
2000
1000
0
12000
10000
8000
6000
4000
2000
0
0.5
1.0
1.5
2.0
Step Size

Figure 6

walk. The time course of synapse elimination clearly depends more critically upon step size (or equivalently, upon terminal growth rate) when growth-retraction bias is independent of length. Consequently, a much narrower range of growth rates are compatible with realistic rates of synapse loss in the length independent case. While biological systems may operate within this restricted range, it appears more reasonable to conclude that an advantage for larger terminals is required to achieve an effective rate of synapse elimination with the scaffolding mechanism.

Activity. One potential influence of activity considered by the scaffolding model is that the synthesis of scaffolding by a muscle fiber may be dependent upon its activity level. A family of exponential functions (Fig. 7; see Appendix for definition) is employed to describe the dependence of scaffolding synthesis upon activity; the strength of the activity effect depends upon which member of the family is selected to regulate synthesis. Synthesis may be positively or negatively correlated with activity, depending on whether an increasing or decreasing exponential function is selected. Constant rate scaffolding synthesis can be considered a member of this family of curves. The activity distribution of neonatal motor neurons under normal conditions is uncertain (cf. Navarrete and Vrbová, 1983). When a Gaussian distribution of neural activity levels with a moderate variance (e.g., $\sigma/\mu = 0.2$) was assumed, simulations yielded results which did not differ noticeably from those obtained without including activity (data not shown).

More interesting are the results obtained when experimental activity perturbations are simulated. Two such perturbations are allowed by the model: wholesale activity alterations, where the activity of every neuron is blocked or increased, and partial activity blocks, where the activity of a fraction of the motor neurons is reset to zero while the others remain unaffected. The effects of activity-dependent scaffolding synthesis are illustrated by the performance of the model

Figure 7. Three members of the family of exponential curves (defined in Appendix) which are used in the model to describe activity dependent behavior. A representative activity effect occurs when the synthesis of scaffolding is presumed to be regulated by activity. If synthesis were described by the steepest curve shown, then it would be increased over 7-fold during an activity block. Curves from this family are also used to describe trophic factor synthesis, trophic factor uptake, and scaffolding induction.

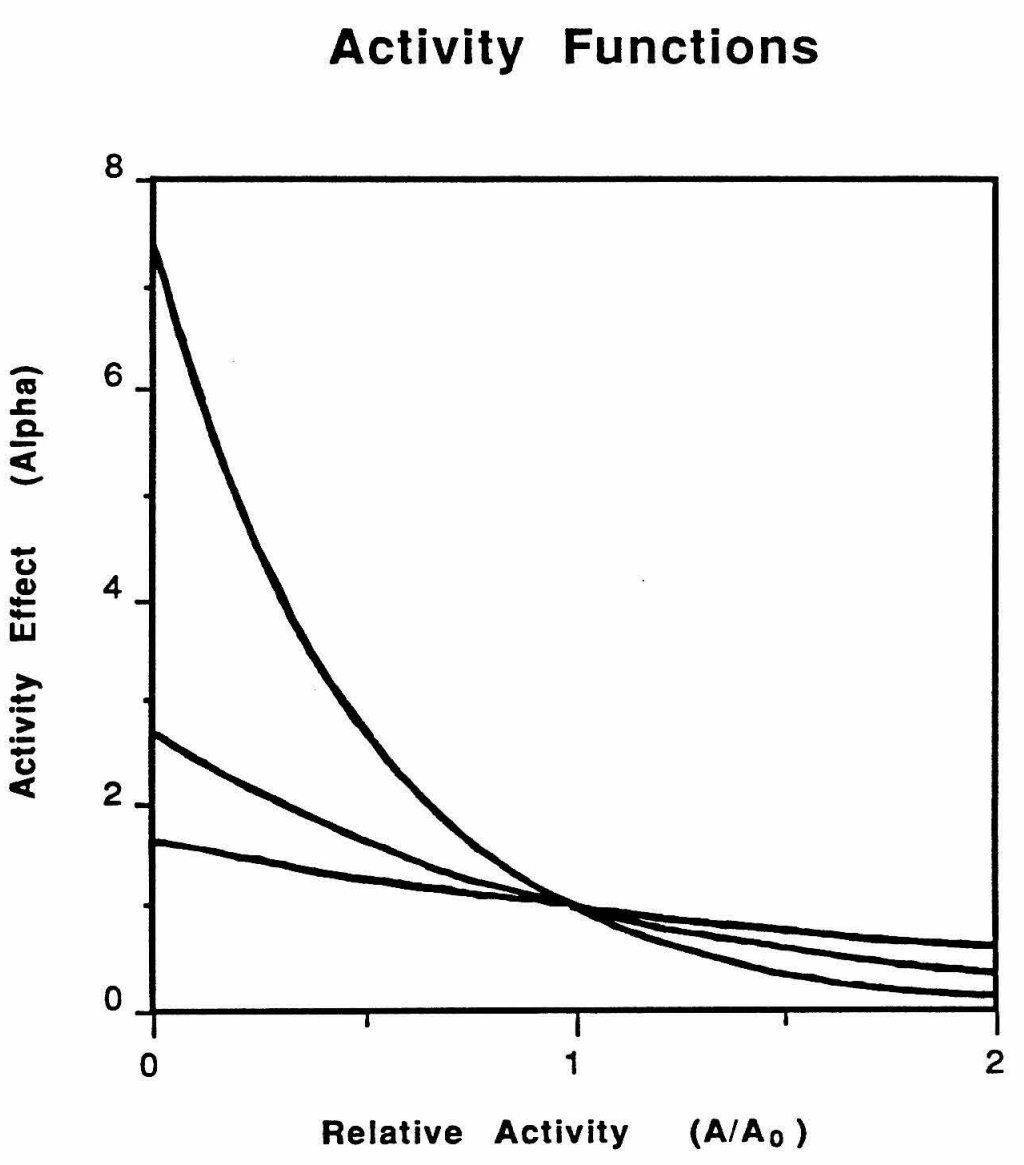
Activity Functions
Activity Effect (Alpha)
8
6
4
2
0
0
1
2
Relative Activity (A/A0)

Figure 7

following wholesale activity perturbations. The ability of a complete activity block to retard or suspend synapse elimination could be correctly simulated by the model (Fig. 8). Interestingly, it was necessary to assume that the rate of synthesis is inversely related to activity as defined by a decreasing exponential curve from Fig. 7. When a 5-fold or greater increase in scaffolding synthesis accompanied the elimination of activity, a realistic slowing of synapse elimination occurred. This increased synthesis leads to greatly enhanced incorporation of scaffolding into the basal lamina and consequent binding to presynaptic terminals. As a result, growth-retraction bias values for all terminals are increased to near unity, and they seek to grow at nearly every iteration. Each terminal is stymied, however, by the similar preference of all other terminals sharing the endplate, and hence the competitive interaction is retarded. Note that synapse elimination proceeds for several hundred iterations following sudden imposition of activity blockade, reflecting the interval required for bound scaffolding levels to equilibrate under the new circumstances. This behavior resembles the dip in polyinnervation observed following transmission block with tetrodotoxin (Thompson *et al.*, 1979; Brown *et al.*, 1981), except that no recovery of polyinnervation could occur in the simulations as new synapse formation by sprouting is not allowed. A small but appropriate effect was also seen when activity levels were increased to simulate whole nerve or muscle stimulation. For example, doubling activity increased the rate of synapse elimination by 5–10%.

A second potential role for activity considered by the model involves modulating the effectiveness of presynaptic terminals in inducing the incorporation of scaffolding into the synaptic basal lamina. Thus the rate of incorporation of scaffolding from the free pool into the basal lamina, and its subsequent binding by the overlying terminal, will vary depending upon the activity level of the particular terminal occupying that endplate position. The functional dependence of induction upon

Figure 8. If scaffolding synthesis is presumed to be inversely dependent on postsynaptic activity, then simulated synapse elimination is retarded by a wholesale activity block. As illustrated, the effect is greater when synthesis is more strongly regulated by activity. The exponential coefficient c is defined in the Appendix

Synapse Elimination with Activity Block for Various Scaffold Synthesis Rates

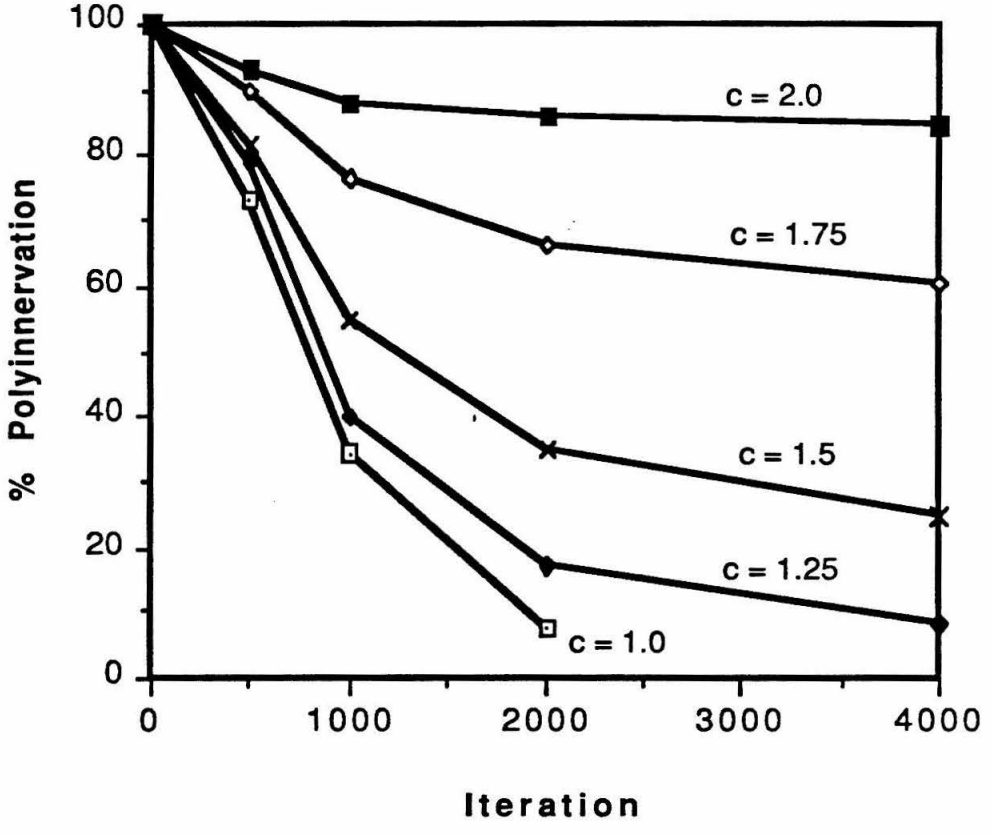

Figure 8

activity is described by an exponential curve selected from the family of Fig. 7. The performance of the model under this assumption is discussed in Results.

Neuronal Energy Model

The neuronal energy mechanism acts by comparing the energy load imposed upon a neuron by its arbor with its capacity to metabolically support that load. If the energy load is smaller than the metabolic capacity, individual terminals of that neuron experience a bias toward growth, whereas if the neuron becomes overextended, the bias alters toward retraction. Motor neuron energy loading E is assumed to be proportional to integrated terminal size, and hence is computed at each iteration as the sum of the lengths of all terminals associated with that neuron. In other words, the energy loading is proportional to motor unit size (i.e., the number of muscle fibers) times the average length of each terminal. The same functional form (Fig. 2) is used to determine the growth-retraction bias as is used in the scaffolding model, except that the horizontal axis represents the difference between metabolic capability M and actual energy load, i.e., $M - E$. When energy loading exactly equals metabolic capacity, there is an equal likelihood of growth or retraction; hence the horizontal axis intercept normally occurs at $M - E = 0$. Essentially, this mechanism defines a negative feedback relationship in which terminal size changes are biased toward correcting deviations in neural energy from its natural target value M. An additional dependence of the bias upon terminal length, such that larger terminals enjoy a relative advantage, can also be introduced as before, by horizontal translation of the bias curve.

Metabolic capacity. Appropriate selection of M is clearly a significant issue. While there is no direct experimental evidence to guide the selection of this parameter, the performance of the model itself during simulations of experimental

observations provides relevant information. The simplest available strategy is to set M equal to a constant and identical value for all motor neurons; a reasonable choice is the initial energy load of an average motor unit. When this was done, synapse elimination proceeded at a realistic rate without the appearance of denervated muscle fibers. Motor unit sizes, however, all converged rapidly to a common value (data not shown), an outcome clearly at variance with the experimental evidence. This behavior illustrates the feedback effect inherent in this mechanism: the energy expenditure of each neuron seeks the common target value M, and because average terminal size varies little between motor units, all units effectively seek a common size. Clearly, introducing variation into neural metabolic capacity values relieves this problem. However, the fact that final motor unit size diversity is so closely regulated by the distribution of M_i (and hence so easily manipulated by the modeler) suggests that the experimental criterion of unchanging motor unit size diversity is of little value in judging the performance of the model.

A somewhat more sophisticated strategy for determining M arises from the notion that, since our model begins at a moment of peak polyinnervation, the full arborization of a motor neuron at that point in time reflects its metabolic capacity. Accordingly, in another series of simulations, the metabolic capacity of each motor neuron was set equal to the initial energy load experienced by that particular neuron. As before, the metabolic capacity of each motor neuron was assumed not to vary with time; a simplifying assumption of our model, that endplates remain constant in size, facilitates this approach. Simulations utilizing this approach again converged to single innervation without giving rise to denervated endplates, but as expected, the distribution of motor unit sizes remained relatively unchanged. When one examines a histogram of bias function values occurring during a simulation employing this strategy (Fig. 9), it is interesting to observe that the distribution, while centered

Figure 9. A histogram of bias function values calculated during a simulation using the neuronal energy model demonstrates a modest bias toward growth even when metabolic capacity is taken to be equal to initial energy loading. The explanation for this effect derives from the frequent mutual hindrance of terminal growth at a crowded endplate, as described in the text.

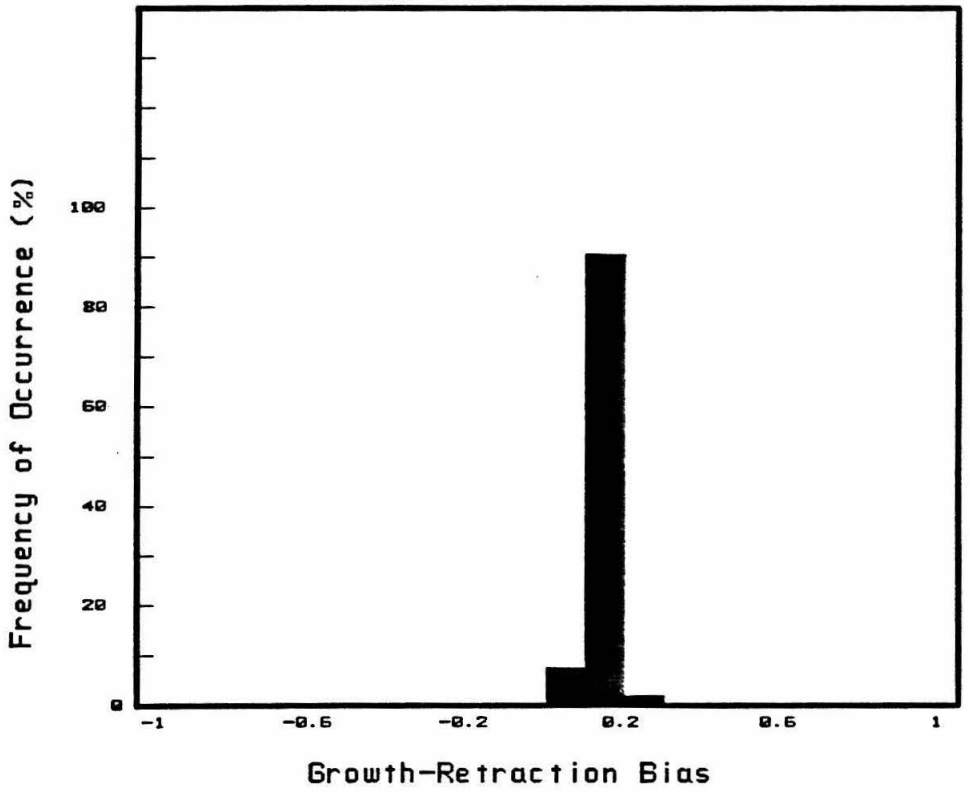
Frequency of Occurrence (%)
100
80
60
40
20
0
-1
-0.6
-0.2
0.2
0.6
1
Growth-Retraction Bias

Figure 9

near zero, is distinctly offset in the positive direction. The explanation for this effect derives from the fact that the model is initialized with endplates almost fully occupied. For the first few iterations, terminals seek to grow or retract with roughly equal probability. Because growth is often hindered by the presence of other terminals, while retraction is not, average terminal size tends to decline slightly from its initial levels, intoducing a slight bias for growth which remains present throughout the simulation. When we began one simulation with endplates only half occupied, the bias function histogram was symmetric about zero, and a large number of denervated endplates arose as development proceeded. This result illustrates the most serious difficulty inherent in the preceding strategy for assigning M: even marginal reductions in M lead to instability in the model, in which a significant degree of retraction bias produces an unacceptable number of denervated endplates.

The instability problem would be resolved if each motor neuron possessed an additional incremental bias toward growth. In the context of the neuronal energy model, this goal would be attained if each motor neuron were granted a reservoir of additional metabolic capacity beyond what is necessary to support its initial energy load. A useful strategy for providing excess capacity while retaining a linkage between metabolic capacity and initial arbor size is to assume that the metabolic capacity of any neuron is a multiple of that neuron's initial energy loading, i.e. $M_i = c_m E_{i_0}$. The preceding approach is thus a special case in which the coefficient is unity.

Partial Denervation. Simulations of partial denervation, the remaining experimental perturbation implemented in our model, both confirm the value of this approach and provide a criterion for selecting the value of c_m. In this procedure, a subset consisting of a specified number of motor neurons (usually a small percentage of the total) is randomly selected to emerge from the procedure

intact. All terminals of the remaining neurons, whose axons are presumed to have been "severed," are removed from endplates, leaving vacant territory. As described earlier (Experimental Framework), experimental motor units shrink considerably from their early size even at the expense of creating denervated muscle fibers, yet remain about 50% larger than mature units in a fully innervated muscle. Partial denervation simulations revealed that motor unit sizes at the completion of synapse elimination increased linearly with increasing values of the coefficient c_m (Fig. 10). Simulations with $c_m = 1$ produced motor units which were clearly too small; a 30–60% excess in metabolic capacity yielded a realistic distribution of motor unit sizes.

Terminal size. Simulations indicated that synapse elimination was accelerated substantially when a relative advantage was conferred upon larger terminals (Fig. 11). In all cases, regardless of the magnitude of the size advantage, the standard sigmoidal time course was observed, and no denervated endplates appeared. As before, variations in the step size of incremental growth and retraction were simulated to evaluate the viability of the neural energy mechanism in the absence of size dependent bias. The rate of synapse elimination varied almost linearly with step size in the length dependent case (Fig. 6B), whereas rate appeared to follow power law behavior when bias was independent of terminal length. As in the case of the scaffolding model, this relationship suggests that only limited range of relative growth rates will allow the process to converge in a reasonable interval of time. However, the number of iterations required to achieve 50% single innervation clearly increases much less dramatically with decreasing step size than was the case for the scaffolding model (cf. Fig. 6A). Hence the neural energy mechanism is convergent over a broader range of incremental step sizes than is the case for the scaffolding mechanism, and it seems more reasonable to suppose that the mechanism

could operate in the absence of an explicit advantage for larger terminals. For this reason, further simulations using the neural energy model were conducted both with and without the assumption of length dependent bias.

Activity. It seems reasonable to speculate that energy loading may be greater in motor neurons which experience higher levels of activity. Hence the model optionally allows activity to modulate neural energy in a linear fashion, such that energy remains equal to integrated terminal length at a specified nominal activity level (see Appendix). For normal, unperturbed activity ranges, metabolic capacity is calculated as before, based on the activity adjusted value of initial energy. Care is taken during activity perturbations to ensure that M is determined based upon normal unperturbed activity. Simulations in which activity plays a role are described in Results.

Trophic Factor Model (Local Mode)

In this positive feedback mechanism, a soluble factor synthesized and secreted by muscle fibers is taken up by presynaptic terminals, where it acts locally to increase the bias toward growth. Trophic factor synthesis is inversely proportional to muscle fiber activity in a relationship defined by any of the family of decreasing exponential functions of Fig. 7 (see Appendix), and is then secreted into an available pool in the synaptic cleft where it is subject to diffusional loss. Uptake by terminals is proportional to the available concentration, and is optionally dependent upon presynaptic activity in a manner once again defined by the curves of Fig. 7. Factor accumulates in the terminal, but is also removed by decay or axonal transport. Axonally transported trophic factor will, in a future enhancement of the model, accumulate in the cell body and optionally act to regulate global neuronal tendencies. Locally, the concentration of trophic factor within a terminal determines

Figure 10. An extra reservoir of metabolic capacity, beyond the minimum required to support the neuronal arbor, is necessary if the neuronal energy model is to successfully simulate the development of motor unit sizes following experimentally induced partial denervation. In treated animals, motor units still lose many synapses, yet emerge from synapse elimination with about 50% more than the normal number of muscle fibers. The degree of extra capacity required to match this finding varies depending upon the initial level of polyinnervation and whether terminal size plays a role in the determination of growth-retraction bias.

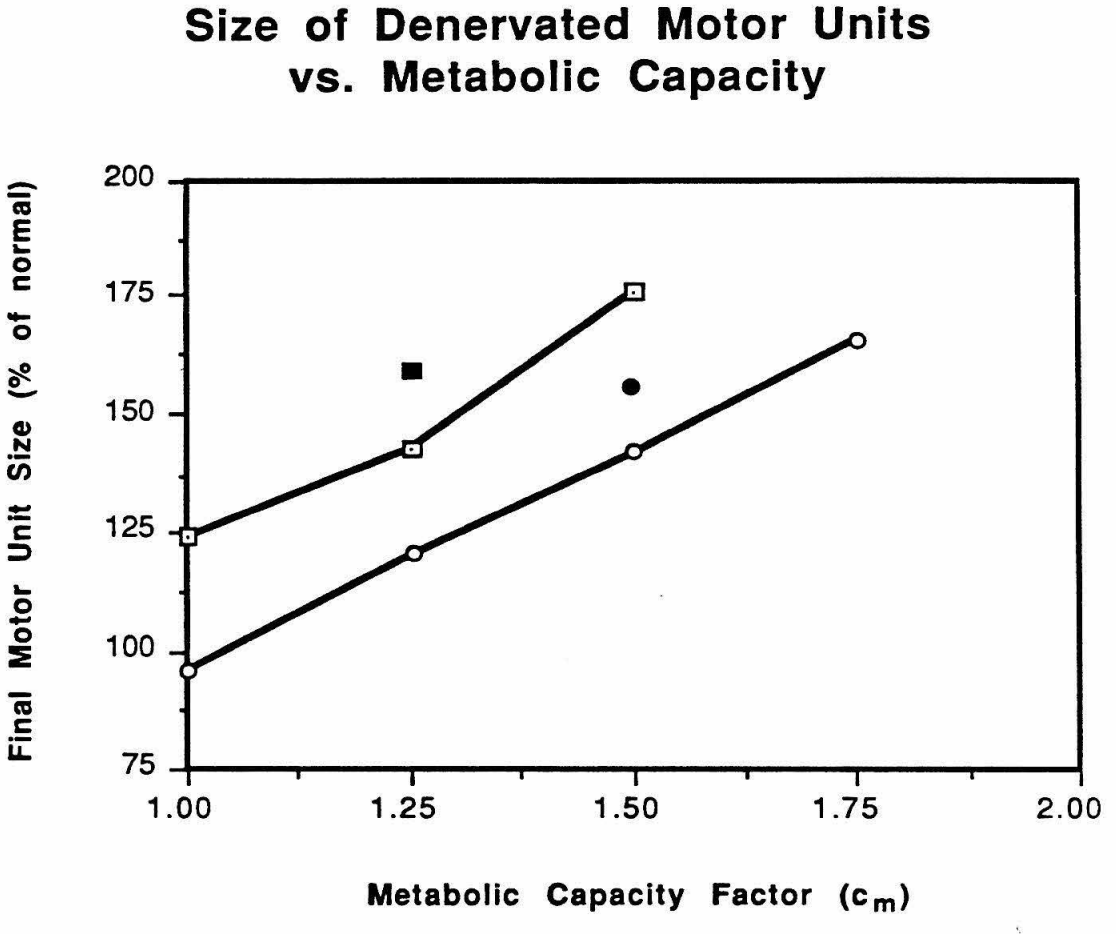
Size of Denervated Motor Units
vs. Metabolic Capacity
Final Motor Unit Size (% of normal)
200
175
150
125
100
75
1.00
1.25
1.50
1.75
2.00
Metabolic Capacity Factor (c_m)
no length dependence, initial PI = 3
length dependence, initial PI = 3
no length dependence, initial PI = 6
length dependence, initial PI = 6

Figure 10

Figure 11. Conferring a relative advantage upon larger terminals accelerates the rate of synapse elimination in the neuronal energy model.

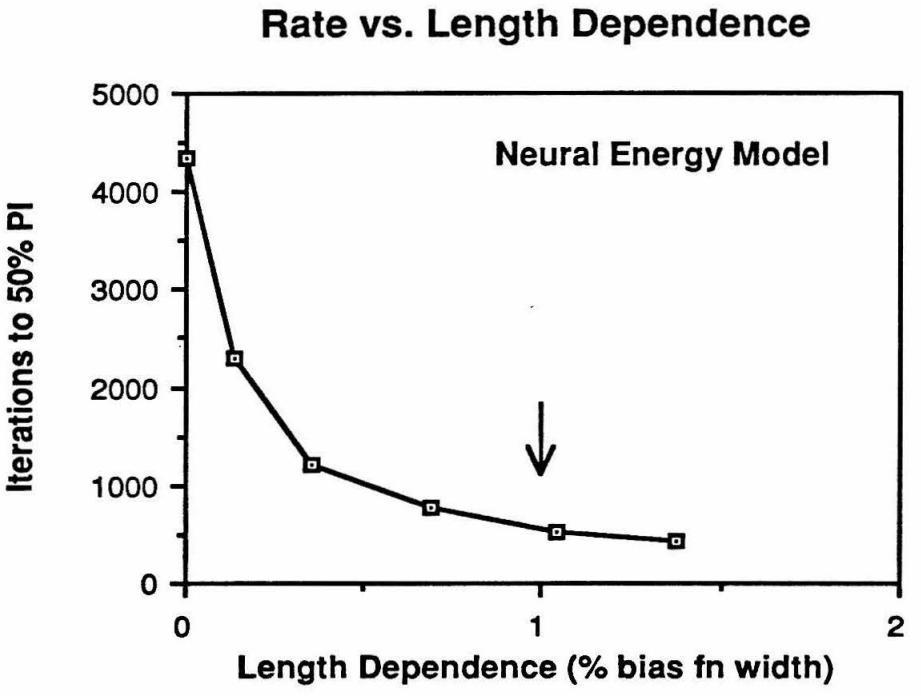
Rate vs. Length Dependence
Neural Energy Model
Iterations to 50% PI
5000
4000
3000
2000
1000
0
0
1
2
Length Dependence (% bias fn width)

Figure 11

its growth-retraction bias according to a sigmoidal curve defined similarly to that of Fig. 2 (Appendix).

In initial simulations with the local trophic factor model, synapse elimination proceeded extremely slowly. This stems from a provision of the model that inherently resists convergence to single innervation: We assumed that, excluding uptake, decay and transport, trophic factor is conserved within presynaptic terminals. Thus when a terminal retracts, the concentration of trophic factor within the terminal increases proportionately, increasing the subsequent likelihood of growth. Similarly, growth reduces the internal trophic factor concentration, thereby tending to promote retraction. The combination of these two effects tends to stabilize the polyinnervated state. This problem can be moderated by assuming a rapid rate of decay or transport of intraterminal trophic factor. Regulating terminal uptake of trophic factor based on presynaptic activity level also accelerates synapse elimination, even at lower intraterminal decay or transport rates. This effect depends upon the unproven assumption that activity differences exist among neonatal motor neurons. The associated competitive advantage for either more or less active neurons also affects other properties of the process, as will be described later. A third strategy for increasing the rate of synapse loss was actually adopted: an explicit dependence on terminal length was introduced into the bias function (Fig. 12), as was done with other mechanisms. We used a degree of length dependence consistent with that employed in simulations with the other mechanism (see Appendix).

Figure 12. Terminal size dependence also plays a significant role in the rate of synapse elimination in the local trophic factor model. This curve is virtually identical to that of the scaffolding model (Fig. 5).

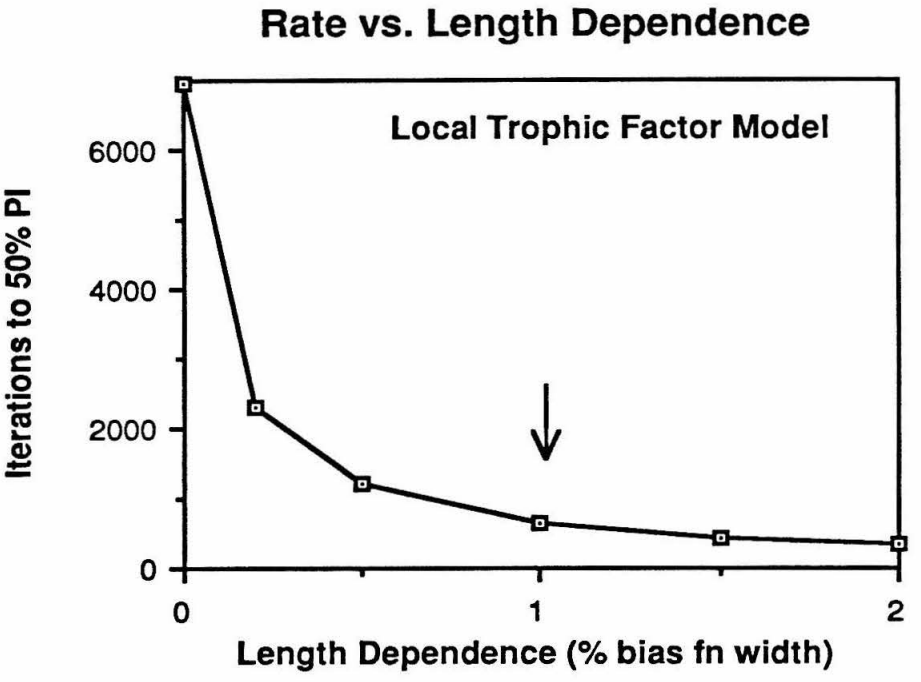
Rate vs. Length Dependence
Local Trophic Factor Model
Iterations to 50% PI
6000
4000
2000
0
0
1
2
Length Dependence (% bias fn width)

Figure 12

SUMMARY OF EXPERIMENTAL SIMULATIONS

To assess and compare the ability of the three proposed mechanisms to accurately describe the process of synapse elimination, we used the model to simulate the 9 experimental observations listed in Table 1. Some of these simulations were presented in the previous section to illustrate the operation of the model. These are noted briefly below, while the remaining simulations are described in greater detail. Our findings concerning the performance of the model in simulating the experimental criteria are summarized for comparison in Table 2. In addition to testing the model against the experimental criteria, we were interested in examining whether a competitive role for activity during synapse elimination could promote the recruitment ordering of motor units according their size, as speculated by Callaway *et al.* (1987).

Scaffolding Model

Simulations using the scaffolding model were conducted assuming a competitive advantage for larger terminals, based on our earlier finding (see Model Formulation and Performance) that this provision ensured convergence over a suitable range of incremental step sizes. Our experience during these earlier tests led us to suspect that similar results would follow simulations in which length dependence was omitted from calculation of growth-retraction bias, but that vastly more model iterations would be required. Simulations assuming terminal length dependence yielded an appropriate sigmoidal time course for the disappearance of multiple innervation. No endplates became denervated during the process, and in fact, surviving terminals expanded to occupy virtually the entire available endplate region. Diversity in the distribution of motor unit sizes was compared before and after synapse elimination by combining the results of 7 independent model

SELECTED EXPERIMENTAL OBSERVATIONS

Normal Synapse Elimination

1. No denervated endplates appear under normal conditions.

2. Appearance of singly innervated fibers follows a sigmoidal time course.

3. Similar endpoint timing despite initial level of polyinnervation.

4. Motor unit size diversity changes little during synapse elimination.

Activity Perturbations

5. Wholesale activity block retards synapse elimination.

6. Increased overall activity hastens synapse elimination.

7. In partial activity blocks, less active units enjoy a competitive advantage.

Partial Denervation

8. In partially denervated muscle, motor units remain larger than normal, but nevertheless decrease in size even though denervated muscle fibers consequently appear.

9. Partial denervation retards synapse elimination among remaining polyinnervated muscle fibers.

Table 1

Experimental Observations	Scaffolding	Neuronal Energy	Local Trophic Factor
No Denervated Endplates	YES	YES	YES
Normal Time Course	YES – Requires Size Dependence	YES	YES – Requires Size Dependence
Synchronous Endpoint	YES	YES	MARGINAL
Equivalent MU Size Diversity	YES – Affected by Activity	YES – Affected by Activity	YES – Affected by Activity
Activity Block Retards SE	YES	YES	YES
Stimulation Hastens SE	YES	YES	YES
Competitive Activity Role	YES	YES	YES
Partial Denervation Affects MU Size	NO	YES	NO
Partial Denervation Retards SE	NO	NO	NO

Table 2

simulations. The pooled distributions, shown in Fig. 13, reveal little change in motor unit size diversity. Two scale invariant measures of diversity, the standard deviation normalized by the mean, and the interquartile ratio, confirm this conclusion.

Another performance issue concerns the relationship between the time course of synapse elimination and the initial level of polyinnervation. Specifically, how well does the scaffolding model simulate the evidence (Soha *et al.*, 1987) for a nearly synchronous endpoint of the synapse elimination process for the fast and slow fiber populations in the rabbit soleus muscle? Because of the specific innervation of fiber types in rat and rabbit soleus (Thompson *et al.*, 1984; Gordon and Van Essen, 1985), fast and slow motor units are largely distinct. Hence we were able to conduct the simulation by comparing different model runs with varying initial levels of polyinnervation (6-fold for slow units vs. 3-fold for fast units). The results of this analysis are summarized in Fig. 14. While small differences in the percentage of multiply innervated fibers are apparent at the earlier age ("d7" in Fig. 14A), variation is negligible at the later age ("d11"). This surprising similarity in polyinnervation at both times results from a much larger early rate of synapse loss when initial polyinnervation is higher (Fig. 14B).

As described in the preceding section, the observed slowing of the rate of synapse elimination following a wholesale activity block could be correctly simulated by the model (Fig. 8) provided that the exponential relationship selected to describe scaffolding synthesis as a function of muscle fiber activity produced as sufficiently large increase in synthesis in the absence of activity. The same exponential relationship then yielded an appropriate increase in the rate of synapse loss when activity was increased above normal levels. The assumption of activity dependent scaffolding synthesis yielded no discernible effects in response to the third activity perturbation, a partial activity block. This is not surprising, considering that the

Figure 13. The relative diversity of motor unit sizes determined by scale invariant measures remains largely unchanged during normal synapse elimination as simulated by the scaffolding model.

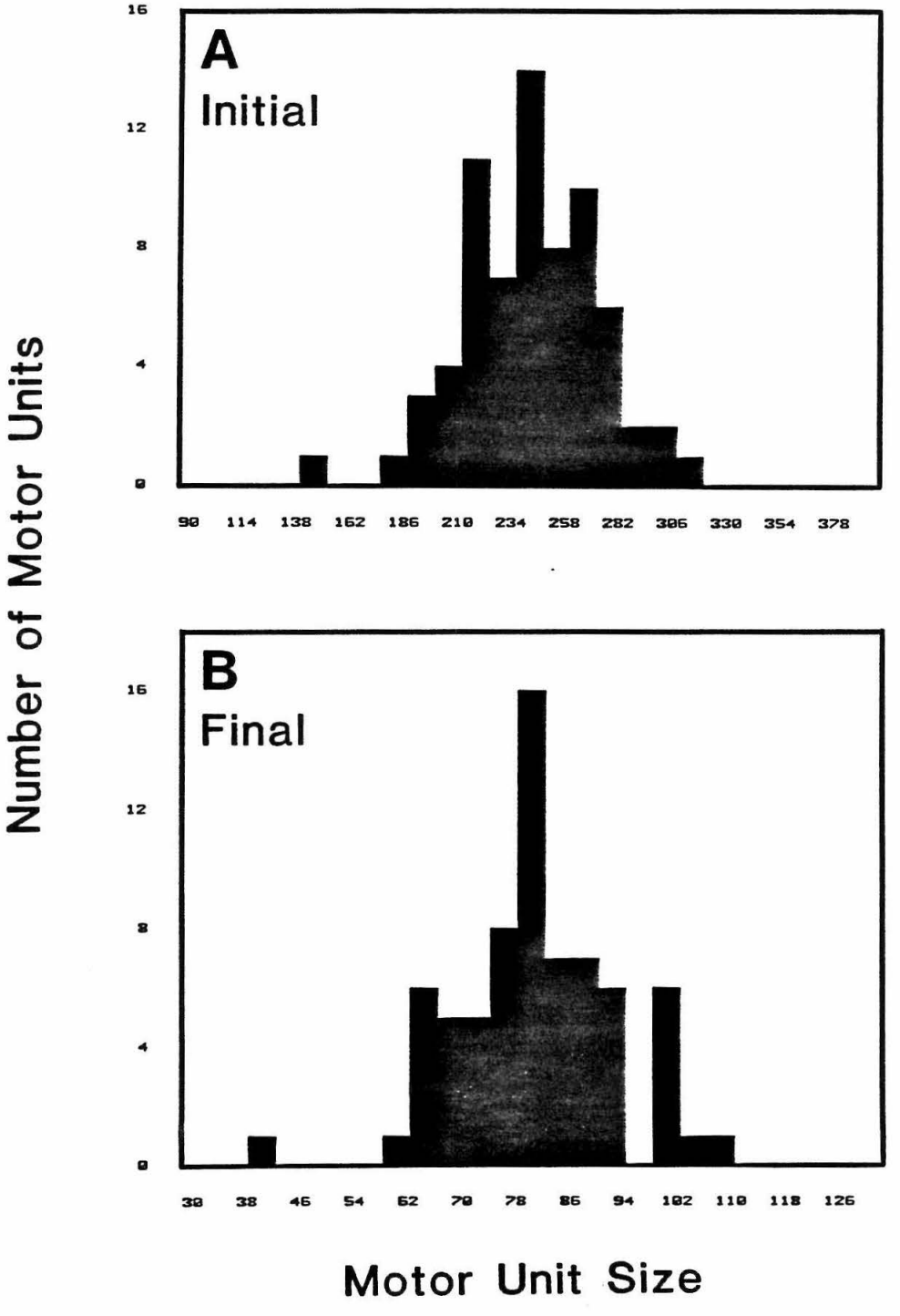
A
Initial
B
Final
Number of Motor Units
Motor Unit Size
0
4
8
12
16
90 114 138 162 186 210 234 258 282 306 330 354 378
30 38 46 54 62 70 78 86 94 102 110 118 126

Figure 13

Figure 14. The scaffolding model is remarkably accurate in simulating experimental evidence indicating a nearly synchronous endpoint for synapse elimination regardless of the initial level of polyinnervation (A). A greater initial degree of polyinnervation (6-fold vs. 3-fold) leads to the early loss of a substantially higher fraction of terminals (B), presumably owing to their smaller size. Iterations corresponding to days 7 and 11 in the rabbit soleus muscle are indicated by arrows.

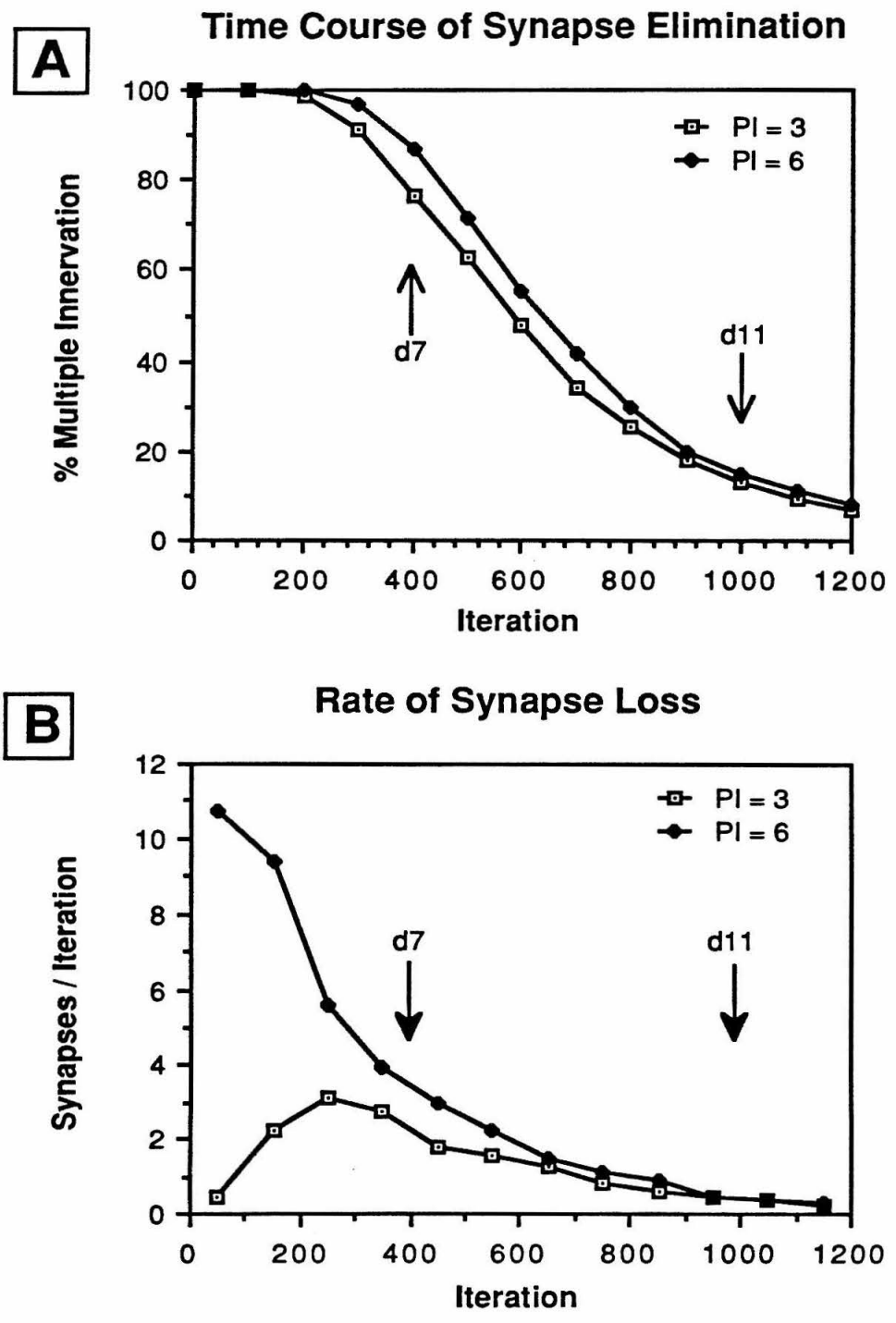
A
Time Course of Synapse Elimination
% Multiple Innervation
100
80
60
40
20
0
0
200
400
600
800
1000
1200
Iteration
PI = 3
PI = 6
d7
d11
B
Rate of Synapse Loss
Synapses / Iteration
12
10
8
6
4
2
0
0
200
400
600
800
1000
1200
Iteration
PI = 3
PI = 6
d7
d11

Figure 14

altered rate of scaffolding synthesis at an endplate affects all terminals at that endplate similarly, regardless of their particular activity.

A complementary constellation of effects was observed when the activity of presynaptic terminals was allowed to regulate the incorporation of scaffolding into the synaptic basal lamina, while scaffolding synthesis remained independent of activity. In this circumstance, a total block of activity had virtually no effect upon the rate of synapse elimination, suggesting that scaffolding synthesis was indeed a rate limiting step. Similarly, no change in rate was observed when overall activity levels were doubled. In contrast, this hypothesized role for activity enabled the model to correctly simulate the effect of a partial activity block upon the development of motor unit size, but only if less active terminals were assumed to induce greater incorporation of scaffolding ($c_{bl} \geq 0$, Appendix). In this case, while both lost the majority of their terminals, inactive axons retained control of larger motor units than did their active rivals, reflecting a competitive advantage for less active units (Callaway *et al.*, 1987). In some model experiments, the block was maintained for the entire run, while in other cases, to simulate the experiments of Callaway *et al.* (1988), the partial block was removed at a model iteration found to be roughly equivalent to 9 days postnatal in rabbits based on the level of polyinnervation at this iteration in unperturbed model runs. An appropriate slope for the activity dependence ($c_{bl} = 1.25$, Appendix) correctly simulated the magnitude of the inactivity advantage reported by Callaway *et al.* (1988). Interestingly, the ultimate size of both blocked and active motor units depended little on whether the block was lifted at the iteration corresponding to 9 days. However, the ratio of motor unit sizes for blocked vs. active units continued to increase after removal of the block, reaching about twice its value at the moment the block was lifted. In the experiments of Callaway *et al.* (1988), only a moderate

further increase in this ratio was seen following failure of the block.

Having selected parameters which correctly simulated partial activity block experiments, we employed these same parameters in a series of normal, unperturbed model runs. While activity dependent scaffolding incorporation was assumed in all cases, simulations were conducted with and without activity dependent scaffolding synthesis. Two issues were addressed, one regarding changes in motor unit size diversity, the other concerning the conjecture of Callaway *et al.* (1987) that activity differences in neonates might promote recruitment order sorting of motor units during synapse elimination. The assumption that scaffolding incorporation is dependent on activity of the overlying presynaptic terminal led to a clear increase in motor unit size diversity during synapse elimination (data not shown). A further consequence was the development of a substantial degree of recruitment order sorting consistent with the size principle (Fig. 15), especially evident when the results of several simulations were pooled. Inclusion of postsynaptic activity dependent synthesis moderated both effects.

The final developmental perturbation simulated with the scaffolding model was partial denervation. When the majority of motor neurons and their terminals were suddenly removed, synapse elimination continued with a moderately accelerated time course at the remaining polyinnervated endplates, regardless of which of the postulated activity influences were invoked. More significantly, no additional denervated endplates appeared as synapse elimination progressed, so that the remaining motor units emerged from the process much larger than has been observed experimentally (Brown *et al.*, 1976; Thompson and Jansen, 1977). The rate of synapse elimination among remaining polyinnervated terminals was marginally increased. Hence the scaffolding model was unable to simulate the experimentally observed effects of partial denervation.

Figure 15. Simulations suggest that the ordering of motor unit sizes according to their recruitment thresholds can be enhanced during synapse elimination under appropriate assumptions. In these simulations of unperturbed synapse elimination, we assumed that the induction and incorporation of scaffolding into the synaptic basal lamina is inversely dependent upon presynaptic activity. This assumption was successful in simulating the competitive advantage experienced by less active terminals during a partial activity block. While initial motor unit sizes are not correlated with activity (A), a clear negative correlation develops during synapse elimination (B), as less active motor units retain more terminals. Activity presumably reflects recruitment threshold, so that more active units are recruited first.

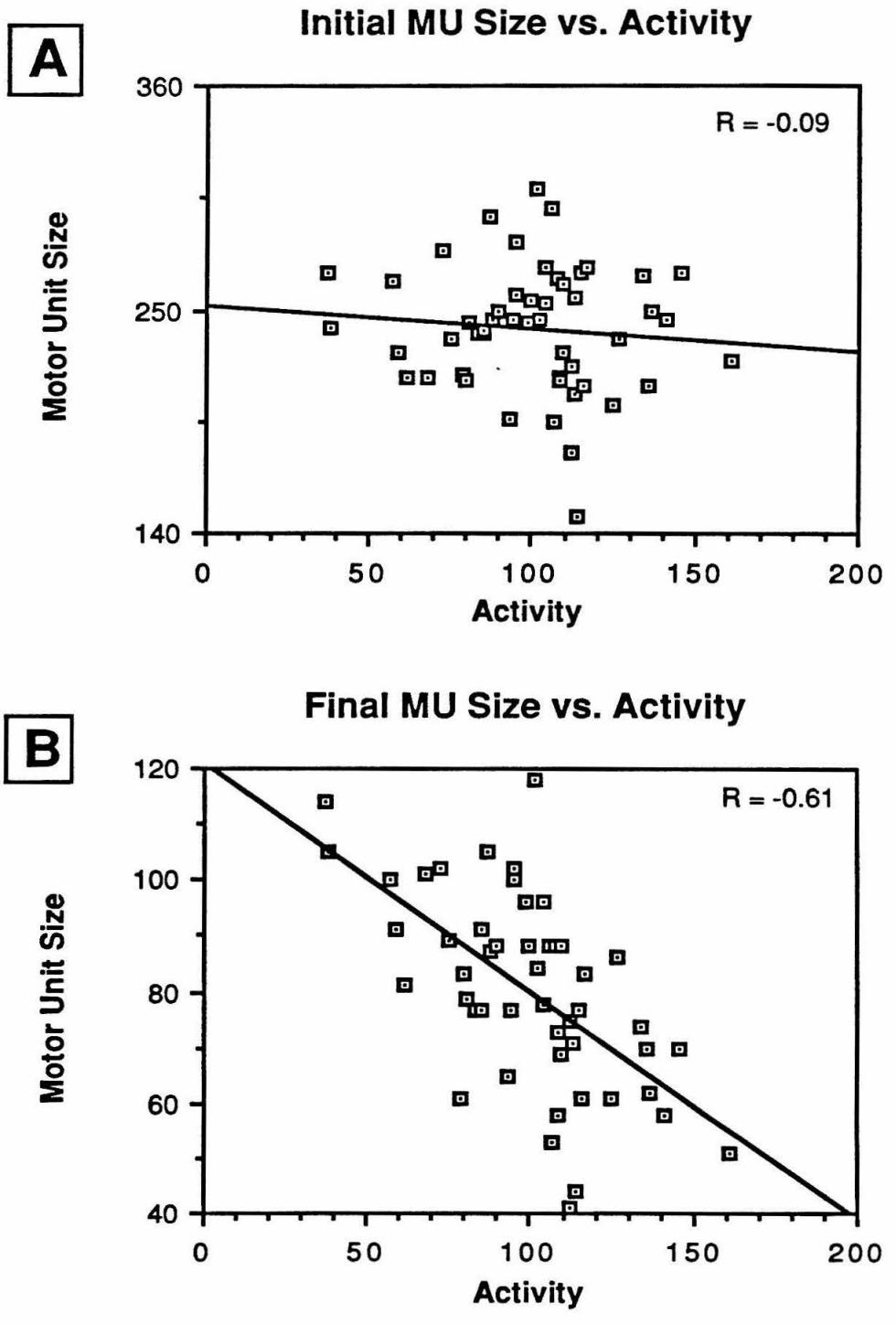
A
Initial MU Size vs. Activity
R = -0.09
Motor Unit Size
360
250
140
0
50
100
150
200
Activity
B
Final MU Size vs. Activity
R = -0.61
Motor Unit Size
120
100
80
60
40
0
50
100
150
200
Activity

Figure 15

Neural Energy Model

Because a growth advantage for larger terminals appears to be less important for convergence in the neural energy model (see Model Formulation and Performance), simulations were run both with and without terminal length dependence. In either case, the model produced synapse elimination which proceeded to completion with a normal time course and without producing denervated endplates. Motor unit size diversity closely matched the assigned diversity in metabolic capacity.

Simulations demonstrated that the time course of synapse elimination initiated with either 3-fold or 6-fold polyinnervation were similar at the two time points corresponding to days 7 and 11 in the rabbit soleus muscle (Fig 16), at least to within the 1 day experimental resolution of Soha *et al.* (1987). A much greater early rate of synapse loss in the 6-fold case was again responsible for this similarity. Timing differences were greater under the assumption of a terminal size advantage, averaging 0.7 days (shown in Fig. 16) compared to an average difference of 0.3 days (data not shown) when bias was assumed to be independent of terminal length.

When neural energy was modulated by activity, wholesale activity block simulations produced a delay in the rate of synapse elimination (Fig. 17), whether or not terminal length dependence was included in the bias function. While the delay was significant (approximately 5-fold), the maximal effect was less than that produced by the scaffolding model, where polyinnervation could be maintained indefinitely. As with the scaffolding mechanism, the retarding effect resulted from an increased preference for growth among all competing terminals. Increased activity accelerated synapse elimination moderately. In partial activity block simulations, blocked units enjoyed a competitive advantage and became relatively larger than their active rivals, in accordance with the observations of Callaway *et al.* (1987).

Figure 16. Simulations with the neuronal energy model show a considerable similarity in the time course of synapse elimination for widely varying initial levels of polyinnervation (A), although the behavior is somewhat less striking than that shown by the scaffolding model. Again, a much higher early rate of synapse loss for 6-fold vs. 3-fold initial polyinnervation (B) accounts for the phenomenon.

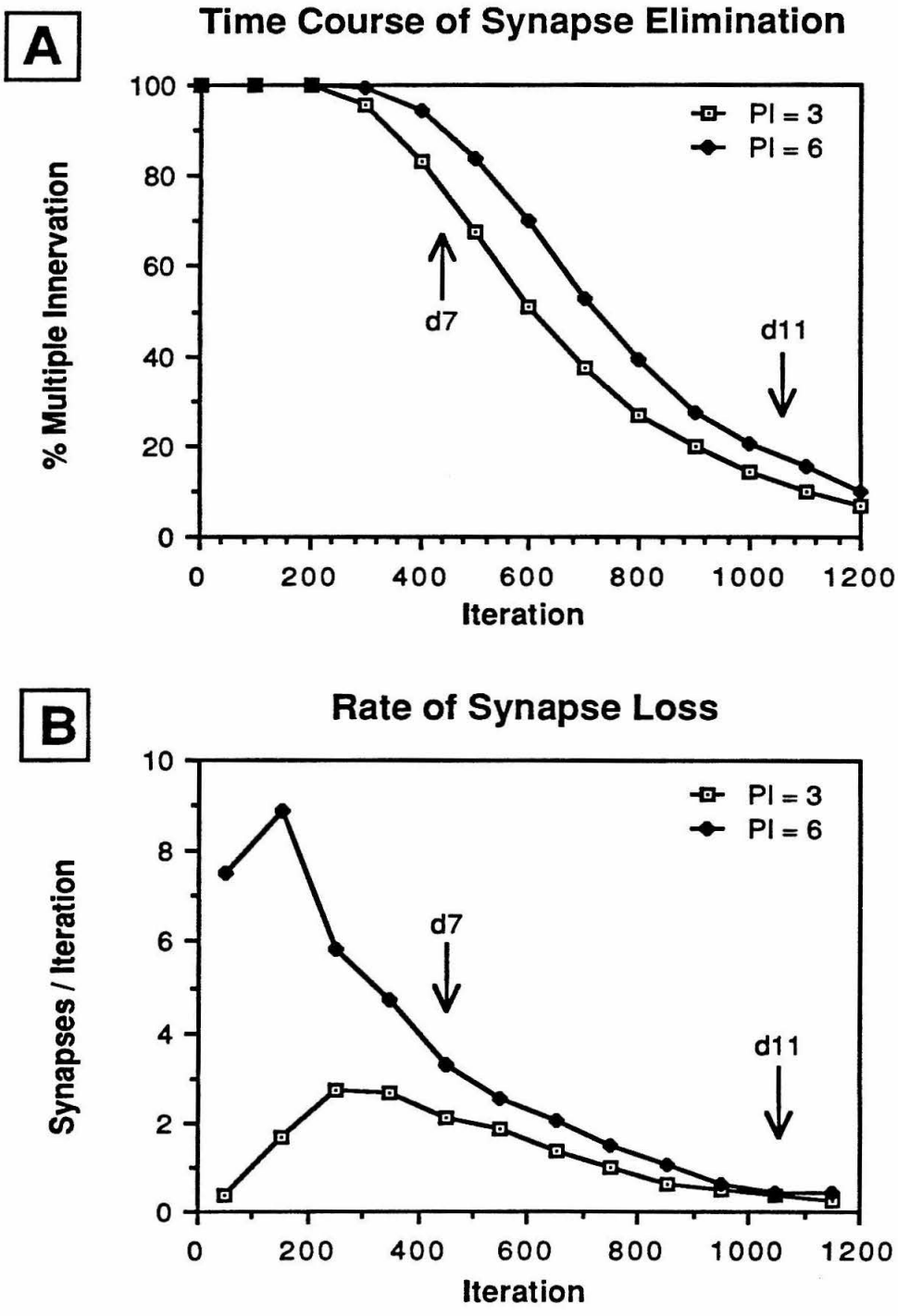
A
Time Course of Synapse Elimination
% Multiple Innervation
100
80
60
40
20
0
0
200
400
600
800
1000
1200
Iteration
PI = 3
PI = 6
d7
d11
B
Rate of Synapse Loss
Synapses / Iteration
10
8
6
4
2
0
0
200
400
600
800
1000
1200
Iteration
PI = 3
PI = 6
d7
d11

Figure 16

Figure 17. If activity modulates neural energy loading such that more active neurons must support greater demands, the the neural energy model is able to simulate the retarding effect of a presynaptic activity block, or the hastening of synapse elimination when activity is increased by neural stimulation. Because the mechanism works presynaptically, it cannot simulate the effect of a postsynaptic activity block.

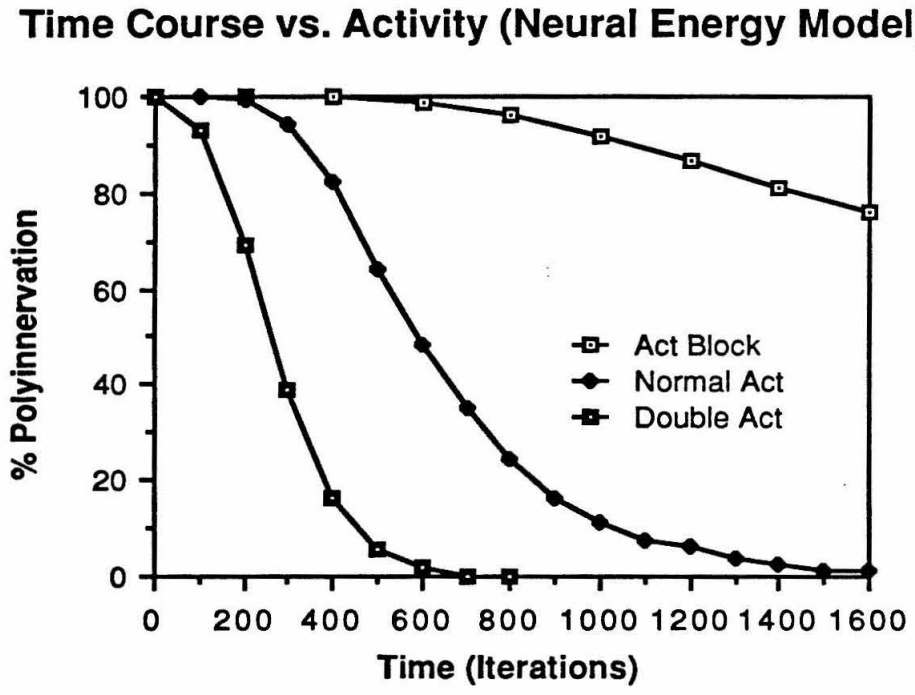
Time Course vs. Activity (Neural Energy Model)
% Polyinnervation
100
80
60
40
20
0
0
200
400
600
800
1000
1200
1400
1600
Time (Iterations)
Act Block
Normal Act
Double Act

Figure 17

Interestingly, however, activity differences during normal synapse elimination do not yield an increased correlation between motor unit size and the presumptive recruitment order reflected by the level of neural activity.

The neural energy model was particularly successful in simulating the altered development of motor unit size following partial denervation, provided that each neuron's metabolic capacity exceeded the energy demands of its arbor by an adequate percentage. No delay in the rate of synapse elimination was apparent, however; if anything, the presence of fewer competing terminals accelerated synapse elimination at endplates which remained polyinnervated following experimental perturbation.

Trophic Factor Model

Conferring a competitive advantage upon terminals in proportion to their length was necessary to obtain timely convergence with the locally acting trophic factor model. Synapse elimination then proceeded in an orderly fashion without the development of denervated endplates. Motor unit size diversity was largely unchanged during synapse elimination. Pooling results of 5 simulations with differing random number seeds yielded a final diversity (s.d./mean) of 0.149 vs. an initial diversity of 0.135. Simulations were also conducted to compare the timing of synapse elimination for differing initial levels of polyinnervation. Early synapse loss was substantially greater for 6-fold vs. 3-fold initial polyinnervation (Fig. 18). However, a moderately higher percentage of muscle fibers remained multiply innervated both at "day 7" and "day 11." The differences in both cases were close to the limit of detectability in the experiments of Soha *et al.* (1987).

The interruption of synapse loss which follows wholesale activity block has

Figure 18. Under the local trophic factor model, the time course of synapse elimination differs by less than a day despite substantial differences in the initial level of polyinnervation. Iterations corresponding to days 7 and 11 in rabbit soleus can be estimated based on the average percentage of polyinnervation remaining at those times.

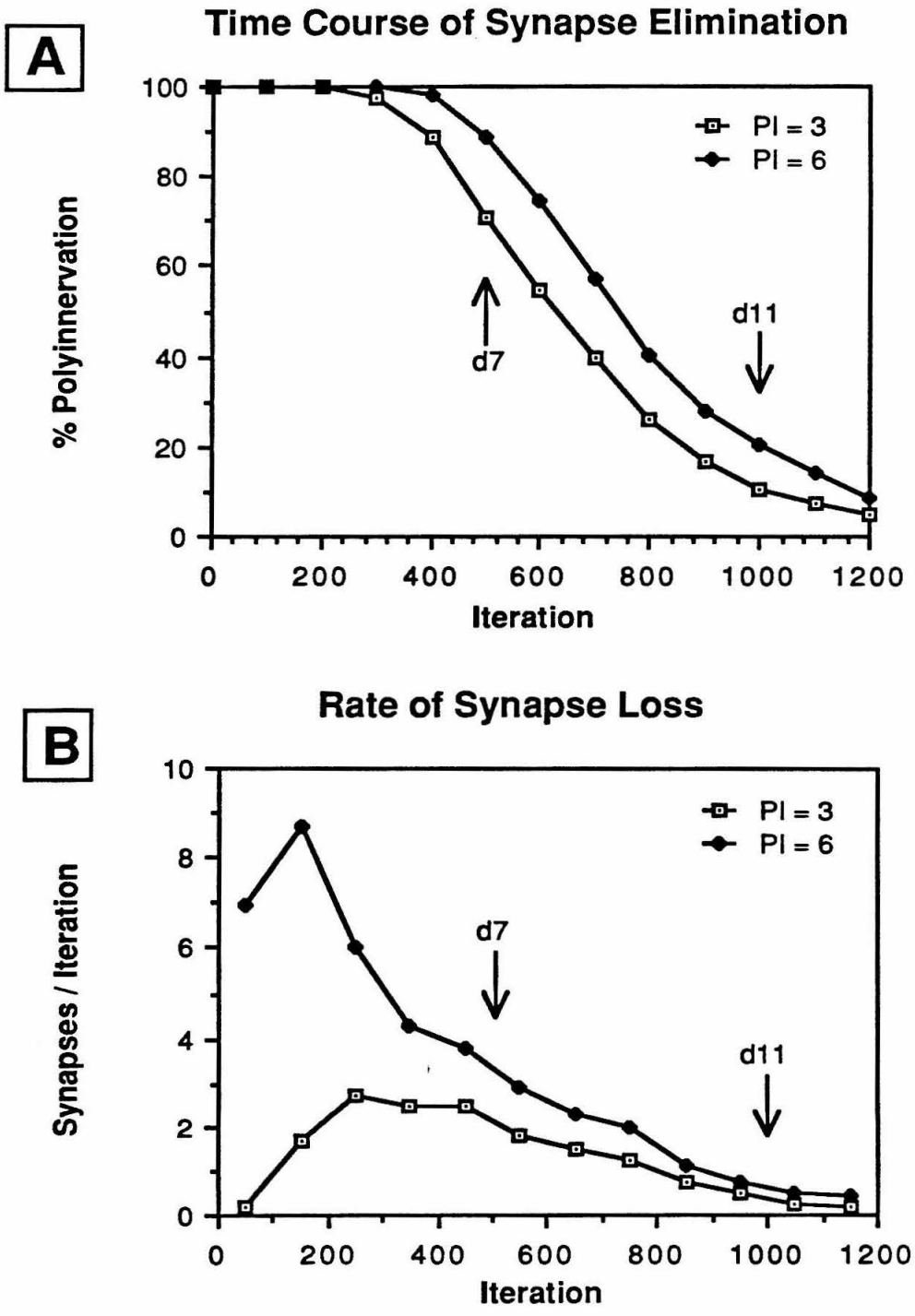
A
Time Course of Synapse Elimination
% Polyinnervation
100
80
60
40
20
0
0
200
400
600
800
1000
1200
Iteration
PI = 3
PI = 6
d7
d11
B
Rate of Synapse Loss
Synapses / Iteration
10
8
6
4
2
0
0
200
400
600
800
1000
1200
Iteration
PI = 3
PI = 6
d7
d11

Figure 18

been a primary consideration in motivating previous theroretical consideration of trophic factors in synapse elimination (Jansen *et al.*, 1978; Thompson, 1985). The local trophic factor model simulates this experimental observation successfully with or without inclusion of terminal size dependence. Clearly it is the hypothesized reciprocal exponential dependence of trophic factor synthesis upon postsynaptic activity (see Model Formulation and Performance) which is responsible for this behavior. The degree to which the process is retarded is strongly dependent upon the selected steepness of the exponential activity dependence (Fig. 19). Acceleration of synapse elimination following experimentally increased activity was also simulated correctly. When only trophic factor synthesis depends on activity, a partial activity block has no apparent on the development of motor unit sizes.

When the uptake of trophic factor by presynaptic terminals was also presumed to be dependent upon activity, the response of the process to either a removal or increase of activity increased modestly. More importantly, this assumption allowed successful simulation of partial activity block experiments. Blocked motor units retained a significantly larger fraction of their original synaptic connections than did more active units, but only if a decreasing exponential function of activity (Fig. 7) was employed to describe trophic factor uptake. The effect was greater for steeper exponential functions. At first glance, it would seem intuitively dissatisfying to postulate that uptake might proceed at a greater rate at less active terminals. It is possible, however, that uptake itself is independent of activity, while the inactivation of trophic factor could be positively regulated by intracellular Ca^{2+}. We again examined whether this process could contribute to recruitment order sorting during normal synapse elimination. First, we determined the slope of the activity uptake dependence which yielded an increase in relative motor unit size for blocked units comparable to that observed by Callaway *et al.* (1988) when the activity

Figure 19. The inverse dependence of trophic factor synthesis upon muscle fiber activity allows the local trophic factor model to simulate the effects of wholesale activity perturbations.

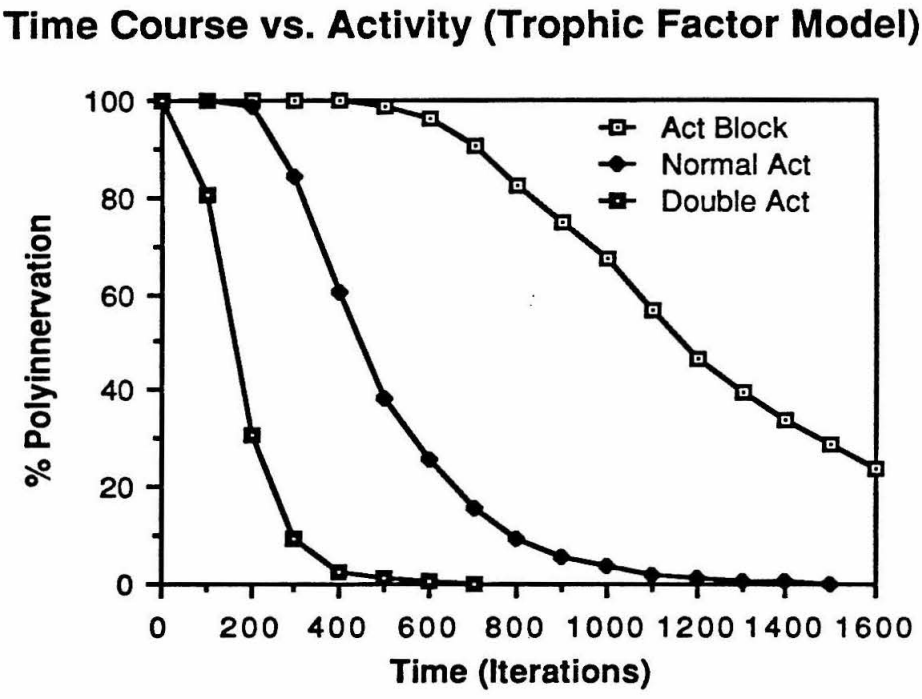
Time Course vs. Activity (Trophic Factor Model)
% Polyinnervation
100
80
60
40
20
0
0
200
400
600
800
1000
1200
1400
1600
Time (Iterations)
Act Block
Normal Act
Double Act

Figure 19

block was removed at an appropriate time. Then we simulated normal synapse elimination, assuming a systematic variability in neural activity, and observed the development of motor unit sizes. As shown in Fig. 20, final motor unit sizes were indeed negatively correlated with neural activity as would be appropriate were the recruitment ordering implicit in this activity pattern to be maintained into adulthood.

The local operation of trophic factor as described in our model is not effective in simulating the effects of partial denervation. Synapse elimination is accelerated modestly, presumably due to the reduced competition for space at endplates which remain polyinnervated. After the initial denervation, no additional endplates become denervated. Hence, motor unit sizes remain much larger than is observed in experimental animals.

Figure 20. If uptake of trophic factor is inversely dependent upon the activity of a presynaptic terminal, then recruitment order sorting may develop during synapse elimination. The inverse dependence might occur if uptake were independent of activity, but removal of factor depended upon intracellular Ca^{2+} levels.

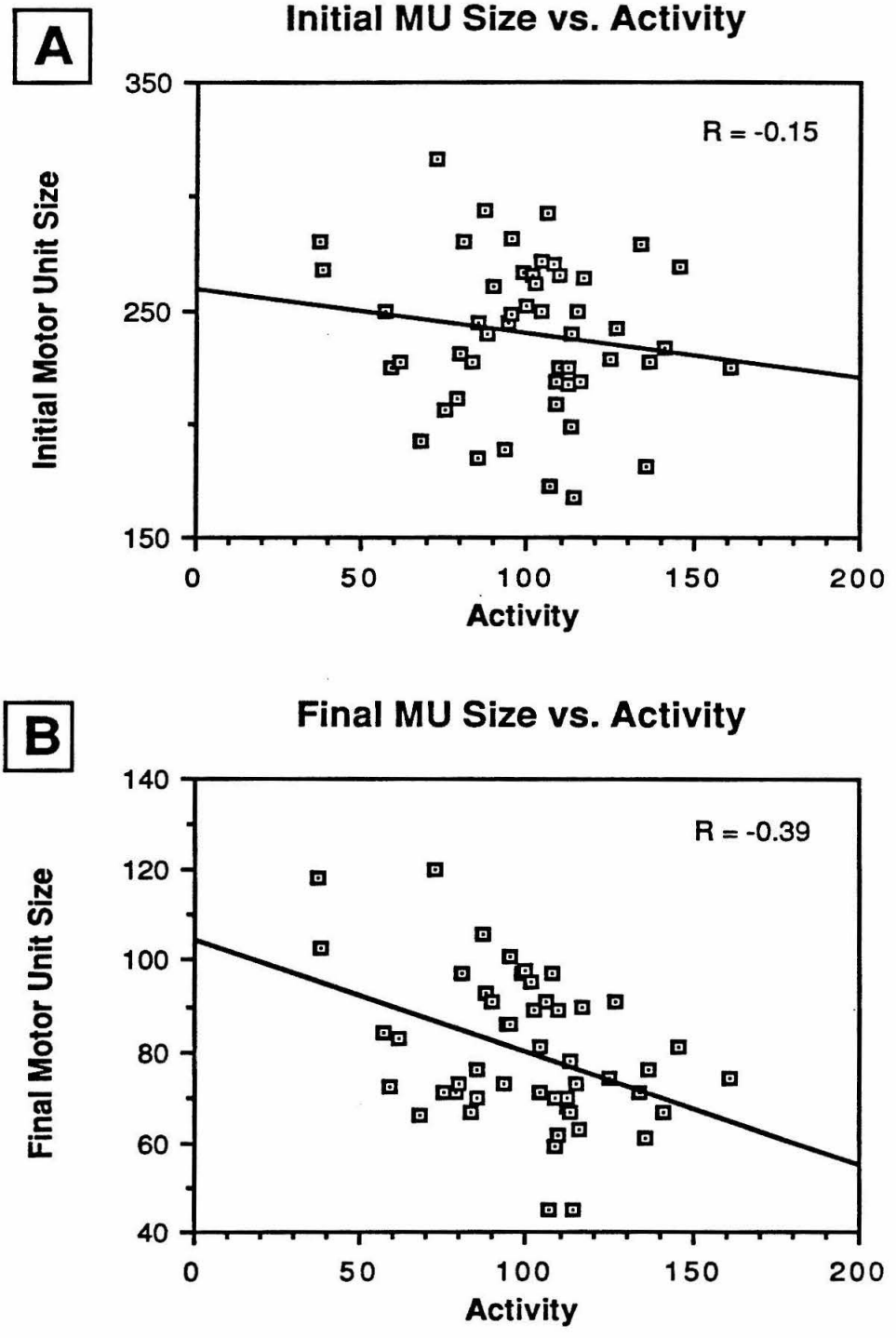
A
Initial MU Size vs. Activity
Initial Motor Unit Size
350
250
150
R = -0.15
0
50
100
150
200
Activity
B
Final MU Size vs. Activity
Final Motor Unit Size
140
120
100
80
60
40
R = -0.39
0
50
100
150
200
Activity

Figure 20

DISCUSSION

Several interesting findings have emerged from the modeling experiments. The most fundamental of these is that synapse elimination, as simulated by the model, proceeds in an orderly and appropriate manner under a very simple set of rules. Two key assumptions are largely responsible for this result: (1) Terminals compete for limited endplate space, and (2) all terminals experience an overall bias for growth. In a basic scaffolding simulation, without length dependence or activity effects, all terminals are on an approximately equal footing. Even so, synapses are gradually lost without producing denervated endplates, and the distribution of motor unit sizes maintains appropriate diversity as all units shrink in size. Adding a terminal size dependence, so that larger terminals enjoy a competitive advantage, accelerates synapse elimination to a perhaps more realistic rate, but does not disturb the orderly nature of the process. The neural energy model displays similar behavior, with or without length dependence. Because of our assumptions concerning the internal localization of factor, the local trophic factor model requires that terminal size modulate growth-retraction bias in order to converge to the singly innervated state.

Several findings are particularly interesting because they would not have been readily predictable in advance. One of these concerns the comparative time course of synapse elimination for differing initial levels of polyinnervation. The underlying experimental observation, that fast and slow muscle fibers in rabbit soleus muscle reach the latter stages of synapse elimination at approximately the same time (Chapter 3), was itself surprising, considering that earlier in the process, slow fibers receive about twice the synaptic input of fast fibers (Gordon, 1983; Callaway *et al.*, 1988). We were curious, and somewhat doubtful, as to whether the model would yield a similar result. In fact, as described earlier, all three mechanisms yielded remarkably similar timing near the endpoint, regardless of the initial level

of polyinnervation, although the trophic factor model was less effective in simulating this observation. The explanation for this result involves the substantially elevated rate of early synapse loss associated with greater initial polyinnervation.

Another example of a non-intuitive result concerns the role of scaffolding synthesis in accounting for the delay in synapse elimination that follows a wholesale block of neural activity. While it seemed likely that modulating synthesis by activity would alter the rate of competition, we were uncertain what the sign of the effect might be. It seemed reasonable to suppose that if scaffolding were important in establishing a competitive framework, then more scaffolding might accelerate the competition. In fact, the opposite is true: higher levels of scaffolding increase the growth preference of all terminals. Each terminal clings to its territory, thereby slowing the rate of synapse loss. Thus to correctly simulate the effect of an activity block, it is necessary that there be an inverse dependence of scaffolding synthesis upon muscle fiber activity. Furthermore, synthesis in inactive fibers must increase by several fold over normal rates to adequately mimic experimental evidence. A similar relationship links the rate of trophic factor synthesis to the rate of synapse elimination under the trophic factor mechanism.

A third example concerns the relationship between potential activity differences among neonatal motor neurons and the early development of correct recruitment ordering among motor units according to their size. Recruitment ordering consistent with the size principle (Henneman and Olson, 1965) could develop in two fundamentally different ways. The recruitment thresholds of motor neurons could develop according to their motor unit size, or alternatively, motor unit sizes might develop so as to become consistent with existing recruitment thresholds. When Callaway *et al.* (1987) observed that blocking the activity of a small fraction of motor neurons gave their terminals a competitive advantage over their normally

active rivals, they noted that this non-Hebbian behavior could in fact promote recruitment ordering according to the second of these two mechanisms. This process would of course require that there be consistent differences in activity among neonatal motor neurons, an issue which has not yet been fully resolved. In this example, while it seems intuitively likely that any activity dependence which simulated the results of a partial activity block would indeed tend to promote recruitment ordering, one cannot readily predict whether the magnitude of this effect would be sufficient to produce meaningful changes in relative motor unit size. Additionally, one would like to determine how large the activity differences must be to produce substantial ordering in the relatively short interval available. For both the scaffolding and local trophic factor models, simulations established that presynaptic mechanisms which could mimic the effect of a partial activity block would also promote recruitment order sorting in response to consistent differences in activity. Furthermore, a relatively small range of activity levels (20-40%) was sufficient to produce a significant degree of ordering. Surprisingly, this relationship did not apply to the neural energy model. While the effect of a partial activity block could be simulated if presynaptic activity were presumed to modulate energy loading, moderate differences in normal activity produced no noticeable recruitment order sorting.

These three examples illustrate the rationale for modeling, and confirm its practical value in understanding the behavior of a complex system. In each case, the inherent complexity of the situation was too great to permit the outcome to be assessed in advance with a high degree of confidence. In some cases, overtly surprising or unpredictable results were obtained, although in retrospective analysis, these results seem entirely reasonable. In other situations, modeling can confirm initial expectations, while providing greater detail or a quantitative perspective.

Two of the models work through interactions which are local to the endplate, while the other operates on a system-wide basis. It is interesting to examine more fully the underlying similarities and differences in these mechanisms. While certainly not identical, the locally acting trophic factor mechanism is similar in several interesting respects to the scaffolding model. In both cases, the growth-retraction bias of presynaptic terminals is influenced by a molecule synthesized and secreted by muscle fibers. Scaffolding remains external to a terminal, while trophic factor acts intracellularly. Synthesis of each is regulated in an inverse exponential manner by muscle fiber activity. The scale at which the mechanisms operate differs. Scaffolding affects only a local region at a terminal boundary, hence it operates at a sub-micron scale. Trophic factor is presumed to distribute equally throughout a presynaptic terminal. The rates at which the two molecules are removed (by decay or transport) were presumed to differ by two orders of magnitude (with scaffolding being more stable); otherwise the intracellular accumulation of trophic factor could effectively prevent the removal of any terminals. Activity dependent trophic factor uptake is analogous to assuming that the induction of scaffolding incorporation into the basal lamina is dependent on presynaptic activity. We allow the efficacy of either scaffolding or trophic factor in promoting terminal growth to be modulated by activity, mediated in both cases by shifts in the bias function.

Given the degree of structural similarity between the two models one would expect a corresponding similarity in performance. As described earlier (Model Formulation and Performance), the local trophic model manifests an inherent tendency to resist convergence. Hence, a relative growth advantage for larger terminals is even more critical in this model if the process is to proceed at a reasonable rate. As with the scaffolding mechanism, once a terminal size dependence is introduced into the bias function, the model is quite successful in simulating the

selected experimental features of synapse elimination, with one possible exception: The initial level of polyinnervation retains greater influence on the timing of synapse elimination in the trophic factor model, although the difference in single innervation at the equivalent to days 7 and 11 would be only marginally detectable in the labeling experiment of Soha *et al.* (1987). An inverse exponential relation between activity and trophic factor synthesis leads to appropriate behavior in response to overall activity perturbations, as did the activity dependent synthesis of scaffolding. This effect is stronger in the local trophic factor model, in that a smaller value of the exponential coefficient (c_f vs. c_s, see Appendix) is required to produce a similar degree of retardation following activity block. Including activity dependent uptake of trophic factor in the model allows partial activity block experiments to be simulated, but only if increased activity results in less uptake. This is another example of a finding which at first glance would seem counter-intuitive. As described earlier, however, it is conceivable that uptake itself might be unaffected by activity, while inactivation of trophic factor could be positively regulated by intracellular Ca^{2+} in an activity dependent manner. The necessary inverse dependence of uptake on activity is similar to the relationship between scaffolding incorporation and activity required to simulate partial activity block experiments. Another similarity in these aspects of the models is the effect on motor unit size. Given that one assumes a range of activity levels among unperturbed neonatal motor neurons, activity dependent uptake of trophic factor and the activity dependent induction of scaffolding both lead to substantially increased diversity in motor unit size, regardless of the sign of the exponential dependence on activity. In both cases, an inverse dependence can produce recruitment order sorting during synapse elimination. A final similarity between the local trophic factor and scaffolding models is their failure to simulate the effects of partial denervation.

The neural energy model differs fundamentally from the scaffolding and local trophic factor models in that, at any iteration, all terminals in the arbor of a given motor neuron experience the same growth-retraction bias, subject to optional modulation by terminal length. Conversely, terminals are unaffected by local endplate considerations save for the inevitable competition for synaptic space. While conferring a growth advantage onto larger terminals hastens synapse elimination considerably, terminal size dependence is less critical for convergence in the neural energy model in that synapse elimination proceeds at a credible rate across a fairly broad range of dynamic step sizes. Hence we conducted simulations both with and without the assumption of terminal size dependence. In either case, the tested aspects of normal synapse elimination were accurately simulated. To investigate activity perturbations, we allowed activity to modulate the calculated energy load such that more active neurons require additional metabolic support. This assumption accurately simulates the effect of a presynaptic activity block or of neural stimulation, but because it is independent of muscle fiber activity, it cannot duplicate the effect of a postsynaptic block with α-bungarotoxin (Duxson, 1982; Callaway and Van Essen, 1988), or the possible effect of direct muscle stimulation (Thompson, 1983). Also, while this assumption produces the correct response to a partial activity block, it does not promote recruitment order sorting. Because motor neurons resist excessive expansion of their arbors, the neural energy model responds appropriately to the reduced competitive environment which follows partial denervation by withdrawing completely from some endplates, even though these may become denervated as a result. Even this mechanism, although specifically formulated to explain partial denervation, fails to simulate the delay in synapse elimination which is seen following partial denervation.

The results of our simulations are highly dependent upon several key

assumptions inherent in our model. The first of these is that the development of presynaptic terminals is a highly dynamic process, alternating between brief episodes of growth and retraction. Indirect evidence of dynamic behavior from both light and EM level observations has been cited (Wernig *et al.*, 1980; Bixby, 1981). Two other critical assumptions are that terminals compete for limited endplate space, and that available endplate space is almost fully occupied during the dynamic competitive process. While these assumptions represent reasonable (perhaps even likely) possibilities, there are plausible alternatives. If there is no lateral competition for space between the multiple terminal profiles underlying a single Schwann cell in ultrastructural cross-sectional views of the endplate, then perhaps all available endplate space could be simultaneously occupied by several presynaptic terminals. In this case, an alternative substrate for the competitive interaction among terminals would be required. It has also been suggested, based upon repeated observations of dye-labeled terminals (Balice-Gordon and Lichtman, 1987), that once a terminal has withdrawn from a significant region of an endplate, no terminal may reoccupy the vacated territory. If strictly true, such a behavior is potentially in conflict with all three of the critical assumptions itemized above. However, such behavior might apply only to regions which become totally vacant, while dynamic behavior and competition for space continue within local regions. Alternative assumptions such as these can ultimately be addressed within the framework of our model.

Our model was constructed in a manner designed to retain generality, and as such is intended to evolve. Additional mechanisms can be readily implemented and analyzed within the same general framework. For example, a prevalent conception of trophic factors suggests that their central effects on overall neuronal vigor may be more significant than any local effects. A muscle-derived trophic factor may operate

in this manner, and we intend to implement this capability soon. Experimental evidence has been reported which implicates proteases, particularly Ca^{2+}-activated neutral protease, as key agents in mediating synapse elimination (O'Brien *et al.*, 1978, 1984; Connold *et al.*, 1986). The structure of our model should allow this mechanism to be simulated. Another objective is to identify means by which partial denervation might delay synapse elimination. Allowing a diffusional spreading of trophic factor among adjacent endplates, or invoking a distinct sprouting factor, are possible approaches. Finally, the model was designed to support studies of these mechanisms in various combinations, and with differing relative weightings. We intend to undertake these studies in the near future.

APPENDIX: MATHEMATICAL DESCRIPTION

In accordance with a basic design goal of the model, changes in terminal size are determined stochastically, while the probabilities of either growth or retraction depend upon the recent state of the system. Two state variables regulate terminal growth and retraction at each model iteration. The dynamic state d $(0 \leq d \leq 1)$ describes the probability that a terminal will seek to change its size at the next iteration, and thereby controls the overall rate of development. While $d = 1$ in all simulations described earlier in the text, other possibilities are that d might vary as a function of time or presynaptic activity. Another state variable b $(-1 < b < 1)$ determines the relative bias for growth or retraction. Bias increases linearly in favor of growth as b increases. Together, these state variables define the preference for growth $P_G(b, d)$, the preference for retraction $P_R(b, d)$, and the preference for no change in size $P_N(d)$ (see Fig. 1):

$$P_G = \frac{d}{2}(b + 1)$$

$$P_R = -\frac{d}{2}(b - 1)$$

$$P_G + P_R = d$$

$$P_N = 1 - d$$

Because terminals are not allowed to grow into occupied or contested territory, the term "preference" is used to make clear that these values differ somewhat from the true probabilities of growth, retraction, or no change.

It is convenient to group terms contributing to the bias function according to the mechanism they describe, thereby treating b as the weighted average of mechanism-specific bias functions:

$$b = \sum_i a_i b_i, \qquad \sum_i a_i = 1, \quad (-1 \leq b_i \leq 1)$$

As before, more negative values of b_i reflect a greater bias toward retraction, while more positive values indicate an increased preference for growth. A general sigmoidal form (Fig. 2) was adopted for the mechanism-specific bias functions:

$$b_i = \frac{2}{1 + e^{\pm\beta(v_i, l)}} - 1,$$

The function β is linear in its dependence on the relevant mechanism specific variable v_i (scaffolding, trophic factor, or neural energy load). In some simulations, terminal length l was included explicitly in the bias function. The sign of the exponential function varies depending on the mechanism.

Among the possible roles for activity which we simulate in the model are regulation of the synthesis and incorporation or uptake of both scaffolding and trophic factor. The family of exponential curves (Fig. 7) defined by

$$\alpha(A) = e^{c(1-A/A_0)}$$

possesses certain features which appropriately describe the potential effects of activity in these cases. When activity A is constant at the reference level A_0, generally taken to be the average activity of a motor neuron under normal conditions, then $\alpha(A) = 1$, and activity has no effect. The exponential coefficient c determines the rate at which the function increases or decreases monotonically with increasing activity. In either case, small activity differences have their greatest effect at low activity levels.

Mechanisms of Synapse Elimination: Bias Functions

Scaffolding (b_1). Scaffolding is synthesized by muscle fibers at a rate which is optionally a function of postsynaptic activity A_{MF},

$$\Delta S_{MF} = r_{S_1}\alpha_{syn}(A) + r_{S_2} = r_{S_1}e^{c_s(1-A_{MF}/A_0)} + r_{S_2},$$

and accumulates to form a pool of available scaffolding S_{MF}, For $r_{S_1} > 0$ and $c_s > 0$, the inverse exponential dependence on activity implies that maximum synthesis occurs when all activity is blocked, and that increasing activity through stimulation results in a moderate decrease in scaffolding synthesis. At each iteration, a percentage of the available pool of scaffolding is incorporated into the basal lamina at each occupied endplate position and bound by the resident presynaptic terminal, in a manner optionally dependent on presynaptic activity:

$$\Delta S_{BL} = r_3 \alpha_{in}(A) S_{MF} = r_3 e^{c_{b1}(1-A/A_0)} S_{MF}.$$

A weighted average of bound scaffolding is computed for each boundary region of every terminal,

$$S = \frac{\sum_{i=0}^{k} w_i S_{i_0 \pm i}}{\sum_{i=0}^{k} w_i},$$

where S_i is the bound scaffolding at endplate position i, and i_0 is a boundary position. A typical set of weights is $w = (1, 1, .5, .5)$, with $k = 4$. The bias component b_1 due to scaffolding is then determined according to

$$b_1 = \frac{2}{1 + e^{-c_1(S - S_0 + \lambda(l))/S_{eq}}} - 1,$$

where S_0 controls the position of the S-axis intercept and S_{eq}, an estimate of the average equilibrium value of bound scaffolding at an occupied endplate position, provides a convenient unit for scaling the slope c_s of b_1 (but can be replaced if desired). The function

$$\lambda(l) = c_{l_1}(l - l_0),$$

permits the bias to depend explicitly upon terminal length, and can be viewed as introducing a horizontal translation into b_1. Typically, $l_0 = 50$, or half of the total endplate length. The magnitude of the competitive advantage enjoyed by larger

terminals is regulated by c_{l_1}. In the majority of our simulations, $c_{l_1} = 0.01 S_{eq}$. Coefficients regulating length advantage were selected similarly in simulations with the other mechanisms.

Neural Energy (b_2). The energy demand imposed upon a neuron by its arbor is proportional to the combined lengths l_i of all of its terminals, optionally modulated by its activity A,

$$E = c_E(\frac{A}{A_0}) \sum_{arbor} l_i + (1 - c_E) \sum_{arbor} l_i,$$

where the coefficient c_E controls the magnitude of the activity influence. The neural energy bias b_2 is defined by

$$\begin{aligned} b_2 &= \frac{2}{1 + e^{(E-M-\lambda(l)/E_w}} - 1 \\ &= \frac{2}{1 + e^{-((M-E)-\lambda(l))/E_w}} - 1. \end{aligned}$$

The metabolic capacity M of the neuron is the coordinate of the E-axis intercept, and b_2 is anti-symmetric about this point. A fundamental distinction of this mechanism lies in the sign of the exponential: viewed as a function of $(M - E)$, b_2 is sigmoidal as in Fig. 2, but if b_2 is regarded as a function of E, it is a monotonically decreasing sigmoidal function similar to Fig. 2 but reflected about the E-axis intercept. Terminal length dependence λ (l) is implemented as in the scaffolding mechanism. The width or slope of b_2 is controlled by E_w, which is generally set to a fraction of the average initial energy, e.g., $E_w = 0.4\mu_{E_0}$ in certain length dependent simulations.

Trophic Factor (b_3). Trophic factor f is synthesized at a rate inversely dependent upon activity

$$\Delta f = r_f \alpha_{syn}(A) = r_f e^{c_f(1-A/A_0)}$$

and secreted into an available pool. Uptake by a presynaptic terminal is proportional to the available concentration f, and is optionally dependent upon

the level of activity:

$$\Delta f_T = r_u f \alpha_u(A) = r_u f e^{c_u(1-A/A_0)}$$

Trophic factor within a terminal is subject to removal by decay and axonal transport. The intracellular quantity of factor f_T is converted to a concentration f_t which regulates the bias according to

$$b_3 = \frac{2}{1 + e^{-c_3(f_t - f_{t_0} + \lambda(l))/f_{t_{eq}}}} - 1.$$

The f-axis intercept is controlled by f_{t_0}, while the slope of the sigmoidal function is determined by c_3 and the expected average equilibrium concentration of trophic factor $f_{t_{eq}}$. Length dependence $\lambda(l)$ is defined as before.

REFERENCES

Al-Ghaith, L. K., and Lewis, J. H. (1982). Pioneer growth cones in virgin mesenchyme: an electron-microscope study in the developing chick wing. *J. Embryol. Exp. Morphol.* **68**, 149–160.

Bagust, J., Lewis, D. M., and Westerman, R. A. (1973). Polyneuronal innervation of kitten skeletal muscle. *J. Physiol. (London)* **229**, 241–255.

Balice-Gordon, R. J., and Lichtman, J. W. (1987). The relationship between pre- and postsynaptic elements at developing neuromuscular junctions. *Soc. Neurosci. Abstr.* **13**, 375.

Balice-Gordon, R. J., and Thompson, W. J. (1988). The organization and development of compartmentalized innervation in rat extensor digitorum longus muscle. *J. Physiol. (London),* in press.

Barany, M., and Close, R. I. (1971). The transformation of myosin in cross-innervated rat muscles. *J. Physiol. (London)* **213**, 455–474.

Barker, D., and Ip, M. C. (1966). Sprouting and degeneration of mammalian motor axons in normal and deafferented skeletal muscle. *Proc. R. Soc. Lond. B* **163**, 538–554.

Barstad, J. A. B. (1962). Presynaptic effect of the neuromuscular transmitter. *Experientia* **18**, 579–580.

Bastiani, M. J., and Goodman, C. S. (1984). Neuronal growth cones: specific interactions mediated by filopodial insertion and induction of coated vesicles. *Proc. Natl. Acad. Sci. USA* **81**, 1849–1853.

Bennett, M. R., and Ho, S. (1988). The formation of topographical maps in developing rat gastrocnemius muscle during synapse elimination. *J. Physiol.* **396**, 471–496.

Bennett, M., Ho, S., and Lavidis, N. (1986). Competition between segmental

nerves at end-plates in rat gastrocnemius muscle during loss of polyneuronal innervation. *J. Physiol. (London)* **381**, 351–376.

Bennett, M. R., and Lavidis, N. A. (1984a). Development of the topographical projection of motor neurons to a rat muscle accompanies loss of polyneuronal innervation. *J. Neurosci.* **4**, 2204–2212.

Bennett, M. R., and Lavidis, N. A. (1984b). Segmental motor projections to rat muscles during the loss of polyneuronal innervation. *Dev. Brain Res.* **13**, 1–7.

Bennett, M. R., McGrath, P. A., Davey, D. F., and Hutchinson, I. (1983). Death of motorneurons during the postnatal loss of polyneuronal innervation of rat muscles. *J. Comp. Neurol.* **218**, 351–363.

Bennett, M. R., and Pettigrew, A. G. (1974). The formation of synapses in striated muscle during development. *J. Physiol. (London)* **241**, 515–545.

Bennett, M. R., and Pettigrew, A. G. (1975). The formation of synapses in amphibian striated muscle during development. *J. Physiol. (London)* **252**, 203–239.

Bennett, M. R., and Raftos, J. (1977). The formation and regression of synapses during the re-innervation of axolotl striated muscle. *J. Physiol. (London)* **265**, 261–295.

Berg, H. C. (1983). "Random Walks in Biology." Princeton University Press, Princeton, NJ.

Beresford, B. (1983). Brachial muscles in the chick embryo: the fate of individual somites. *J. Embryol. Exp. Morphol.* **77**, 99–116.

Bernstein, J. J., and Guth, L. (1961). Nonselectivity in the establishment of neuromuscular connections following nerve regeneration in the rat. *Exp. Neurol.* **4**, 262–275.

Betz, W. J., Caldwell, J. H., and Ribchester, R. R. (1979). The size of motor units during post-natal development of rat lumbrical muscle. *J. Physiol. (London)*

297, 463–478.

Betz, W. J., Caldwell, J. H., and Ribchester, R. R. (1980). The effects of partial denervation at birth on the development of muscle fibres and motor units in rat lumbrical muscle. *J. Physiol. (London)* **303**, 265–279.

Bixby, J. L. (1981). Ultrastructural observations on synapse elimination in neonatal rabbit skeletal muscle. *J. Neurocytol.* **10**, 81–100.

Bixby, J. L., and Van Essen, D. C. (1979a). Regional differences in the timing of synapse elimination in skeletal muscles of the neonatal rabbit. *Brain Res.* **169**, 275–286.

Bixby, J. L., and Van Essen, D. C. (1979b). Competition between foreign and original nerves in adult mammalian skeletal muscle. *Nature (London)* **282**, 726–728.

Bray, D. (1970). Surface movements during growth of single explanted neurons. *Proc. Natl. Acad. Sci. USA* **65**, 905–910.

Brooke, M. H., Williamson, E., and Kaiser, K. K. (1970). Muscle fiber types: how many and what kind? *Arch. Neurol.* **25**, 360–366.

Brown, M. C., and Booth, C. M. (1983). Postnatal development of the adult pattern of motor axon distribution in rat muscle. *Nature (London)* **304**, 741–742.

Brown, M. C., Holland, R. L., and Hopkins, W. G. (1981). Restoration of focal multiple innervation in rat muscles by transmission block during a critical stage of development. *J. Physiol. (London)* **318**, 355–364.

Brown, M. C., Hopkins, W. G., and Keynes, R. J. (1982). Short- and long-term effects of paralysis on the motor innervation of two different neonatal mouse muscles. *J. Physiol. (London)* **329**, 439–450.

Brown, M. C., and Ironton, R. (1978). Sprouting and regression of neuromuscular synapses in partially denervated mammalian muscles. *J. Physiol. (London)* **278**, 325–348.

Brown, M. C., Jansen, J. K. S., and Van Essen, D. C. (1976). Polyneuronal innervation of skeletal muscle in new-born rats and its elimination during maturation. *J. Physiol. (London)* **261**, 387–422.

Buller, A. J., Eccles, J. C., and Eccles, R. M. (1960). Interaction between motoneurones and muscles in respect of the characteristic speeds of their responses. *J. Physiol. (London)* **150**, 417–439.

Buller, A. J., Mommaerts, W. F. H. M., and Seraydarian, K. (1969). Enzymic properties of myosin in fast and slow twitch muscles of the cat following cross-innervation. *J. Physiol. (London)* **205**, 581–597.

Burden, S. J., Sargent, P. B., and McMahan, U. J. (1979). Acetylcholine receptors in regenerating muscle accumulate at original synaptic sites in the absence of the nerve. *J. Cell Biol.* **82**, 412–425.

Burke, R. E. (1967). Motor unit types of cat triceps surae muscle. *J. Physiol. (London)* **193**, 141–160.

Burke, R. E., Levine, D. N., Tsairis, P., and Zajac, F. E. (1973). Physiological types and histochemical profiles in motor units of the cat gastrocnemius. *J. Physiol. (London)* **234**, 723–748.

Butler, J., Cosmos, E., and Brierley, J. (1982). Differentiation of muscle fiber types in aneurogenic brachial muscles of the chick embryo. *J. Exp. Zool.* **224**, 65–80.

Butler-Browne, G. S., Bugaisky, L. B., Cuenoud, S., Schwartz, K, and Whalen, R. G. (1982). Denervation of newborn rat muscles does not block the appearance of adult fast myosin heavy chain. *Nature (London)* **299**, 830–833.

Butler-Browne, G. S., and Whalen, R. G. (1984). Myosin isozyme transitions occurring during the postnatal development of the rat soleus muscle. *Dev. Biol.* **102**, 324–334.

Callaway, E. M., Soha, J. M., and Van Essen, D. C. (1987). Competition favouring inactive over active motor neurons during synapse elimination. *Nature (London)*

328, 422–426.

Callaway, E. M., Soha, J. M., and Van Essen, D. C. (1988). Differential loss of neuromuscular connections according to activity level and spinal position of neonatal rabbit soleus motor neurons. Maunuscript in preparation.

Callaway, E. M., and Van Essen, D. C. (1988). α-Bungarotoxin induced partial activity block slows synapse elimination as assessed both physiologically and anatomically in the neonatal rabbit soleus muscle. Manuscript in preparation.

Campenot, R. B. (1977). Local control of neurite development by nerve growth factor. *Proc. Natl. Acad. Sci. U. S. A.* **74**, 4516–4519.

Chevallier, A., Kieny, M., and Mauger, A. (1977). Limb-somite relationships: origin of the limb musculature. *J. Embryol. Exp. Morphol.* **41**, 245–258.

Chun, L. L. Y., and Patterson, P. H. (1977). Role of nerve growth factor in the development of rat sympathetic neurons in vitro: I. Survival, growth, and differentiation of catecholamine production. *J. Cell Biol.* **75**, 694–704.

Connold, A. L., Evers, J. V., and Vrbová, G. (1986). Effect of low calcium and protease inhibitors on synapse elimination during postnatal development in the rat soleus muscle. *Dev. Brain Res.* **28**, 99–107.

Covault, J., and Sanes, J. R. (1985). Neural cell adhesion molecule (N-CAM) accumulates in denervated and paralyzed skeletal muscles. *Proc. Natl. Acad. Sci. U. S. A.* **82**, 4544–4548.

Covault, J., and Sanes, J. R. (1986). Distribution of N-CAM in synaptic and extrasynaptic portions of developing and adult skeletal muscle. *J. Cell Biol.* **102**, 716–730.

Cowan, W. M., Fawcett, J. W., O'Leary, D. D. M., and Stanfield, B. B. (1984). Regressive events in neurogenesis. *Science* **225**, 1258–1265.

Crepel, F., Mariani, J., and Delhaye-Bouchaud, N. (1976). Evidence for a multiple innervation of Purkinje cells by climbing fibers in the immature rat cerebellum.

J. Neurobiol. **7**, 567–578.

Crow, M. T., and Stockdale, F. E. (1986). Myosin expression and specialization among the earliest muscle fibers of the developing avian limb. *Dev. Biol.* **113**, 238–254.

Cull-Candy, S. G., Lundh, H., and Thesleff, S. (1976). Effects of botulinum toxin on neuromuscular transmission in the rat. *J. Physiol. (London)* **260**, 177–203.

Dennis, M. J., and Yip, J. W. (1978). Formation and elimination of foreign synapses on adult salamander muscle. *J. Physiol. (London)* **274**, 299–310.

Dennis, M. J., Ziskind-Conhaim, L., and Harris, A. J. (1981). Development of neuromuscular junctions in rat embryos. *Dev. Biol.* **81**, 266–279.

Dhoot, G. K. (1986). Selective synthesis and degradation of slow skeletal myosin heavy chains in developing muscle fibers. *Muscle Nerve* **9**, 155–164.

Dhoot, G. K., and Perry, S. V. (1983). Effect of denervation at birth on the development of skeletal muscle cell types in the rat. *Exp. Neurol.* **82**, 131–142.

Donahue, S. P., and English, A. W. (1987). The role of synapse elimination in the establishment of neuromuscular compartments. *Dev. Biol.* **124**, 481–489.

Duron, B., Marlot, D., and Macron, J. M. (1979). Segmental motor innervation of the cat diaphragm. *Neurosci. Lett.* **15**, 93–96.

Duxson, M. J. (1982). The effect of postsynaptic block on the development of the neuromuscular junction in postnatal rats. *J. Neurocytol.* **11**, 395–408.

Duxson, M. J., Ross, J. J., and Harris, A. J. (1986). Transfer of differentiated synaptic terminals from primary myotubes to new-formed muscle cells during embryonic development in the rat. *Neurosci. Lett.* **71**, 147–152.

Ecob, M. S., and Whalen, R. G. (1986). The expression of myosin heavy chain isoforms in a nerve-muscle culture system. In "Molecular Biology of Muscle Development," UCLA Symp. Mol. Cell. Biol. New Series **29**, 272–282.

Edstrom, L., and Kugelberg, E. (1968). Histochemical composition, distribution of fibers and fatiguability of single motor units. *J. Neurol. Neurosurg. Psychiatry* **31,** 424–433.

Eisen, J. S., Myers, P. Z., and Westerfield, M. (1986). Pathway selection by growth cones of identified motoneurons in live zebrafish embryos. *Nature (London)* **320,** 269–271.

Elizalde, A., Huerta, M., and Stefani, E. (1983). Selective reinnervation of twitch and tonic muscle fibres of the frog. *J. Physiol. (London)* **340,** 513–524.

English, A. W. (1986). Does synapse elimination shape neuromuscular compartments? *Soc. Neurosci. Abstr.* **12,** 1118.

English, A. W., and Ledbetter, W. D. (1982). Anatomy and innervation patterns of cat lateral gastrocnemius muscle. *Amer. J. Anat.* **164,** 67–77.

English, A. W., and Weeks, O. I. (1984). Compartmentalization of single motor units in cat lateral gastrocnemius. *Exp. Brain Res.* **56,** 361–368.

Ferguson, B. (1983). Development of motor innervation of the chick following dorsal-ventral limb bud rotations. *J. Neurosci.* **3,** 1760–1772.

Fladby, T. (1987). Postnatal loss of synaptic terminals in the normal mouse soleus muscle. *Acta Physiol. Scand.* **129,** 229–238.

Fladby, T., and Jansen, J. K. S. (1987). Postnatal loss of synaptic terminals in the partially denervated mouse soleus. *Acta Physiol. Scand.* **129,** 239–246.

Frank, E., and Westerfield, M. (1982). The formation of appropriate central and peripheral connexions by foreign sensory neurones of the bullfrog. *J. Physiol. (London)* **324,** 495–505.

Gerding, R., Robbins, N., and Antosiak, J. (1977). Efficiency of reinnervation of neonatal rat muscle by original and foreign nerves. *Dev. Biol.* **61,** 177–183.

Gordon, H. (1983). Postnatal development of motor units in rabbit and rat soleus muscles. PhD thesis, California Institute of Technology.

Gordon, H., and Van Essen, D. C. (1983). The relation of neuromuscular synapse elimination to spinal position of rabbit and rat soleus motoneurones. *J. Physiol. (London)* **339**, 591–597.

Gordon, H., and Van Essen, D. C. (1985). Specific innervation of muscle fiber types in a developmentally polyinnervated muscle. *Dev. Biol.* **111**, 42–50.

Gouze, J.-L., Lasry, J.-M., and Changeux, J.-P. (1983). Selective stabilization of muscle innervation during development: a mathematical model. *Biol. Cybern.* **46**, 207–215.

Greene, L. A., and Shooter, E. M. (1980). The nerve growth factor: Biochemistry, synthesis and mechanism of action. *Ann. Rev. Neurosci.* **3**, 353–402.

Gundersen, R. W., and Barrett, J. N. (1979). Neuronal chemotaxis: Chick dorsal-root axons turn toward high concentrations of nerve growth factor. *Science* **206**, 1079–1080.

Gurney, M. E. (1984). Suppression of sprouting at the neuromuscular junction by immune sera. *Nature (London)* **307**, 546–548.

Guth, L., and Samaha, F. J. (1969). Qualitative differences between actomyosin ATPase of fast and slow mammalian muscle. *Exp. Neurol.* **25**, 138–152.

Guth, L., and Samaha, F. J. (1970). Procedure for the histochemical demonstration of actomyosin ATPase. *Exp. Neurol.* **28**, 365–367.

Hamburger, V. (1939). The development and innervation of transplanted limb primordia of chick embryos. *J. Exp. Zool.* **80**, 347–389.

Hamburger, V. (1975). Cell death in the development of the lateral motor column of the chick embryo. *J. Comp. Neurol.* **160**, 535–546.

Hamburger, V., and Hamilton, H. L. (1951). A series of normal stages in the development of the chick embryo. *J. Morphol.* **88**, 49–92.

Hardman, V. J., and Brown, M. C. (1985). Spatial organization within rat motor neuron pools. *Neurosci. Lett.* **60**, 325–329.

Hardman, V. J., and Brown, M. C. (1987). Accuracy of reinnervation of rat internal intercostal muscles by their own segmental nerves. *J. Neurosci.* **7**, 1031–1036.

Harris, A. J. (1981). Embryonic growth and innervation of rat skeletal muscles. I. Neural regulation of muscle fibre numbers. *Proc. R. Soc. Lond. B* **293**, 257–277.

Henneman, E., and Olson, C. B. (1965). Relations between structure and function in the design of skeletal muscles. *J. Neurophysiol.* **28**, 581–598.

Hennig, R., and Lømo, T. (1985). Firing patterns of motor units in normal rats. *Nature (London)* **314**, 164–166.

Herrera, A. A., and Banner, L. R. (1987). Direct observation of motor nerve terminal remodeling in living frogs. *Soc. Neurosci. Abstr.* **13**, 1665.

Herrup, K. and Sunter, K. (1987). Numerical matching during cerebellar development: quantitative analysis of granule cell death in staggerer mouse chimeras. *J. Neurosci.* **7**, 829–836.

Hilfer, S. R., Searls, R. L., and Fonte, V. G. (1973). An ultrastructural study of early myogenesis in the chick wing bud. *Dev. Biol.* **30**, 374–391.

Hill, R., and Robbins, N. (1987). Transient filopodial-like structures observed at the living mammalian neuromuscular junction. *Soc. Neurosci Abstr.* **13**, 1007.

Hoh, J. F. Y. (1975). Active and nonselective reinnervation of fast-twitch and slow-twitch rat skeletal muscle. *J. Physiol. (London)* **251**, 791–801.

Hollyday, M. (1980). Organization of motor pools in chick lumbar lateral motor column. *J. Comp. Neurol.* **194**, 143–170.

Hollyday, M. (1981). Rules of motor innervation in chick embryos with supernumerary limbs. *J. Comp. Neurol.* **202**, 439–465.

Hollyday, M., and Hamburger, V. (1977). An autoradiographic study of the formation of the lateral motor column in the chick embryo. *Brain Res.* **132**, 197–208.

Hopkins, W. G., Brown, M. C., and Keynes, R. J. (1985). Postnatal growth of motor nerve terminals in muscles of the mouse. *J. Neurocytol.* **14,** 525–540.

Horder, T. J. (1978). Functional adaptability and morphogenetic opportunism, the only rules for limb development? *Zoon* **6,** 181–192.

Innocenti, G. M. (1981). Growth and reshaping of axons in the establishment of visual callosal connections. *Science* **212,** 824–827.

Ivy, G. O., and Killackey, H. P. (1982). Ontogenetic changes in the projections of neocortical neurons. *J. Neurosci.* **2,** 735–743.

Jacob, M., Christ, B., and Jacob, H. J. (1979). The migration of myogenic cells from the somites into the leg region of avian embryos: an ultrastructural study. *Anat. Embryol.* **157,** 291–309.

Jansen, J. K. S., Thompson, W. and Kuffler, D. P. (1978). The formation and maintenance of synpatic connections as illustrated by studies of the neuromuscular junction. *Prog. Brain Res.* **48,** 3–18.

Jansen, J. K. S., Van Essen, D. C., and Brown, M. C. (1976). Formation and elimination of synapses in skeletal muscles of rat. *Cold Spring Harbor Symp. Quant. Biol.* **40,** 425–434.

Johnson, D. A., and Purves, D. (1981). Postnatal reduction of neural size in the rabbit ciliary ganglion. *J. Physiol. (London)* **318,** 143–159.

Jones, S. P., Ridge, R. M. A. P., and Rowlerson, A. (1987). The non-selective innervation of muscle fibres and mixed composition of motor units in a muscle of neonatal rat. *J. Physiol. (London)* **386,** 377–394.

Karpati, G., and Engel, W. K. (1968). "Type grouping" in skeletal muscles after experimental reinnervation. *Neurology* **18,** 447–455.

Katz, M. J., and Lasek, R. J. (1978). Evolution of the nervous system: role of ontogenetic buffer mechanisms in the evolution of matching populations. *Proc. Natl. Acad. Sci. USA* **75,** 1349–1352.

Kelly, A. M., and Rubinstein, N. A. (1980). Why are fetal muscles slow? *Nature (London)* **288**, 266–269.

Kelly, A. M., and Zacks, S. I. (1969). The histogenesis of rat intercostal muscle. *J. Cell Biol.* **42**, 135–153.

Keynes, R. J., and Stern, C. D. (1985). Segmentation and neural development in vertebrates. *Trends Neurosci.* **8**, 220–223.

Keynes, R. J., Stirling, R. V., Stern, C. D., and Summerbell, D. (1987). The specificity of motor innervation of the chick wing does not depend upon the segmental origin of muscles. *Development* **99**, 565–575.

Klug, G., Wiehrer, W., Reichmann, H., and Pette, D. (1983). Relationships between early alterations in parvalbumins, sarcoplasmic reticulum and metabolic enzymes in chronically stimulated fast twitch muscle. *Pflügers Arch.* **399**, 280–284.

Korneliussen, H., and Jansen, J. K. S. (1976). Morphological aspects of the elimination of polyneuronal innervation of skeletal muscle fibres in newborn rats. *J. Neurocytol.* **5**, 591–604.

Kugelberg, E. (1973). Histochemical composition, contraction speed and fatiguability of rat soleus motor neurons. *J. Neurol. Sci.* **20**, 177–198.

Kugelberg, E. (1976). Adaptive transformation of rat soleus motor units during growth. *J. Neurol. Sci.* **27**, 269–289.

Kugelberg, E., Edstrom, L., and Abbruzzese, M. (1970). Mapping of motor units in experimentally reinnervated rat muscle. *J. Neurol. Neurosurg. Psychiatry* **33**, 319–329.

Laing, N. G., and Lamb, A. H. (1983). The distribution of muscle fibre types in chick embryo wings transplanted to the pelvic region is normal. *J. Embryol. Exp. Morphol.* **78**, 67–82.

Lamb, A. H. (1976). The projection patterns of the ventral horn to the hind limb

during development. *Dev. Biol.* **54**, 82–99.

Lamb, A. H. (1977). Neuronal death in the development of the somatotopic projections of the ventral horn in *Xenopus*. *Brain Res.* **134**, 145–150.

Lance-Jones, C. (1985). The somitic origin of limb muscles in the chick embryo: a correlation with motor innervation. *Soc. Neurosci. Abstr.* **11**, 975.

Lance-Jones, C., and Landmesser, L. (1980a). Motoneurone projection patterns in embryonic chick limbs following partial deletions of the spinal cord. *J. Physiol. (London)* **302**, 559–580.

Lance-Jones, C., and Landmesser, L. (1980b). Motoneurone projection patterns in the chick hind limb following early partial reversals of the spinal cord. *J. Physiol. (London)* **302**, 581–602.

Lance-Jones, C., and Landmesser, L. (1981a). Pathway selection by chick lumbosacral motoneurons during normal development. *Proc. R. Soc. Lond.* B **214**, 1–18.

Lance-Jones, C., and Landmesser, L. (1981b). Pathway selection by embryonic chick motoneurons in an experimentally altered environment. *Proc. R. Soc. Lond.* B **214**, 19–52.

Landmesser, L. (1978a). The distribution of motoneurones supplying chick hind limb muscles. *J. Physiol. (London)* **284**, 371–389.

Landmesser, L. (1978b). The development of motor projection patterns in the chick hind limb. *J. Physiol. (London)* **284**, 391–414.

Landmesser, L. (1984). The development of specific motor pathways in the chick embryo. *Trends Neurosci.* **7**, 336–339.

Landmesser, L., and Morris, D. G. (1975). The development of functional innervation in the hind limb of the chick embryo. *J. Physiol. (London)* **249**, 301–326.

Lanser, M. E., Carrington, J. L., and Fallon, J. F. (1986). Survival of motoneurons

in the brachial lateral motor column of *limbless* mutant chick embryos depends on the periphery. *J. Neurosci.* **6**, 2551–2557.

Laskowski, M. B., and Sanes, J. R. (1987a). Topographic mapping of motor pools onto skeletal muscles. *J. Neurosci.* **7**, 252–260.

Laskowski, M. B., and Sanes, J. R. (1987b). Topographically selective reinnervation of adult mammalizn muscles. *Soc. Neurosci. Abstr.* **13**, 1422.

Letinsky, M. S. (1974). The development of nerve-muscle junctions in *Rana catesbeiana* tadpoles. *Dev. Biol.* **40**, 129–153.

LeVay, S., Stryker, M. P., and Shatz, C. J. (1978). Ocular dominance columns and their development in layer IV of the cat's visual cortex: a quantitative study. *J. Comp. Neurol.* **179**, 223-244.

LeVay, S., Wiesel, T. N., and Hubel, D. H. (1980). The development of ocular dominance columns in normal and visually deprived monkeys. *J. Comp. Neurol.* **191**, 1–51.

Levi-Montalcini, R., and Angeletti, P. U. (1963). Essential role of the nerve growth factor in the survival and maintenance of dissociated sensory and sympathetic embryonic nerve cells *in vitro*. *Dev. Biol.* **7**, 653–659.

Levi-Montalcini, R., and Angeletti, P. U. (1968). Nerve growth factor. *Physiol. Rev.* **48**, 534–569.

Lewis, J. (1978). Pathways of axons in the developing chick wing: evidence against chemo-specific guidance. *Zoon* **6**, 175–179.

Lewis, J., Chevallier, A., Kieny, M., and Wolpert, L. (1981). Muscle nerve branches do not develop in chick wings devoid of muscle. *J. Embryol. Exp. Morphol.* **64**, 211–232.

Lichtman, J. W. (1977). The reorganization of synaptic connexions in the rat submandibular ganglion during post-natal development. *J. Physiol. (London)* **273**, 155–177.

Lichtman, J. W., Magrassi, L., and Purves, D. (1987). Visualization of neuromuscular junctions over periods of several months in living mice. *J. Physiol.* **7**, 1215–1222.

Lichtman, J. W., and Purves, D. (1980). The elimination of redundant preganglionic innervation to hamster sympathetic ganglion cells in early post-natal life. *J. Physiol. (London)* **301**, 213–228.

Lichtman, J. W., and Wilkinson, R. S. (1987). Properties of motor units in the transversus abdominis muscle of the garter snake. *J. Physiol. (London)* **393**, 355–374.

Lømo, T., and Rosenthal, J. (1972). Control and ACh sensistivity by muscle activity in the rat. *J. Physiol. (London)* **221**, 493–513.

Lømo, T., Westgaard, R. H., and Dahl, H. A. (1974). Contractile properties of muscle: control by pattern of muscle activity in the rat. *Proc. R. Soc. Lond. B* **187**, 99–103.

Lundh, H., Leander, S., and Thesleff, S. (1977). Antagonism of the paralysis produced by Botulinum toxin in the rat: The effects of tetraethylammonium, guanidine and 4-aminopyridine. *J. Neurol. Sci.* **32**, 29–43.

Mariani, J., and Changeux, J.-P. (1981). Ontogenesis of olivocerebellar relationships. I. Studies by intracellular recordings of the multiple innervation of Purkinje cells by climbing fibers in the developing rat cerebellum. *J. Neurosci.* **1**, 696–702.

McGrath, P. A., and Bennett, M. R. (1979). The development of synaptic connections between different segmental motoneurons and striated muscles in an axolotl limb. *Dev. Biol.* **68**, 133–145.

McLennan, I. S. (1983). Neural dependence and independence of myotube production in chicken hindlimb muscles. *Dev. Biol.* **98**, 287–294.

Miledi, R., and Stefani, E. (1969). Non-selective re-innervation of slow and fast

muscle fibres in the rat. *Nature* **222**, 569–571.

Miller, J. B., Crow, M. T., and Stockdale, F. E. (1985). Slow and fast myosin heavy chain content defines three types of myotubes in early muscle cell cultures. *J. Cell Biol.* **101**, 1643–1650.

Miller, J. B., and Stockdale, F. E. (1986a). Developmental regulation of the multiple myogenic cell lineages of the avian embryo. *J. Cell Biol.* **103**, 2197–2208.

Miller, J. B., and Stockdale, F. E. (1986b). Developmental origins of skeletal muscle fibers: clonal analysis of myogenic cell lineages based on fast and slow myosin heavy chain expression. *Proc. Natl. Acad. Sci. USA* **83**, 3860–3864.

Mommaerts, W. F., Seraydarian, K., Suh, M., Kean, C. J. R., and Buller, A. J. (1977). The conversion of some biochemical properties of mammalian skeletal muscles following cross-reinnervation. *Exp. Neurol.* **55**, 637–653.

Morris, D. G. (1978). Development of functional motor innervation in supernumerary hindlimbs of the chick embryo. *J. Neurophys.* **41**, 1450–1465.

Narusawa, M., Fitzsimons, R. B., Izumo, S., Nadal-Ginard, B., Rubinstein, N. A., and Kelly, A. M. (1987). Slow myosin in developing rat skeletal muscle. *J. Cell Biol.* **104**, 447–459.

Navarrete, R., and Vrbová, G. (1983). Changes of activity patterns in slow and fast muscles during postnatal development. *Dev. Brain Res.* **8**, 11–19.

Nemeth, P. M., Pette, D., and Vrbová, G. (1981). Comparison of enzyme activities among single muscle fibres within defined motor units. *J. Physiol. (London)* **311**, 489–495.

Nemeth, P. M., and Turk, W. R. (1984). Biochemistry of rat single muscle fibres in newly assembled motor units following nerve crush. *J. Physiol. (London)* **355**, 547–555.

Nurcombe, V., Hill, M. A., Eagleson, K. L., and Bennett, M. R. (1984). Motor neuron survival and neuritic extension from spinal cord explants induced by

factors released from denervated muscle. *Brain Res.* **291**, 19–28.

O'Brien, R. A. D., Östberg, A. J. C., and Vrbová, G. (1978). Observations on the elimination of polyneuronal innervation in developing mammalian skeletal muscle. *J. Physiol. (London)* **282**, 571–582.

O'Brien, R. A. D., Östberg, A. J. C., and Vrbová, G. (1984). Protease inhibitors reduce the loss of nerve terminals induced by activity and calcium in developing rat soleus muscles *in vitro*. *Neuroscience* **12**, 637–646.

O'Leary, D. D. M., Fawcett, J. W., and Cowan, W. M. (1986). Topographic targeting errors in the retinocollicular projection and their elimination by selective ganglion cell death. *J. Neurosci.* **6**, 3692–3705.

O'Leary, D. D. M., Stanfield, B. B., and Cowan, W. M. (1981). Evidence that the early postnatal restriction of the cells of origin of the callosal projection is due to the elimination of axonal collaterals rather than to the death of neurons. *Dev. Brain Res.* **1**, 607–617.

Oppenheim, R. W. (1986). The absence of significant postnatal motoneuron death in the brachial and lumbar spinal cord of the rat. *J. Comp. Neurol.* **246**, 281–286.

Papoulis, A. (1965). "Probability, Random Variables, and Stochastic Processes." McGraw-Hill, New York.

Pette, D. Müller, W., Leisner, E., and Vrbová, G. (1976). Time dependent effects on contractile properties, fibre populations, myosin light chains and enzymes of energy metabolism in intermittently and continuously stimulated fast twitch muscles of the rabbit. *Pflügers Arch.* **364**, 103–112.

Pettigrew, A. G., Lindeman, B., and Bennett, M. R. (1979). Development of segmental innervation of the chick forelimb. *J. Embryol. Exp. Morphol.* **49**, 115–137.

Phillips, W. D., and Bennett, M. R. (1984). Differentiation of fiber types in wing

muscles during embryonic development: effect of neural tube removal. *Dev. Biol.* **106,** 457–468.

Purves, D., and Lichtman, J. W. (1980). Elimination of synapses in the developing nervous system. *Science* **210,** 153–157.

Purves, D., and Lichtman, J. W. (1985). "Principles of Neural Development." Sinauer, Sunderland, MA.

Redfern, P. A. (1970). Neuromuscular transmission in new-born rats. *J. Physiol. (London)* **209,** 701–709.

Ridge, R. M. A. P., and Betz, W. J. (1984). The effect of selective, chronic stimulation of motor units size in developing rat muscle. *J. Neurosci.* **4,** 2614–2620.

Riley, D. A. (1977a). Spontaneous elimination of nerve terminals from the endplates of developing skeletal myofibers. *Brain Res.* **134,** 279–285.

Riley, D. A. (1977b). Multiple innervation of fiber types in the soleus muscles of postnatal rats. *Exp. Neurol.* **56,** 400–409.

Riley, D. A. (1981). Ultrastructural evidence for axon retraction during spontaneous elimination of polyneuronal innervation of the rat soleus muscle. *J. Neurocytol.* **10,** 425–440.

Robbins, N., and Polak, J. (1987). Forms of growth and retraction at mouse neuromuscular junctions revealed by a new nerve terminal stain and correlative electron microscopy. *Soc. Neurosci. Abstr.* **13,** 1007.

Rosenthal, J. L., and Taraskevich, P. S. (1977). Reduction of multiaxonal innervation at the neuromuscular junction of the rat during development. *J. Physiol. (London)* **270,** 299–310.

Ross, J. J., Duxson, M. J., and Harris, A. J. (1987). Neural determination of muscle fibre numbers in embryonic rat lumbrical muscles. *Development* **100,** 395–409.

Rubinstein, N. A., and Kelly, A. M. (1978). Myogenic and neurogenic contributions

to the development of fast and slow twitch muscles in rat. *Dev. Biol.* **62,** 473–485.

Rubinstein, N. A., and Kelly, A. M. (1981). Development of muscle fiber specialization in the rat hindlimb. *J. Cell Biol.* **90,** 128–144.

Rutz, R., and Hauschka, S. D. (1982). Clonal analysis of vertebrate myogenesis. VII. Heritability of muscle colony type through sequential subclonal passages *in vitro*. *Dev. Biol.* **91,** 103–110.

Salmons, S., and Sréter, F. A. (1976). Significance of impulse activity in the transformation of skeletal muscle type. *Nature (London)* **263,** 30–34.

Salmons, S., and Vrbová, G. (1969). The influence of activity on some contractile characteristics of mammalian fast and slow muscles. *J. Physiol. (London)* **201,** 533–549.

Sanes, J. R., Marshall, L. M., and McMahan, U. J. (1978). Reinnervation of muscle fiber basal lamina after removal of myofibers. Differentiation of regenerating axons at original synaptic sites. *J. Cell Biol.* **78,** 176–198.

Schafer, D. A., Miller, J. B., and Stockdale, F. E. (1987). Cell diversification within the myogenic lineage: in vitro generation of two types of myoblasts from a single myogenic progenitor cell. *Cell* **48,** 659–670.

Schmalbruch, H. (1982). Skeletal muscle fibers of newborn rats are coupled by gap junctions. *Dev. Biol.* **91,** 485–490.

Schmidt, H., and Stefani, E. (1976). Re-innervation of twitch and slow muscle fibres of the frog after crushing the motor nerves. *J. Physiol. (London)* **258,** 99–123.

Seed, J., and Hauschka, S. D. (1984). Temporal separation of the migration of distinct myogenic precursor populations into the developing chick wing bud. *Dev. Biol.* **106,** 389–393.

Shafiq, S. A., Asiedu, S. A., and Milhorat, A. T. (1972). Effect of neonatal neurectomy on differentiation of fiber types in rat skeletal muscle. *Exp. Neurol.*

35, 529–540.

Shellswell, G. B. (1977). The formation of discrete muscles from the chick wing dorsal and ventral muscle masses in the absence of nerves. *J. Embryol. Exp. Morphol.* **41**, 269–277.

Smalheiser, N. R., and Crain, S. M. (1984). The possible role of "sibling neurite bias" in the coordination of neurite extension, branching, and survival. *J. Neurobiol.* **15**, 517–529.

Smith, C. L., and Frank, E. (1987). Peripheral specification of sensory neurons transplanted to novel locations along the neuraxis. *J. Neurosci.* **7**, 1537–1549.

Soha, J. M., Yo, C., and Van Essen, D. C. (1987). Synapse elimination by fiber type and maturational state in rabbit soleus muscle. *Dev. Biol.* **123**, 136–144.

Soileau, L. C., Silberstein, L., Blau, H. M., and Thompson, W. J. (1987). Reinnervation of muscle fiber types in the newborn rat soleus. *J. Neurosci.* **7**, 4176–4194.

Sperry, R. W. (1963). Chemoaffinity in the orderly growth of nerve fiber patterns and connections. *Proc. Natl. Acad Sci. USA* **50**, 703–710.

Sréter, F. A., Gergely, J., Salmons, S., and Romanul, F. (1973). Synthesis by fast muscle of myosin light chains characteristic of slow muscle in response to long term stimulation. *Nature (London)* **241**, 17–19.

Stein, J. M., and Padykula, H. A. (1962). Histochemical classification of individual skeletal muscle fibers of the rat. *Am. J. Anat.* **110**, 103–123.

Stockdale, F. E., and Miller, J. B. (1987). The cellular basis of myosin heavy chain isoform expression during development of avian skeletal muscles. *Dev. Biol.* **123**, 1–9.

Sulston, J. E., and Horvitz, H. R. (1977). Post-embryonic cell lineages of the nematode *Caenorhabditis elegans*. *Dev. Biol.* **56**, 110–156.

Summerbell, D., and Stirling, R. V. (1981). The innervation of dorsoventrally

reversed chick wings: evidence that motor axons do not actively seek out their appropriate targets. *J. Embryol. Exp. Morphol.* **61**, 233–247.

Swett, J. E., Eldred, E., and Buchwald, J. S. (1970). Somatotopic cord-to-muscle relations in efferent innervation of cat gastrocnemius. *Am. J. Physiol.* **219**, 762–766.

Taxt, T. (1983). Local and systemic effects of tetrodotoxin on the formation and elimination of synapses in reinnervated adult rat muscle. *J. Physiol. (London)* **340**, 175–194.

Taxt, T., Ding, R., and Jansen, J. K. S. (1983). A note on the elimination of polyneuronal innervation of skeletal muscles in neonatal rats. *Acta Physiol. Scand.* **117**, 557–560.

Thompson, W. J. (1983a). Lack of segmental selectivity in elimination of synapses from soleus muscle of new-born rats. *J. Physiol. (London)* **335**, 343–352.

Thompson, W. J. (1983b). Synapse elimination in neonatal rat muscle is sensitive to pattern of muscle use. *Nature (London)* **309**, 709–711.

Thompson, W. J. (1985). Activity and synapse elimination at the neuromuscular junction. *Cell. Mol. Neurobiol.* **5**, 167–182.

Thompson, W., and Jansen, J. K. S. (1977). The extent of sprouting of remaining motor units in partly denervated immature and adult rat soleus muscles. *Neuroscience* **2**, 523–535.

Thompson, W., Kuffler, D. P., and Jansen, J. K. S. (1979). The effect of prolonged, reversible block of nerve impulses on the elimination of polyneuronal innervation of new-born rat skeletal muscle fibers. *Neuroscience* **4**, 271–281.

Thompson, W. J., Sutton, L. A., and Riley, D. A. (1984). Fiber type composition of single motor units during synapse elimination in neonatal rat soleus muscle. *Nature (London)* **309**, 709–711.

Tosney, K. W., and Landmesser, L. T. (1984). Pattern and specificity of axonal

outgrowth following varying degrees of chick limb bud ablation. *J. Neurosci.* **4**, 2518–2527.

Tosney, K. W., and Landmesser, L. T. (1985a). Development of the major pathways for neurite outgrowth in the chick hindlimb. *Dev. Biol.* **109**, 193–214.

Tosney, K. W., and Landmesser, L. T. (1985b). Specificity of early motoneuron growth cone outgrowth in the chick embryo. *J. Neurosci.* **5**, 2336–2344.

Tosney, K. W., and Landmesser, L. T. (1985c). Growth cone morphology and trajectory in the lumbosacral region of the chick embryo. *J. Neurosci.* **5**, 2345–2358.

Toutant, M., Montarras, D, and Fiszman, M. Y. (1984). Biochemical evidence for two classes of myoblasts during chick embryonic muscle development. *Expl. Biol. Med.* **9**, 10–15.

Van Essen, D. C. (1982). Neuromuscular synapse elimination: Structural, functional, and mechanistic aspects. In "Neuronal Development" (N. C. Spitzer, ed.), pp. 333-371. Plenum Press, New York.

Van Essen, D. C., and Jansen, J. K. S. (1977). The specificity of re-innervation by identified sensory and motor neurons in the leech. *J. Comp. Neurol.* **171**, 433–454.

Vogel, M., and Landmesser, L. (1987). Distribution of fiber types in embryonic chick limb muscles innervated by foreign motoneurons. *Dev. Biol.* **119**, 481–495.

Weeks, O. I., and English, A. W. (1985). Compartmentalization of the cat lateral gastrocnemius motor nucleus. *J. Comp. Neurol.* **235**, 255–267.

Weiss, P., and Hoag, A. (1946). Competitive reinnervation of rat muscles by their own and foreign nerves. *J. Neurophysiol.* **9**, 413–418.

Wernig, A, Pécot-Dechavassine, M., and Stöver, H. (1980). Sprouting and regression of the nerve at the frog neuromuscular junction in normal conditions and after prolonged paralysis with curare. *J. Neurocytol.* **9**, 277–303.

Westerfield, M., and Eisen, J. S. (1988). Neuromuscular specificity: pathfinding by identified motor growth cones in a vertebrate embryo. *Trends Neurosci.* **11,** 18–22.

Weydert, A., Barton, P., Harris, A. J., Pinset, C., and Buckingham, M. (1987). Developmental pattern of mouse skeletal myosin heavy chain gene transcripts in vivo and in vitro. *Cell* **49,** 121–129.

White, N. K., Bonner, P. H., Nelson, D. R., and Hauschka, S. D. (1975). Clonal analysis of vertebrate myogenesis. IV. Medium-dependent classification of colony-forming cells. *Dev. Biol.* **44,** 346–361.

Whitelaw, V., and Hollyday, M. (1983a). Thigh and calf discrimination in the motor innervation of the chick hindlimb following deletions of limb segments. *J. Neurosci.* **3,** 1199–1215.

Whitelaw, V., and Hollyday, M. (1983b). Position-dependent motor innervation of the chick hindlimb following serial and parallel duplications of limb segments. *J. Neurosci.* **3,** 1216–1225.

Whitelaw, V., and Hollyday, M. (1983c). Neural pathway constraints in the motor innervation of the chick himdlimb following dorsoventral rotations of distal limb segments. *J. Neurosci.* **3,** 1226–1233.

Wigston, D. J. (1987). Repeated imaging of neuromuscular junctions in mouse soleus. *Soc. Neurosci. Abstr.* **13,** 1007.

Wigston, D. J., and Kennedy, P. R. (1987). Selective reinnervation of transplanted muscles by their original motoneurons in the axolotl. *J. Neurosci.* **7,** 1857–1865.

Wigston, D. J., and Sanes, J. R. (1982). Selective reinnervation of adult mammalian muscle by axons from different segmental levels. *Nature (London)* **299,** 464–467.

Wigston, D. J., and Kennedy, P. R. (1987). Selective reinnervation of transplanted muscles by their original motorneurons in the axolotl. *J. Neurosci.* **7,** 1857–1865.

Willshaw, D. J. (1981). The establishment and the subsequent elimination of polyneuronal innervation of developing muscle: Theoretical considerations. *Proc. R. Soc. Lond. B* **212**, 233–252.

Wirsen, C., and Larsson, K. S. (1964). Histochemical differentiation of skeletal muscle in foetal and newborn mice. *J. Embryol. Exp. Morphol.* **12**, 759–767.

Zajac, F. E., and Faden, J. S. (1985). Relationship among recruitment order, axonal conduction velocity, and muscle-unit properties of type-identified motor units in cat plantaris muscle. *J. Neurophysiol.* **53**, 1303–1322.